

University of Louisville

ThinkIR: The University of Louisville's Institutional Repository

Electronic Theses and Dissertations

12-2023

BioCaRGOS: Capture and release gels for optimized storage of biologics.

Chinmay Shashank Potnis
University of Louisville

Follow this and additional works at: <https://ir.library.louisville.edu/etd>



Part of the [Life Sciences Commons](#)

Recommended Citation

Potnis, Chinmay Shashank, "BioCaRGOS: Capture and release gels for optimized storage of biologics." (2023). *Electronic Theses and Dissertations*. Paper 4205.
<https://doi.org/10.18297/etd/4205>

This Doctoral Dissertation is brought to you for free and open access by ThinkIR: The University of Louisville's Institutional Repository. It has been accepted for inclusion in Electronic Theses and Dissertations by an authorized administrator of ThinkIR: The University of Louisville's Institutional Repository. This title appears here courtesy of the author, who has retained all other copyrights. For more information, please contact thinkir@louisville.edu.

BioCaRGOS: CAPTURE AND RELEASE GELS FOR OPTIMIZED STORAGE
OF BIOLOGICS

By

Chinmay Shashank Potnis

M.S., University of Louisville, 2021

A Dissertation

Submitted to the Faculty of the
College of Arts and Sciences of the University of Louisville
in Partial Fulfilment of the Requirements
for the Degree of

Doctor of Philosophy
in Chemistry

Department of Chemistry
University of Louisville
Louisville, KY

December 2023

Copyright 2023 by Chinmay Shashank Potnis
All rights reserved

BioCaRGOS: CAPTURE AND RELEASE GELS FOR OPTIMIZED STORAGE
OF BIOLOGICS

By

Chinmay Shashank Potnis
M.S., University of Louisville, 2021

A Dissertation Approved on

August 31st, 2023

By the following Dissertation Committee

Dissertation Director
Dr. Craig A. Grapperhaus

Dr. Gautam Gupta

Dr. Robert M. Buchanan

Dr. Vance Jager

Dr. Xiang Zhang

DEDICATION

To my loving parents Sonia and Shashank and my brother Manas Potnis your unwavering love and support have been my greatest source of strength throughout this journey. This thesis is dedicated to each of you, with heartfelt gratitude for your constant encouragement and belief in my abilities.

ACKNOWLEDGEMENTS

I would like to express my deepest gratitude to my research advisors Dr. Craig Grapperhaus and Dr. Gautam Gupta, for their invaluable mentorship, guidance, and unwavering motivation throughout my journey. I am immensely thankful to Dr. Mark Linder for his invaluable assistance and expertise in chemical biology, always willing to lend a helping hand and clear my doubts and for amazing collaboration. I extend my sincere appreciation to the National Institutes of Health (NIH) for their crucial funding support, which has been instrumental in the completion of my thesis. I would like to thank the University of Louisville for conferring me the Dissertation Completion Award (Summer 2023) that supported my research.

I am grateful to Evan Alexander for helping me with the biological studies included in this dissertation. I would also like to thank Dr. Meenakshi Bansal for her valuable expertise in Raman spectroscopy experiments and train me on the instrument related to some of the experiments in this dissertation and for excellent collaboration. I am also grateful to Dr. Rajat Chauhan for his assistance towards my research and his guidance. I also want to thank the members of my dissertation committee; Dr. Vance Jager, for his unconditional support for my research activities, Dr. Xiang Zhang for his time, contribution, and valuable suggestions; Dr. Robert M. Buchanan for his commitment in making this journey come to a smooth

end. Also, thanks to Sherry Nalley and other administrative staff of the department of chemistry for their support. I would also like to thank the current chair, Dr. Wittebort, for his support and motivation during my PhD.

My heartfelt appreciation goes to my lab mates Kritika Bajaj, Sashil Chapagain, Peter Armstrong, Christine Phipps, Mohan Paudel, Kelley Lee, and Rishad Khan who have been instrumental in my PhD journey. I would like to thank my friends Sudripet, Yuhao, Sagar, Hari, Vasu, and Deepika who have made this ride enjoyable and memorable.

I am deeply grateful to my parents, Sonia, and Shashank, for their unwavering support and love during the toughest moments of this journey. My heartfelt appreciation goes to my brother, Manas, for standing by my side throughout. And last but certainly not least, I want to express my deepest gratitude to Kritika Bajaj, whose invaluable support, guidance, and unwavering belief in me kept me motivated and inspired me to pursue my goals.

ABSTRACT

BioCaRGOS: CAPTURE AND RELEASE GELS FOR OPTIMIZED STORAGE OF BIOLOGICS

Chinmay Shashank Potnis

Aug 31st, 2023

The preservation of proteins and nucleic acids is crucial for scientific and medical applications. Storing them at ultra-low temperatures is expensive and impractical. This thesis explores alternative strategies for room temperature storage, focusing on sol gel encapsulation. The challenges of maintaining biomolecule stability during storage are discussed, and strategies like additives, lyophilization, and encapsulation are explored.

Silica sol gel encapsulation is investigated as an innovative storage method. It preserves biomolecule activity and allows customization of properties. The development of BioCaRGOS, a sol gel system for optimized room temperature storage, is presented. Hemoglobin and miRNA-21 are used as model bio molecules, showcasing stability and compatibility with clinical processes. Efforts are made to optimize BioCaRGOS for compatibility with downstream applications by addressing methanol interference. The release of pancreatic cancer biomarkers is evaluated, demonstrating compatibility with droplet digital PCR. The study further explores the stability of heme proteins under degradation and low pH

conditions using BioCaRGOS, highlighting challenges in storing therapeutic proteins.

In conclusion, sol gel encapsulation, particularly BioCaRGOS, shows potential for stabilizing and storing biomolecules at room temperature. It offers stability, ease of recovery, and compatibility with downstream applications. This research contributes to cost-effective storage methods, eliminating the need for specialized freezers and reducing energy consumption in biomolecule preservation.

TABLE OF CONTENTS

| | |
|---|-------|
| ACKNOWLEDGEMENTS | iv |
| ABSTRACT..... | vi |
| LIST OF FIGURES..... | xiii |
| LIST OF TABLES..... | xviii |
| CHAPTER 1..... | 1 |
| INTRODUCTION | 1 |
| 1.1 Lay summary | 1 |
| 1.2 Scope of dissertation..... | 2 |
| 1.3 Preservation of proteins and nucleic acids | 6 |
| 1.4 Storage techniques..... | 9 |
| 1.4.1 Low temperature storage methods | 9 |
| 1.4.2 Room temperature storage methods | 11 |
| 1.4.3 Silica sol gel process..... | 13 |
| 1.5 Summary..... | 14 |
| CHAPTER 2..... | 16 |
| SOL GEL CHEMISTRY | 16 |
| 2.1 Introduction | 16 |
| 2.2 Types of precursors in sol gels..... | 17 |

| | | |
|--|---|----|
| 2.3 | Mechanisms of sol gel synthesis | 18 |
| 2.3.1 | Hydrolysis and condensation reactions of metal alkoxides..... | 19 |
| 2.4 | Process parameters affecting sol gel structures | 21 |
| 2.4.1 | Effect of water to silica ratio (H ₂ O: Si), r | 21 |
| 2.4.2 | Effect of precursor concentration | 22 |
| 2.4.3 | Effect of pH | 23 |
| 2.4.4 | Effect of solvents | 24 |
| 2.4.5 | Effect of catalyst | 26 |
| 2.5 | Encapsulation of biospecimens via sol gel process | 27 |
| 2.6 | Limitations of conventional sol gel approaches | 29 |
| 2.7 | Introduction to BioCaRGOS | 30 |
| CHAPTER 3..... | | 33 |
| BioCaRGOS: CAPTURE AND RELEASE GELS FOR OPTIMIZED STORAGE OF PROTEINS AND NUCLEIC ACIDS AT AMBIENT TEMPERATURES | | 33 |
| 3.1 | Introduction | 33 |
| 3.2 | Experimental..... | 37 |
| 3.2.1 | Materials | 37 |
| 3.2.2 | BioCaRGOS synthesis | 38 |
| 3.2.3 | Storage of hemoglobin in BioCaRGOS | 39 |
| 3.2.4 | Release of hemoglobin..... | 39 |
| 3.2.5 | Evaluation of BioCaRGOS by Raman spectroscopy | 40 |
| 3.2.6 | Evaluation of gel formation using IR spectroscopy | 40 |

| | | |
|--|--|----|
| 3.2.7 | Degradation of miRNA 21 with enhancement of RNase A concentration | 40 |
| 3.2.8 | Reverse transcription | 41 |
| 3.2.9 | Real-time qPCR amplification | 41 |
| 3.3 | Results | 41 |
| 3.3.1 | UV-vis characterization of hemoglobin content within the BioCaRGOS formulations..... | 41 |
| 3.3.2 | Long term storage of hemoglobin in BioCaRGOS | 47 |
| 3.3.3 | Raman analysis of BioCaRGOS formulations..... | 48 |
| 3.3.4 | Polyethylene glycol (PEG) induced hemoglobin release in BioCaRGOS formulations..... | 49 |
| 3.3.5 | Investigation of compatibility of BioCaRGOS with miRNA 21 | 51 |
| 3.3.6 | Long term evaluation of miRNA 21 concentration in BioCaRGOS | 53 |
| 3.3.7 | Evaluation of stability in the presence of RNase A..... | 55 |
| 3.4 | Conclusion | 57 |
| CHAPTER 4..... | | 59 |
| ENHANCING THE COMPATIBILITY OF BioCaRGOS WITH DOWNSTREAM APPLICATIONS..... | | 59 |
| 4.1 | Introduction | 59 |
| 4.2 | Experimental..... | 62 |
| 4.2.1 | Materials | 62 |
| 4.2.2 | BioCaRGOS synthesis | 62 |
| 4.2.3 | Evaluation of BioCaRGOS using Raman spectroscopy..... | 63 |
| 4.2.4 | Circulating cell free (cfDNA) nucleic acid extraction | 63 |

| | | |
|--|---|----|
| 4.2.5 | Circulating tumor (ctDNA) analysis using Seracare samples | 63 |
| 4.2.6 | Invert Syringe Filtration | 64 |
| 4.2.7 | Droplet digital PCR (ddPCR)..... | 64 |
| 4.2.8 | Elimination of Methanol from BioCaRGOS samples..... | 66 |
| 4.3 | Results | 67 |
| 4.3.1 | BioCaRGOS compatibility with ddPCR..... | 67 |
| 4.3.2 | BioCaRGOS compatibility with ctDNA extraction process | 70 |
| 4.3.3 | Elimination of silica from BioCaRGOS to minimize the interference ... | 71 |
| 4.4 | Conclusions | 75 |
| CHAPTER 5..... | | 77 |
| INVESTIGATING BioCaRGOS FOR STABILITY OF HEME PROTEINS | | |
| UNDER ENZYMATIC DEGRADATION AND LOW pH | | 77 |
| 5.1 | Introduction | 77 |
| 5.2 | Experimental..... | 80 |
| 5.2.1 | Materials | 80 |
| 5.2.2 | BioCaRGOS Synthesis | 80 |
| 5.2.3 | Encapsulation of protein in BioCaRGOS..... | 81 |
| 5.2.4 | Release of Mb post encapsulation..... | 81 |
| 5.2.5 | Spectroscopic Characterization | 81 |
| 5.2.6 | Proteolysis experiment..... | 81 |
| 5.3 | Results | 82 |
| 5.3.1 | BioCaRGOS synthesis and encapsulation of Mb..... | 82 |
| 5.3.2 | Stability of Mb against Proteinase K..... | 84 |
| 5.3.3 | Long term storage of Mb in presence of Proteinase K..... | 88 |

| | |
|---|-----|
| 5.3.4 Release of encapsulated Mb from BioCaRGOS matrix | 89 |
| 5.3.5 Effect of BioCaRGOS and their concentration on the stability of Cyt c at low pH..... | 91 |
| 5.4 Conclusions | 93 |
| CHAPTER 6..... | 95 |
| CONCLUSIONS | 95 |
| REFERENCES | 100 |
| Appendix for Chapter 3 | 112 |
| Appendix for Chapter 5 | 120 |
| CURRICULUM VITA..... | 121 |

LIST OF FIGURES

| | |
|--|----|
| Figure 1-1. Various factors (external and internal) leading to denaturation of biologics. | 8 |
| Figure 1-2. Different types of storage methods for proteins and nucleic acids..... | 9 |
| Figure 2-1. Schematic for CVD process for immobilization. | 31 |
| Figure 3-1. Synthesis and Raman characterization of BioCaRGOS formulations. (a and b) Schematic of BioCaRGOS formulations and encapsulation of hemoglobin for long-term room-temperature storage and (c) complete hydrolysis of 5.0 v/v % tetramethyl orthosilicate (TMOS..... | 44 |
| Figure 3-2. UV-vis analysis of hemoglobin content within BioCaRGOS formulations. (a) Incremental increase in the hemoglobin stability with incremental increase in BioCaRGOS concentrations (0–5.0) v/v %. An unaltered UV-vis absorbance band (406 nm) of heme group of hemoglobin framework is observed in BioCaRGOS formulations (5.0 v/v %). (b) Hemoglobin stability with incremental increase in BioCaRGOS concentrations (0–7.5) v/v %. An unaltered UV-vis absorbance band (406 nm) of heme group in hemoglobin framework is observed in BioCaRGOS formulations (5.0 and 7.5 v/v %). | 46 |
| Figure 3-3. Excellent long-term stability of hemoglobin in BioCaRGOS formulations (5.0 v/v % TMOS; 0.01 w/v % hemoglobin; 0.15 M PB, pH 8.2) against control hemoglobin solutions (0.01 w/v % hemoglobin; 0.15 M PB, pH 8.2). (a) Refrigeration (5 °C) and (b) room- temperature (23 °C) conditions.. | 48 |

| | |
|---|----|
| Figure 3-4. Raman spectra of BioCaRGOS. An unaltered Raman spectrum of BioCaRGOS (5.0 v/v %) formulations (with and without hemoglobin) over 21 days..... | 49 |
| Figure 3-5. Polyethylene glycol (PEG) induced hemoglobin content release. a) Schematic of PEG addition to the BioCaRGOS formulation for facile hemoglobin extraction and b) significant hemoglobin release in BioCaRGOS formulations upon PEGylation. | 50 |
| Figure 3-6. Investigation of compatibility of BioCaRGOS with miRNA: (a) miRNA concentration level (nM) in CaRGOS (0.5 v/v %) in low salt buffer and high salt buffer (b) representative schematic of the significant electrostatic-repulsions between negatively charged silica-colloids and miRNA 21 (c) a plot of miRNA concentrations (nM) vs. TMOS concentrations (v/v) % with their pH levels..... | 53 |
| Figure 3-7. Long term evaluation of miRNA concentrations in BioCaRGOS: A plot of miRNA 21 concentrations (nM) with sol-gel for 82 days at varying temperatures (4, 25, 40) °C; miRNA 21 concentrations (nM) without BioCaRGOS (Control) at 25 °C..... | 54 |
| Figure 3-8. Evaluation of stability in the presence of RNase A: (a) A schematic of dual-character of negatively charged silica-colloids demonstrating the electrostatic-attraction induced denaturation of positively charged RNase A and a simultaneous immobilization of miRNA 21 within BioCaRGOS formulations via electrostatic repulsion (b) A plot of relative fluorescence intensity of Ethidium bromide versus RNase A concentrations in (0-320) nM range..... | 57 |

| | |
|---|----|
| Figure 4-1. Raman spectra of 5 v/v % TMOS pre-distillation demonstrating methanol intensity at A) 45 °C, B) 55 °C, and C) 70 °C at 25 mbar after timed intervals..... | 67 |
| Figure 4-2. ddPCR analysis of KRAS (G12D) ctDNA levels showing low copies due to interference of methanol present in BioCaRGOS. | 68 |
| Figure 4-3. Addition of 98% MeOH to control samples [10 mM Tris-HCl (pH 7.5), 1 mM EDTA, 0.15 M NaCl] to see the negative effect on KRAS ctDNA samples..... | 69 |
| Figure 4-4. ddPCR analysis showing no interference in ctDNA count post removal of methanol by distillation..... | 70 |
| Figure 4-5. ddPCR characterization of KRAS (G12D) ctDNA concentrations (ng/mL) extracted from Seracare reference materials containing BioCaRGOS (+ silica), prior to the ctDNA extraction against controls. | 71 |
| Figure 4-6. A) Representation of Invert Syringe Filtration technique (ISF) using a 0.45 µm pore size filter to remove silica from BioCaRGOS samples prior to analysis. B) Plot of DLS counts showing > 70-80% removal of colloidal silica from BioCaRGOS by ISF. C) KRAS (G12D) ctDNA concentrations (ng/mL) extracted from Seracare reference material containing BioCaRGOS (w/o MeOH and limited silica) employing rotary evaporation and ISF, prior to cfDNA extractions, against controls..... | 74 |
| Figure 4-7. Percentage yield enhancement of ctDNA in BioCaRGOS samples demonstrating ~96% recovery..... | 75 |
| Figure 4-8. BioCaRGOS synthesis and complete workflow of ctDNA extraction | 76 |

Figure 5-1. (A) Schematic overview of BioCaRGOS synthesis and Mb encapsulation. (B) Mechanism of BioCaRGOS sol gel synthesis. 83

Figure 5-2. UV-vis spectra of metaquo Mb upon addition of 0.1 wt/v % proteinase K at 25 °C at pH 7.4 over 24 h period. The Soret bands of metaquo mb (409 nm) and the denatured, free heme are shown in (A), while the Q-band region is shown in (B). The 633 nm band in the Q region is from metaquo Mb. 85

Figure 5-3. Myoglobin stability with incremental increase in BioCaRGOS concentration (0 – 7.5 v/v %). An unaltered UV-vis absorbance band (409 nm) of heme group of Mb was observed in BioCaRGOS formulations (5 and 7.5 v/v %). 86

Figure 5-4. CD spectra of Mb encapsulated in 1 and 2.5 v/v % BioCaRGOS vs controls. Note: Day 0 Control was similar to Day 0 1 and 2.5 v/v % BC. Denatured Mb conformation indicated by dotted line (purple). CD spectra of Mb encapsulated in 2.5 v/v % BioCaRGOS vs controls demonstrating intact 2° structure of Mb as compared to Mb in controls which was denatured over 24 h. 87

Figure 5-5. Long term storage in presence of proteinase K of Mb encapsulated in 5 and 7.5 v/v % BioCaRGOS demonstrating excellent stability as compared to Mb in control samples. 89

Figure 5-6. Schematic representation of release of Mb from 5 v/v % BioCaRGOS solution. 90

Figure 5-7. UV-vis absorption spectrum of Cyt c encapsulated at pH 2.5 over the period of 1 h (A) in control samples (w/o BioCaRGOS) (B) in 7.5 v/v % BioCaRGOS. 92

Figure 5-8. Cyt c stability with incremental increase in BioCaRGOS concentration (0-7.5 v/v %). An unaltered UV-vis absorbance band (409 nm) of heme group of Cyt c was observed in BioCaRGOS formulations (7.5 v/v %).
..... 93

LIST OF TABLES

| | |
|---|----|
| Table 2-1. Parameters for sol gel encapsulation..... | 28 |
| Table 4-1. ddPCR sample preparation..... | 65 |
| Table 4-2. Thermal cycler program..... | 66 |

CHAPTER 1

INTRODUCTION

1.1 Lay summary

Proteins and nucleic acids, which are important biological molecules, are commonly stored at low temperatures, typically at $-80\text{ }^{\circ}\text{C}$, to maintain their stability and functionality. Cold storage slows down enzymatic and chemical reactions that can cause degradation or denaturation of these molecules over time. However, preserving proteins and nucleic acids at such low temperatures requires specialized equipment and consumes a lot of energy, making it expensive and not always practical for long-term storage on a large scale. As a result, various researchers have explored alternative storage methods that can be more cost-effective and practical for long-term storage of proteins and nucleic acids at room temperature. This is important because room temperature storage would eliminate the need for specialized freezers and reduce energy consumption, making the storage process more accessible and affordable.

Several strategies are being explored for room temperature storage of proteins and nucleic acids, including the use of stabilizing additives, lyophilization (freeze-drying), and encapsulation in protective matrices. Stabilizing additives, such as sugars or other stabilizing agents, can help prevent degradation and denaturation of biomolecules at room temperature. Lyophilization, which involves freeze-drying the biomolecules, removes water from the samples and

can stabilize them at room temperature. Encapsulation in protective matrices, such as polymers or hydrogels, can provide a physical barrier against degradation factors and maintain the stability of the biomolecules at room temperature. This dissertation focuses on the use of novel sol-gel encapsulation technique called BioCaRGOS for protecting and stabilizing biomolecules, specifically proteins and nucleic acids. It discusses the sensitivity of these biomolecules to environmental variations and the need for effective encapsulation methods to protect them from degradation and denaturation. The dissertation highlights the progress made in recent years in the development of sol-gel encapsulation methods for proteins and nucleic acids, including the use of sol-gel matrices to protect enzymes from high temperatures, proteases from proteolysis, and DNA from degradation by nucleases. It also discusses the advantages of sol-gel encapsulation, such as controlled release of encapsulated biomolecules and biocompatibility of sol-gel matrices with downstream analytical techniques. The dissertation further describes the development BioCaRGOS which offers improved stability and long-term storage of biomolecules, such as proteins and miRNA, and compatibility with clinical practices. It also focuses on the potential utility of BioCaRGOS in enhancing the shelf life of drugs and its compatibility with extraction and analysis of cell-free DNA for cancer biomarkers is also discussed.

1.2 Scope of dissertation

This dissertation describes a series of studies on the synthesis and characterization of a novel sol gel technique called BioCaRGOS. These studies include synthesis and applicability of BioCaRGOS for the storage of proteins, such as hemoglobin, and nucleic acids, such as DNA and miRNA 21.

Furthermore, studies were conducted on minimization of the interference caused by methanol, a by-product of the hydrolysis reaction arising from BioCaRGOS synthesis, and the removal of silica nanoparticles post encapsulation to minimize the interference in the analysis of biologics on downstream analytical instruments. The study focuses on demonstrating the applicability of BioCaRGOS for the storage of heme proteins, specifically myoglobin and cytochrome c, under various stresses. These proteins were chosen due to their different isoelectric points and susceptibility to denaturation in the presence of proteinase K and low pH conditions.

BioCaRGOS were characterized using Raman spectroscopy and Fourier transform infrared (FT-IR) for monitoring synthesis. Dynamic light scattering (DLS) and zeta analysis were used for investigating the size of the silica nanoparticles and their colloidal stability over time. The stability studies of various proteins such as hemoglobin, myoglobin, and cytochrome C was characterized on UV-visible spectroscopy and circular dichroism spectroscopy. The KRAS ctDNA was characterized using droplet digital PCR was performed using the QX200™ Droplet Digital™ PCR System from BioRad for investigating the stability in BioCaRGOS formulations.

Chapter 1 of this dissertation provides an overview of the need for biospecimen storage and different storage methods. It discusses the preservation of proteins and nucleic acids and describes the challenges faced in terms of maintaining their stability and structure during storage. It also discusses different techniques for storage of biospecimens. Overall, this chapter provides an overview of the importance of preserving proteins and

nucleic acids, the challenges associated with their stability during storage, and the different storage techniques commonly used in the field.

Chapter 2 provides an overview of silica sol gel encapsulation as an alternative technique for the storage of biospecimens, such as proteins and nucleic acids. Biospecimens are susceptible to environmental stresses that can lead to denaturation and loss of activity, and silica sol gel encapsulation provides a physical barrier against these stresses, preserving the activity and functionality of the biomolecules. The chapter discusses the advantages of silica sol gel encapsulation over cold storage techniques, including the ability to tailor the properties of silica sol gel materials, such as porosity, mechanical strength, and chemical composition, to optimize protection against environmental stresses. The chapter also describes the two main types of precursors used in sol gel synthesis, namely alkoxysilanes and alkali metal salts, and their hydrolysis and condensation reactions that result in the formation of a three-dimensional network of silica nanoparticles. Factors associated with sol gel synthesis and how they can affect the stability of biomolecules are also discussed in this chapter.

Chapter 3 discusses the development of BioCaRGOS, a capture and release gel system for optimized storage of proteins and nucleic acids at ambient temperatures. The chapter focuses on the stability of hemoglobin, a model protein, in BioCaRGOS as a proof of concept. The advantages of BioCaRGOS over conventional sol-gel techniques include a clinically compatible process with rapid hydrolysis, minimal presence of methanol, effective long-term storage of biospecimens, and an easy post-encapsulation recovery method. The stability of hemoglobin in BioCaRGOS is attributed to

factors such as the isoelectric point (pI) of proteins, where the net charge on the protein is zero, and the role of electrolytes in maintaining protein stability. Additionally, miRNA-21, a small non-coding RNA molecule involved in cancer regulation, is mentioned as a potential biomolecule for encapsulation in BioCaRGOS for storage and release studies.

Chapter 4 focuses on enhancing the compatibility of BioCaRGOS, a sol-gel encapsulation approach for biospecimen storage, with downstream applications. It specifically addresses the need to optimize BioCaRGOS for the removal of methanol, a by-product of its synthesis, which can interfere with polymerase chain reaction (PCR) used for DNA amplification. The chapter also discusses the release of biomarkers post-encapsulation and the effect of silica interference, with a focus on circulating tumor DNA (ctDNA) in plasma as a potential biomarker for pancreatic cancer. The compatibility of BioCaRGOS with ctDNA extraction protocols and droplet digital PCR (ddPCR) is evaluated to establish its effectiveness in preserving ctDNA integrity for downstream analysis. The chapter presents results on the successful minimization of methanol interference and elimination of silica colloidal particles from BioCaRGOS prior to ctDNA extraction, demonstrating the compatibility of BioCaRGOS with ddPCR for the storage of pancreatic cancer biomarkers at ambient temperatures.

Chapter 5 of the thesis focuses on investigating the stability of heme proteins, specifically myoglobin (Mb) and cytochrome c (Cyt c), under enzymatic degradation and low pH conditions using BioCaRGOS. The chapter introduces the challenges associated with the storage and stability of therapeutic proteins, including their large molecular size and degradation due

to harsh process conditions. The long-term stability of myoglobin in the presence of proteinase K at ambient temperature is also demonstrated. We used two model proteins, Mb and Cyt c, to assess the stability of the proteins in the presence of proteinase K and under pH stress, respectively. Remarkably, both proteins showed exceptional stability when encapsulated in 5 and 7.5 v/v % BioCaRGOS, with Mb being preserved efficiently for over 25 days even in the presence of proteinase K. This stabilization effect is attributed to the inhibitory action of BioCaRGOS formulations on proteinase K, possibly due to electrostatic attractions.

Chapter 6 of this study elucidated the potential of sol-gel encapsulation, specifically the developed BioCaRGOS (Biocompatible Capture and Release Gels for Optimized Biospecimen Storage), as an effective technique for the stabilization and storage of biomolecules, including proteins and nucleic acids. The results indicated that BioCaRGOS has the potential to stabilize a wide range of biomolecules, as most proteins and nucleic acids exhibit a pI (isoelectric point) below the pH of BioCaRGOS solution, facilitating easy recovery.

1.3 Preservation of proteins and nucleic acids

Cells are fundamental units of living organisms. The genetic information for making an individual is stored in and replicated through DNA (deoxyribonucleic acid), which is located inside the nucleus. DNA is a sequence of four different types of nucleotides. Certain segments of the DNA correspond to genes, which under appropriate condition would be used to make a molecule called mRNA (ribonucleic acid), whose sequence directly corresponds to the DNA sequence. This process is called transcription. The resulting mRNA

migrates out of the nucleus into cell cytoplasm. There, a protein is synthesized in a process called translation using the mRNA as a template. A protein is a sequence of 20 different kinds of amino acids. Each amino acid is uniquely determined by three nucleotides on the DNA and RNA. Proteins work with each other to form various biological processes and pathways in a hierarchical fashion. First, the primary sequence of the protein, which is a linear sequence of 20 amino acids, dictates the folding of the protein into 3-D structure. Through this hierarchical structure, the limited number of proteins are able to combine with each other to perform diverse kinds of cellular functions. These proteins have the most dynamic and diverse role of any macromolecule in the body, catalysing biochemical reactions, forming receptors and channels in membranes, providing intracellular and extracellular scaffolding support, and transporting molecules from one organ to another. From therapeutic point of view, they represent a tremendous opportunity in terms of harnessing protein therapeutics to treat various diseases.

Protein therapeutics, enzymes, and vaccines are all made up of proteins and these three industries have a common problem: most proteins are subjected to denaturation if exposed to high temperatures or other environmental variables. The efficiency of protein therapeutics, enzymes and vaccines is highly dependent on protein secondary and tertiary structure and heat exposure disrupts the intermolecular interactions needed to maintain the structure. In addition to temperature, ionic properties such as ion concentration, charge, and size play an important role in determining the stability of protein and nucleic acid folding kinetics. pH is another important factor that plays an important role in maintaining folded structure of proteins and nucleic acids.

When the pH value of the reaction medium changes, the shape and structure of enzyme or protein will change. There are carboxyl groups on the side chain of amino acids and there are amine containing functional groups in the side chain of basic amino acids. If the ionized state of amino acids in the protein is changed, the ionic bonds that maintain the three-dimensional structure of the protein will change, thus change in pH will lead to structural modifications and damage the protein function or lead to enzyme inactivation (Figure 1-1).

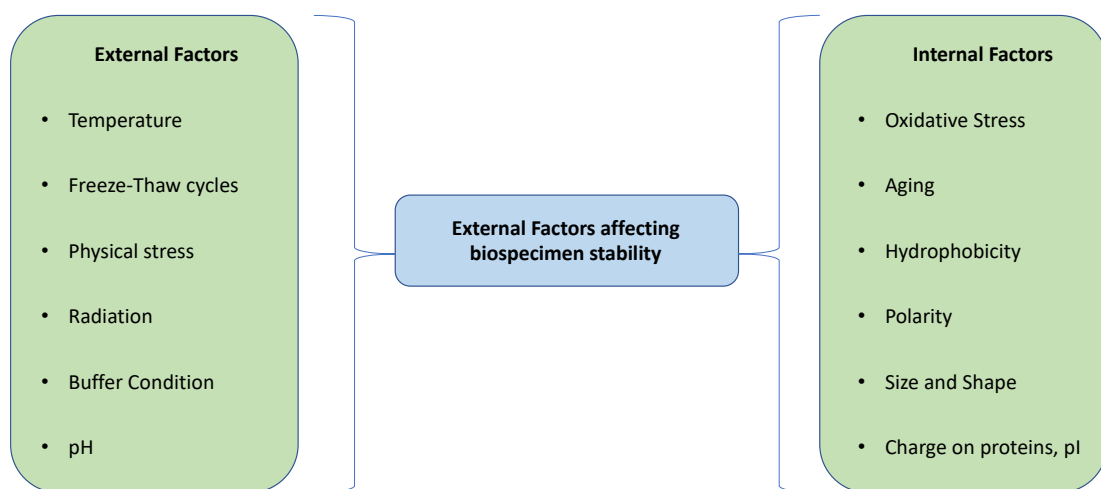


Figure 1-1. Various factors (external and internal) leading to denaturation of biologics.

RNA, DNA, and proteins are used in many fields such as molecular and cellular biology, medicine, and nanotechnology. For most of these uses, integrity of these biospecimens is very crucial and must be maintained during storage. However, these biospecimens are susceptible to multiple degradation reactions. First, it is very sensitive to oxidation by reactive oxygen species. Degradation can also occur through the activity of some metallic complexes catalyzing the hydrolytic cleavage of the phosphodiester bond or by contaminating nucleases. In order to maintain the integrity of these biospecimens, temperature is one of the crucial factors biospecimens have to

deal with while transportation and plays a key role in many complex physiological mechanisms.¹ In selecting biospecimen storage temperature, consideration should be given to the biospecimen type, the anticipated length of the storage and the biospecimen of interest. In order to prevent degradation, biospecimens can be stored at various temperatures.

1.4 Storage techniques

Biospecimens should be stored in a stabilize state. As discussed in the previous section, specific temperature for specific biospecimen is crucial and can lead to thermal denaturation if not maintained properly. Currently, the storage methods are classified into low temperature storage methods and room temperature storage methods (Figure 1-2). These will be explained in detail in the next section.

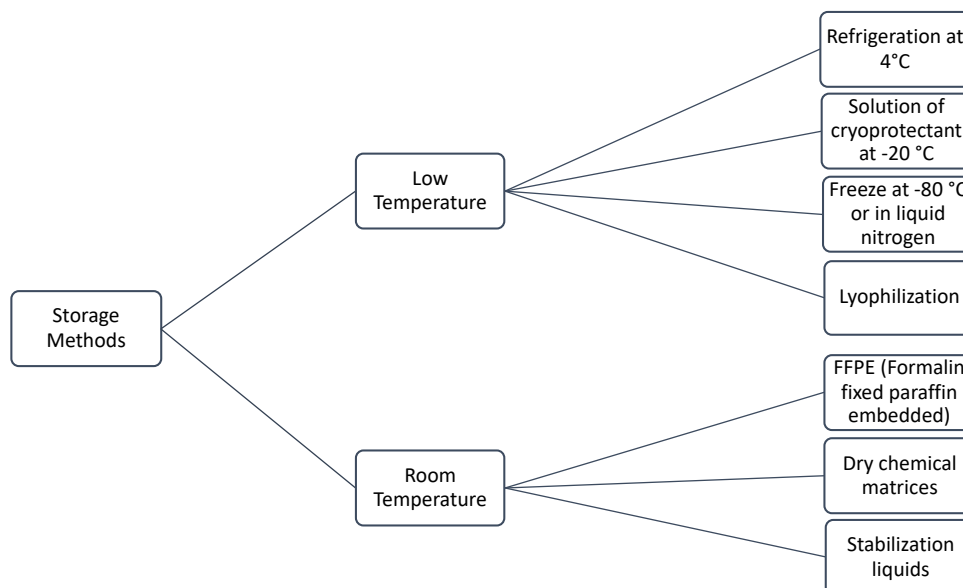


Figure 1-2. Different types of storage methods for proteins and nucleic acids.

1.4.1 Low temperature storage methods

The most common method of preserving biospecimens is freezing and storage of samples at low temperatures in order to inhibit degradation. Formalin

fixed paraffin embedded (FFPE) tissues and ultra-low temperature frozen tissues at (-80 °C to -190 °C) are most widely used to store nucleic acids, protein and other enzymes for diagnostics and research purposes. At, ultra-low temperatures, high molecular weight nucleic acids and enzymatically active protein in tissues are preserved for many years.²⁻⁴ RNA samples are also stored under liquid nitrogen to prevent degradation. The use of low temperature storage to stabilize the biospecimens is mainly carried out to control the behaviour of water in the system and specifically to reduce the mobility of water by freezing.⁵ However, studies have shown that even at low temperature, ribonucleases can be active at -20 °C on frozen RNA and can denature RNA.⁶

Although, cold storage is widely used, it has many challenges associated with respect to stabilizing biospecimens over long term. Moreover, storing up to thousands of samples in biorepositories, biobanks and biological resource centers leads to poor maintenance capacity, costs, and maintenance of cold chain systems.⁷ Protein therapeutics are sensitive to thermal denaturation since the loss of secondary and tertiary structure may cause a decrease in protein activity and the process of thermal denaturation is irreversible in most cases. Unnecessary thawing and refreezing of frozen samples can decrease the integrity of these biospecimens. When the samples are stored at cryogenic temperatures, high usage of liquid nitrogen or liquid carbon dioxide can induce toxicity in biological samples. Shipping of these samples require dry ice and can be very expensive and challenging considering regulations in air transportation. Hence, to address these challenges, effective room temperature storage methods and shipping process is required.

1.4.2 Room temperature storage methods

Clearly, frozen biospecimens have many advantages but also some significant disadvantages. Room temperature storage methods have significant potential to change the widely used cold storage techniques. After relatively upfront costs, room temperature storage requires minimal space and basic overhead for maintaining room temperature. Conversely, the costs of freezers are substantial. This section will include various room temperature techniques used to overcome cold storage methods and their limitations.

Some companies such as Biomatrix (San Diego, CA) and GenVault (Carlsbad, CA) offer commercial solutions in which biospecimens such as RNA and DNA are dehydrated in the presence of hydrophilic additives by entrapment in matrices and stored at room temperature.⁸ Biomatrix's DNA sample matrix is based on a glass polymer that "shrink-wraps" and protect DNA from heat and UV light through a mechanism similar to that used by extremophiles, small organisms that can survive in dry environments for up to 120 years.⁹ In addition, although all these procedures claim to be efficient in storing nucleic acids and proteins being hydrophilic, they cannot be expected to protect the sample against atmospheric water during storage. Whatman's FTA paper binds nucleic acids and inactivates nucleases but the amount to be stored and retrieved are low and storage time is limited. Furthermore, none of them provides with a quantitative estimation of RNA lifetime under the conditions used.

Another technique that has been currently used to preserve biospecimens commercially is lyophilization, which reduces the dependence on cold chain equipment. The lyophilization process involves two main steps: freezing the protein in solution and increasing the pressure to remove the

moisture under vacuum. Although, many proteins are able to retain their structure and activity during both freeze-drying processes, some proteins are unable to tolerate such drastic changes. Furthermore, lyophilized vaccines are still sensitive to heat exposure. Because of all these limitations, the enzyme-protein therapeutics and vaccine industries are interested in finding alternative ways to thermally stabilize proteins.¹⁰

Protein immobilization is an alternative way to cold storage and other room temperature storage methods that are commercially available. Physical immobilization consists of adsorbing or encapsulating a protein within a support material to lock it in place via different interactions such as van der Waals interaction, hydrogen bonding and covalent bonding. The two most commonly used techniques for biospecimen immobilization are adsorption onto inorganic porous materials (e.g., silica, activated carbon, aluminum oxide, iron oxide and metal organic frameworks) and sol-gel encapsulation. According to the IUPAC, mesoporous materials are materials with pore sizes between 2-50 nm in diameter. Microporous materials have pores smaller than 2nm in diameter and macroporous materials have pores larger than 50 nm in diameter. Some of the most common types of mesoporous materials for protein preservation are mesoporous silicas, activated carbon, MOFs.¹⁰ Encapsulation in silica gels normally preserve the functional properties of biospecimens such as proteins, peptides and nucleic acids, or even whole cells, thus allowing a wide range of applications. Since biospecimens cannot withstand extreme temperatures, typically used for synthesizing silica glasses, immobilization of proteins and other biospecimens is achieved via the sol gel process. This technique allows

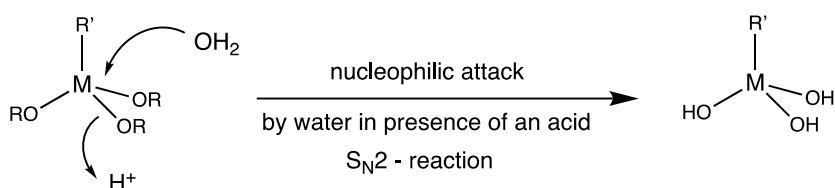
for encapsulation of biospecimens in the silica-based gels and represent a useful alternative to current room temperature storage methods.

1.4.3 Silica sol gel process

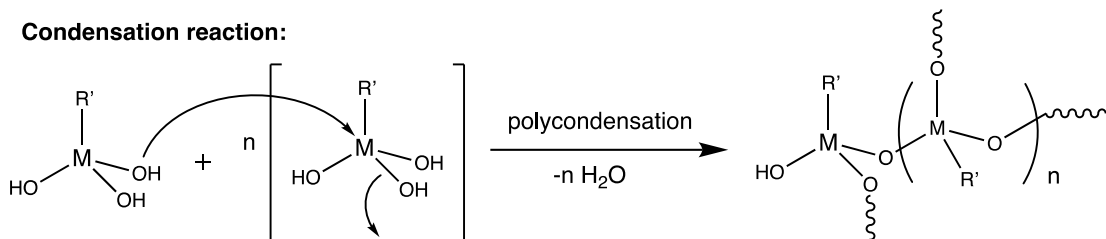
Encapsulation of biospecimens in silica sol gels began in early 1990s.⁹ The chemistry of the encapsulation process must take into account the same requirements to ensure the preservation of biological activity during and after encapsulation.¹¹ This implies to operate in mild temperature conditions, aqueous solution, limited ionic strength and to avoid any additives that may induce biomolecule denaturation or be toxic for the cells. In addition, the resulting encapsulation matrix should exhibit internal surface properties that are not detrimental to the molecule conformation or cell membrane organization. Finally, the host system must have controlled porosity to guarantee the access of substrates and nutrients to guest elements and the recovery of the products while avoiding leaching of the active biologicals. Thus, the primary and limiting step of the encapsulation process is to achieve an aqueous polymerization or gelation reaction in mild conditions.

The pioneer works of Braun and Carturan showed that sol gel process was well suited for bioencapsulation.^{12, 13} These sol gel matrices are obtained from hydrolysis and condensation-polymerization of metal and semimetal alkoxides, mostly but not exclusively SiO₂ materials (Scheme 1-1).¹⁴

Hydrolysis reaction:



Condensation reaction:



Scheme 1-1. Hydrolysis and condensation polymerization reaction mechanism for metal alkoxides

Some of the major advantages of silica sol gels as a matrix for biospecimen encapsulation are listed as follows; a) the synthesis is fast and relatively cheap as compared to other commercially available room temperature storage methods; b) mild pH and temperature conditions that are compatible with retention of protein and nucleic acid functions; c) are open to flexible chemical protocols, allowing the use of a variety of additives and precursor molecules; d) tunable pore size and can be optically transparent facilitating several spectroscopic techniques for characterization of the encapsulated molecules or for biosensor applications; e) enhance the stability of encapsulated molecules by the virtue of the rigidity of the cage thereby preventing leaching of proteins.¹⁵ Thus, silica sol gel process is an attractive alternative as compared to other cold storage and room temperature storage methods for various biomolecules.

1.5 Summary

Proteins and nucleic acids are key components of vaccines, enzymes, and many types of therapeutics, are sensitive to denaturation when exposed to

high temperatures and other stresses such as pH and enzymatic degradation. Maintaining the integrity of these biospecimens is therefore crucial and proper storage is necessary to maintain structural and functional activity of proteins and nucleic acids. As discussed in the introduction, different storage methods are used for preservation of biospecimens. But the limitations associated with most commonly used cold temperature and room temperature storage methods leads to the development of new technique of sol gel encapsulation. This leads to Chapter 2 of this dissertation which describes the mechanism of action for sol gel encapsulation and emphasizes the chemistry of sol gel process.

CHAPTER 2

SOL GEL CHEMISTRY

2.1 Introduction

The need for silica sol gel encapsulation as an alternative technique for the storage of biospecimens, such as proteins and nucleic acids, has been previously described in Chapter 1. Biospecimens are vulnerable to environmental stresses such as exposure to heat, UV light, and oxidation that can lead to denaturation and loss of activity. Silica sol gel encapsulation provides a physical barrier against these physical stresses that can preserve the activity and functionality of the protein or nucleic acid of interest. On the contrary, cold storage techniques do not provide protection against environmental stresses and fluctuations in temperature and humidity levels can affect stability.

Silica sol gel encapsulation is preferred over cold storage techniques for several reasons. First, the properties of silica sol gel materials can be tailored with respect to porosity, mechanical strength, and chemical composition by optimizing synthetic conditions such as the pH, temperature, and concentration of the silica precursor used to maximize the protection against environmental stresses. This allows for the design of silica nanoparticles with specific properties such as controlled drug release or biocompatibility. Second, silica sol

gels are chemically inert, hydrophilic, and exhibit high thermal stability and mechanical strength. This can provide a three-dimensional cage like structure around the biomolecule protecting it from various denaturing factors such as aggregation, dissociation, and denaturation. Lastly, the synthesis of sol gel materials is relatively simple and it can be performed using relatively inexpensive and readily available precursors.^{14, 16} The two main factors associated with sol gel synthesis are hydrolysis and condensation reactions, but there are various other elements that can affect the sol gel synthesis of silica nanoparticles which can eventually affect the encapsulation of biospecimens. In this chapter, factors associated with sol gel synthesis and how they affect the stability of biomolecules will be discussed.

2.2 Types of precursors in sol gels

For the synthesis of sol gels using silicon alkoxides two main routes are most generally used. In the first, the precursors usually involve tetra-alkoxysilanes, tri-alkyl alkoxysilanes, di-alkyl alkoxysilanes, or mono-alkyl alkoxysilanes. Out of these, two most commonly used silica precursors are tetramethyl orthosilicate (TMOS) or tetraethyl orthosilicate (TEOS) as they are easily hydrolyzed in the solution. These traditional TMOS or TEOS precursors are insoluble in water and release denaturing or cytotoxic alcohol (i.e., methanol or ethanol respectively) during the hydrolysis step. As such the typical sol gel reaction involves solubilization of the alkoxide in the parent alcohol and addition of an aqueous solution at a specific pH to achieve hydrolysis and condensation reactions.

The use of water soluble alkoxides incorporating non-cytotoxic alcohols has been reported by Gill *et al.*, where the synthesis of polyglycerylsilane was

carried out and was found compatible with encapsulation of various enzymes.¹⁷ Following this, Brennan *et al.*, developed multiple sugar-modified precursors (sorbitol, maltose, and dextrose), all of which were found compatible for the encapsulation of biospecimens.¹⁸ Lately, tetrakis (2-hydroxyethyl) orthosilicate (THEOS) was developed for encapsulation of mammalian cells.¹⁹ These appeared to be good alternatives as they can be readily dissolved in water at pH 7.0 and are non-cytotoxic. Despite these advantages, they still poses one major drawback, which is the presence of alcohols/sugars that may perturb specific cellular activity.¹³

The second route for sol gel synthesis consists of precursors that are alkali metal salts. The precursors consist of aqueous alkaline silicates of the general formula $M_xSi_yO_z$ where $M = Na^+, K^+$. However, these solutions contain excessive amounts of alkali stabilizing negatively charged poly-silicic acids. Neutralization of these silicates leads to formation of gel but in highly saline environments, the ionic strength exceeds the values compatible with multiple enzymes.

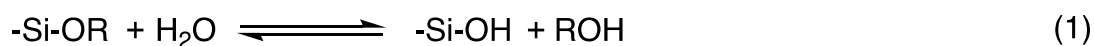
2.3 Mechanisms of sol gel synthesis

In general, the sol gel process involves hydrolysis of an alkoxide precursor under acidic or basic conditions. Hydrolysis of a metal alkoxide (e.g., TMOS or TEOS) precursors results in the formation of silanol functional group (Si-OH). Following this step, the condensation reaction proceeds to form siloxanes (Si-O-Si-). Finally, through polycondensation of silanol and siloxanes, an interconnected three-dimensional network with pores of sub-micrometer dimensions and polymeric chains of SiO_2 are formed.

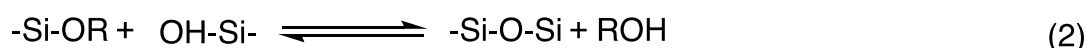
2.3.1 Hydrolysis and condensation reactions of metal alkoxides

At the functional group level, three reactions are generally used to describe the sol gel process where R is an alkyl group.

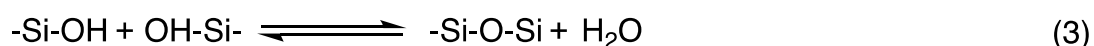
Hydrolysis



Alcohol condensation



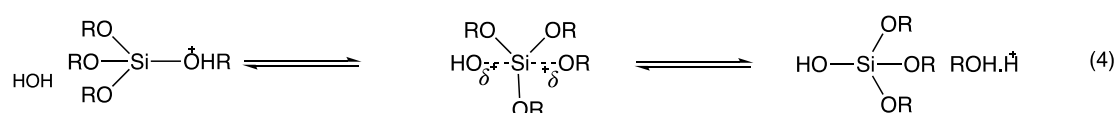
Water condensation



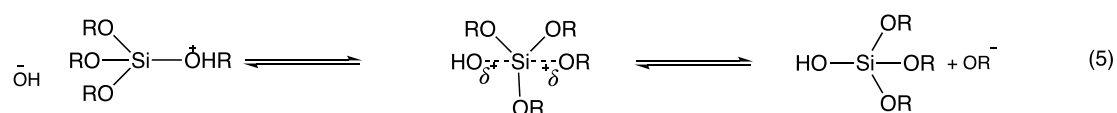
The hydrolysis reaction (Eq. 1) replaces the alkoxide group (OR) with hydroxyl group (OH). The rate and extent of hydrolysis reaction determines the final properties of the sol gel matrix, such as its viscosity, optical transparency, and mechanical strength. Further condensation of silanol groups produces siloxane bonds (-Si-O-Si-) along with the generation of alcohol (R-OH) by-products (Eq. 2). As hydrolysis and condensation reactions are in equilibrium, once the hydrolysis is initiated, condensation reactions proceed simultaneously (Eqs. 2 and 3). As water and most of the alkoxysilanes are immiscible, usually alcohols are added as a co-solvent to homogenize the solution. As the equilibrium reaction suggest, alcohol can be participated in reverse of Eq. 1 and 2 in esterification or alcoholysis of the reactions. Hydrolysis is facilitated in the presence of homogenizing agents like alcohols, dioxane, THF, acetone that are especially beneficial in accelerating hydrolysis of silanes that contain bulky organic or alkoxy groups. Lower alkoxy groups such as methoxy, ethoxy, *n*-propoxy or isopropoxy are preferable as alkoxy group in the silica precursors while any branching of these alkoxy groups or lengthening the chain slows the

hydrolysis rate of the alkoxy silanes. The reaction rate decreases in the order; $\text{Si}(\text{OMe})_4 > \text{Si}(\text{OEt})_4 > \text{Si}(\text{O}^i\text{Pr})_4 > \text{Si}(\text{O}^t\text{Pr})_4$.^{20, 21}

The water to alkoxide ratio in Eqs. 1 and 2 can vary from <1 to 50. The rate and extent of the hydrolysis reaction are mostly influenced by the strength and concentration of acid and base catalyst.²² Hydrolysis and condensation reactions occur through a nucleophilic $\text{S}_{\text{N}}2$ substitution on the Si atom. Usually, weaker acids require longer reaction times to achieve the same extent of reaction compared to strong acids. Base catalyzed hydrolysis of silicon alkoxides proceeds at a much slower rate than acid catalyzed hydrolysis at equivalent catalyst concentration.^{22, 23} Under acidic conditions, an alkoxide group is protonated in a rapid first step. Electron density on the silicon atom is withdrawn, thus making it more electrophilic and more susceptible to attack by water. As shown in equation 4, the water molecule attacks from rear and gains partial positive charge. This positive charge of protonated alkoxide is reduced, making alcohol a better leaving group. The transition state decays by displacement of alcohol accompanied by inversion of the silicon tetrahedron.



Under basic conditions, water dissociates to produce nucleophilic hydroxyl anions in rapid first step as shown in equation 5. The hydroxyl anion then attacks the silicon atom. As the silicon acquires a formal negative charge in the transition state, the $\text{S}_{\text{N}}2$ mechanisms are quite sensitive to inductive as well as steric effects.¹⁴



2.4 Process parameters affecting sol gel structures

Factors such as water to silica ratio, type of precursors, temperature, pH of the medium, solvents, concentration of precursors used, and catalyst highly determine the structure and properties of silica sol gels. Therefore, proper selection of these factors is necessary with respect to the application.^{16, 24} Some of the important factors are described in detail.

2.4.1 Effect of water to silica ratio ($\text{H}_2\text{O}:\text{Si}$), r

Hydrolysis reactions can be affected significantly by the $\text{H}_2\text{O}:\text{Si}$ ratio (r). Depending upon the desired polysilicate product, various values of r ranging from 1 to 25 are selected. As illustrated in Eqs. 1 and 3, water is a reactant in silicon alkoxide hydrolysis and a product in silanol condensation. Hence, a higher $\text{H}_2\text{O}:\text{Si}$ ratio promotes hydrolysis at a faster rate while also slowing the condensation reaction. This results in a sol with a low viscosity, which effects the stability and mechanical strength of the silica nanoparticles. Therefore, the molar ratio of $\text{H}_2\text{O}:\text{Si}(\text{OR})_4$ in the gelation should at least be 2:1 to approach the minimum hydrolysis degree of the alkoxide required for gelation.¹⁶ At higher r values > 4 , due to the presence of excess water, polymerization is slower than condensation, producing cyclization and enhancing the siloxane bond formation within the particles.²⁵ For r values between 6 and 10, due to the presence of optimum amount of water, hydrolysis and condensations reactions proceed systematically yielding lower density and transparent gels.²⁵

The studies of mutual influence of water content and pH can be summarized as follows: at molar ratios of water/silicon of 4 and $\text{pH} < 2$, the condensation of completely hydrolyzed species can be characterized by reaction limited cluster-cluster aggregation (RLCC) producing weakly branched

structure. Under acidic and low water conditions, where the ratio of $H_2O:Si$ is less than 4, the condensation of the incompletely hydrolyzed species is also expected to occur by RLCC aggregation. Due to the reducing effect of OR groups on the functionality of the condensing species, the structures will be weakly branched. At pH 7 and high water content, the growth of gel networks occurs primarily by reaction limited monomer-cluster aggregation (RLMC) and compact structures will be formed.¹⁶ Hence, water to silica ratio is an important parameter that needs to be carefully controlled in the sol gel process to obtain the desired properties of the sol gel material.

2.4.2 Effect of precursor concentration

The bulk density of silica gels are gradually enhanced with increasing precursor concentrations in the initial and aging stages of sol gel processing.¹⁶ At higher concentrations of precursors, condensation is favored due to high amount of solvent that separates the reacting species from each other. At lower precursor concentrations, the hydrolysis reaction is favored rather than the polymerization and hence the polymer size decreases. The precursor concentration has the most dominant effect on the density and the pore size of the final sol gel matrix.²⁶ A high precursor concentration can result in excessive crosslinking and aggregation of gel particles, leading to decrease in transparency and stability of the final sol gel matrix. On the other hand, a low precursor concentration can improve the transparency and stability of sol gel but can also result in lower mechanical strength and a reduced degree of network formation. For example, using TEOS as silicon precursor and ethanol as solvent, clear sols and gels are only formed above two molar ratios of EtOH/TEOS.²⁵ Higher molar ratios of EtOH/TEOS result in lower density,

greater porosity of the aerogels and better transparency. The compact aerogel structures can be characterized by particles of smaller sizes, low pore volume, relatively low specific surface area, and two partly closed pores.²⁶

2.4.3 Effect of pH

The pH of the reaction solution plays a critical role in controlling the rate of hydrolysis and condensation reactions and can greatly influence change in size, shape, and distribution of the resulting silica nanoparticles.^{14, 16, 20, 27} The pH of the reaction also determines the stability of the silica particles as a high pH may lead to the formation of large and unstable particles leading to aggregation, while a low pH may result in a small and highly reactive particles that are prone to aggregation.

Under acidic conditions, hydrolysis involves protonation of the alkoxide group (silica precursor), increasing its leaving group character, followed by nucleophilic attack by water. Under alkaline conditions, hydrolysis proceeds via nucleophilic attack on the silicon atom by the hydroxide ion, forming a negatively charged five coordinated intermediate, followed by the displacement of an alkoxide ion.²⁸ Inorganic acids are considered more effective as catalysts than bases because the silanol groups forming during the reaction can neutralize basic catalysts. The lowest reaction rate for hydrolysis is at pH 7 and for condensation is ~4. Under acidic conditions, (pH <5), the hydrolysis is favored, and condensation reactions are limiting. The acid-catalyzed gelation is primarily characterized by a cluster growth model.^{14, 20} The kinetics of aggregation may be limited by the rate of condensation (e.g., reaction limited cluster aggregation model RLCA)^{20, 24} or by the rate of diffusion (e.g., diffusion limited cluster aggregation model DLCA)²⁹. Above pH 2, the rate of hydrolysis

reaction reduces, and the rate of condensation will be higher, the number of siloxane bonds (-Si-O-Si-) is grows. The growth mechanism changes from cluster to cluster to monomer-cluster. As a result, branched structures are formed which can be characterized by increasing pore volume and lowering specific surface area.¹⁶ Under basic conditions, the hydrolysis and particle nucleation processes are rate determining and the condensation processes are dominant. Hence, the molecules of precursors are aggregated to fewer, larger, and denser particles than acidic conditions. Condensation of clusters with each other is relatively unfavorable.²⁰ More branched networks are obtained under basic conditions compared to the more chain-like network under acidic conditions. The reason is that the condensation reaction on the network silicon atoms [Si-(O-Si)₂₋₃], which are favored at high pH and reactions on the terminal atoms [Si-(O-Si)₁] have important role at low pH. The pH dependence of the gelling time shows the apparent condensation rate to have a maximum at intermediate pH 4.5 and a minimum at pH 2.5 Strongly basic conditions result in non-gelling systems.³⁰

In summary, pH of the solution is a critical parameter in the sol gel synthesis of silica nanoparticles. Considering the effect of pH on sol gel synthesis, it is possible to optimize the reaction conditions and tailor properties for wide range of applications.

2.4.4 Effect of solvents

Solvents are categorized in terms of polarity and capability to bind and release the protons (protic and aprotic). The polarity, viscosity, and the protic or non-protic behavior of the solvent influences the reaction rates and thereby, the structure of the final product. Solvents which have hydrogen bonding interaction

with the OH⁻ ions or H⁺ reduce the catalytic activity under basic and acidic conditions, respectively. Therefore, aprotic solvents that do not hydrogen bond to hydroxyl ions have the effect of making hydroxyl ions more nucleophilic, whereas protic solvents make hydronium ions more electrophilic.¹⁴ Hydrogen bonding may also influence the hydrolysis mechanism. For example, hydrogen bonding with the solvent can sufficiently activate weak leaving groups to realize a bimolecular, nucleophilic (S_N2-Si) reaction mechanism.¹⁴

In the condensation mechanism, protic solvents are expected to slow down the reaction of the base catalyzed condensation to promote acid catalyzed condensation, while aprotic solvents show the opposite effect. The typical polar and protic solvents used in sol gel synthesis are H₂O and alcohols. A typical example of a polar, non-protic solvent is acetone. THF, dioxane, and cyclohexane can be used as non-polar solvents.¹⁶ The polar and protic solvents stabilize the polar siliceous species such as [Si(OR)_x(OH)_y]_n by hydrogen bonding. The non-polar solvents may be used for organoalkoxysilanes or incompletely hydrolyzed systems.¹⁴ The availability of labile protons is a major factor while taking into consideration the reversibility of reactions i.e., re-esterification (reverse of Eq. 1) or siloxane bond alcoholysis or hydrolysis (reverse of Eqs. 2 and 3). Aprotic solvents do not participate in reversible reactions because they lack sufficiently electrophilic protons and are unable to be deprotonated to form sufficiently strong nucleophiles (e.g., OH or OR) necessary for these reactions.

Applying a mixture of solvents can finely regulate the structures in the gelation procedures. For example, aerogels prepared in pure water from silicon alkoxide precursors contain primary particles with smooth surfaces.¹⁶ In the

presence of methanol-water mixtures, the primary particles will be monodisperse and form an aggregated network.³¹ The presence of low dielectric constant solvents such as benzene, toluene or anisole in varying ratios with methanol or other alcohols leads to rapid gelation and a formation of mesoporous materials with fibrous, open web-like structures with high surface area and large pore volume.^{16, 32} The presence of high dielectric constant solvents such as acetone, acetonitrile, DMF, DMSO have no such effect.³³ The density of final aerogel can be controlled by varying the ratio of solvent to precursor in the initial solutions. The amount of solvent defines the pre volume within the silica network. Thus, a high solvent to precursor ratio could result in a low density silica aerogel, similar to the effect of excess water content.¹⁶

2.4.5 Effect of catalyst

The hydrolysis reaction of sol gel usually involves a catalyst. The activity of the catalyst is pH dependent as the catalyst used is typically an acid or a base. HCl, H₂SO₄, HNO₃, HF and acetic acid are some of the commonly used acids whereas NH₃ or NaOH are commonly used bases. It is well known that the catalysts greatly influence the physical properties of silica. In the case of acid catalysis, a dense gel with small pores is produced whereas in base catalysis, a highly cross-linked particles which eventually link to form a network with large pores is produced.

Sol gel catalysts without any acidic or basic features are usually nucleophiles. The nucleophilic catalyst generates 5-coordinated silicon intermediates, which are more reactive than the 4-coordinated silicon atoms. Incomplete hydrolysis results if the catalyst is not used in sufficient amounts.

On the other hand, complete hydrolysis yields a clear and transparent solution.¹⁶

2.5 Encapsulation of biospecimens via sol gel process

Physical entrapment of proteins in a sol gel matrix preserves protein structure and functionality and protects the protein from physiochemical perturbations. It is mainly due to the sol gel matrix “cages” which provide a more rugged environment to the dopant.³⁴ In order to encapsulate the proteins or nucleic acids, several parameters should be taken into consideration (Table 1-1). First, the sol gel method must be aqueous since these are generally required to maintain the biological function of biomolecules. Second, the polymerization reaction must be compatible with pH and ionic strength values that are required for protein function (pH 4-10, ionic strength ranging from 0.01 to 1.0 M). Third, the process must be carried out at room temperature or ambient settings to preserve the native conformation of the biomolecules. Fourth, the material must have a pore size that is sufficiently small to prevent leaching of the biospecimen, but large enough to allow smaller analytes to enter the matrix with ease. Fifth, the material properties or the precursors used for sol gel encapsulation should be tunable to allow for modification of the internal environment to maximize the activity of encapsulated biospecimen. Sixth, it should be possible to form the final material such that it is optically transparent or electrically conductive to allow spectroscopic measurements. Entrapped proteins typically reside in pores that are of a similar size to the protein, thus it is important to determine whether entrapped proteins maintain native conformation during and post entrapment, and whether they are able to undergo changes in conformation once entrapped. The conformational motions

of entrapped biospecimens are examined by absorbance, fluorescence, resonance Raman and other spectroscopic techniques.

Table 2-1. Parameters for sol gel encapsulation

| Parameters | Requirements |
|-------------------------------|---|
| Method | Aqueous sol gel method |
| Compatibility | Polymerization reaction must be compatible with pH (4-10) and ionic strength (0.01-1.0 M) values |
| Temperature | Room temperature or ambient settings |
| Pore Size | Sufficiently small to prevent leaching, but large enough to allow smaller analytes to enter |
| Material Properties | Tunable to modify internal environment for maximizing activity of encapsulated biospecimen |
| Optical/Electrical Properties | Optically transparent or electrically conductive for spectroscopic measurements |
| Conformational Analysis | Ability to maintain native conformation of entrapped proteins and undergo conformational changes |
| Spectroscopic Techniques | Absorbance, fluorescence, resonance Raman, and other spectroscopic techniques for conformational analysis |

Conformational studies of multiple entrapped proteins such as human serum albumin (HSA), bovine serum albumin (BSA), and monellin have indicated that such proteins tend to retain a native conformation upon encapsulation although some proteins such as myoglobin, may undergo

substantial conformational changes upon encapsulation.³⁵ This denaturation has been attributed to the presence of alcohol from the hydrolysis reaction. Moreover, aging of sol gel matrix can induce significant structural changes in entrapped proteins.^{35, 36} Despite the successes over the last few decades, conventional sol gel approaches are inherently complex and require the use of various additives like acids, bases, and alcohols that may be detrimental for biospecimen storage and hence require an alternative method to carry out encapsulation.

2.6 Limitations of conventional sol gel approaches

While conventional sol gel techniques have been shown to be useful in many applications, some drawbacks remain to be overcome. The limitations of conventional sol gel techniques are listed as follows:

1. Most sol gel techniques use high concentrations of silica precursors (typically 25-50%) as the techniques always strived to obtain intact immobilization in a glass like matrix, to restrict the motion of biospecimen, similar to that of freezing.
2. The release of alcohol during the hydrolysis-condensation of silicon alkoxides has been considered an obstacle, due to its potential denaturing activity on the encapsulated biospecimens.
3. Complexity of processing conditions: The sol gel process can be complex and requires precise control over the processing conditions such as temperature, pH, concentration of precursors to achieve optimum matrix for encapsulation.

4. Expensive process: Conventional sol gel approaches can be expensive especially for large scale production due to the costs associated with the precursors, solvents, and processing equipment.
5. Use of high concentrations of silica precursors make the final sol gel a glass like matrix which is less transparent hence difficult to analyze samples spectrophotometrically.

2.7 Introduction to BioCaRGOS

In an effort to reduce the dependence on conventional sol gel techniques for preserving biospecimens, Gupta et al. developed a novel CVD based sol gel route where a solution containing any biomolecule of choice is simply exposed to vapors of silica precursor, TMOS at room temperature for 1 to 12 h in a simple petri dish (Figure 2-1). During this process, TMOS evaporates and hydrolyzes at the interface of the aqueous solution. It then diffuses into the aqueous solution and results in encapsulation of the biomolecule. This process was extremely successful and was proven to work for a variety of proteins, chlorosomes, microbial cells, and liposomes. A key observation made during the CVD process was that low concentration (>10% silica) can preserve the biospecimen. If the concentration can further be decreased, then the release of biospecimen is feasible. This triggered the research in the direction of a process that is compatible with clinical settings that would require minimal expertise and utilizes low concentration of silica precursor.

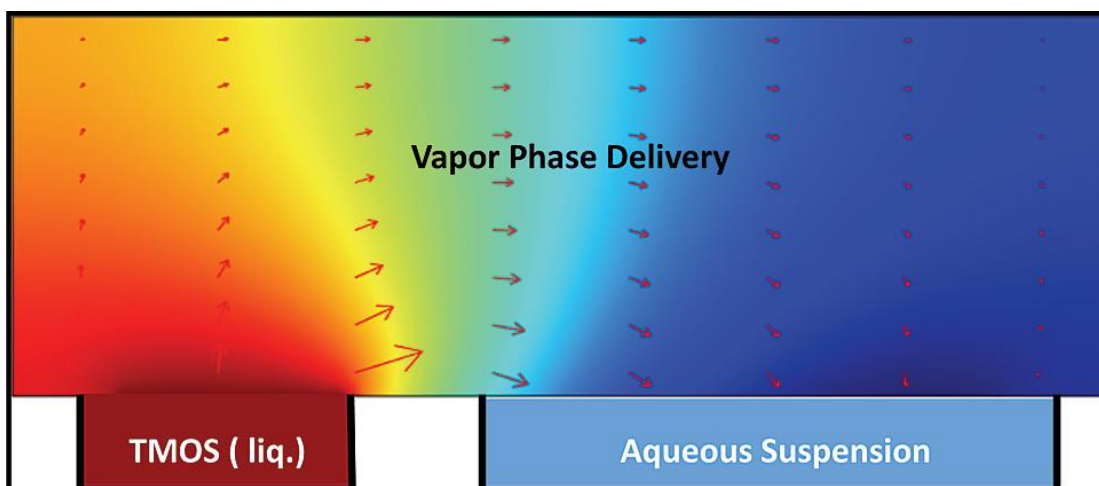


Figure 2-1. Schematic for CVD process for immobilization.

Further studies by Gupta based on the sol gel principle utilized a mixture of the silica precursor TMOS in water that was hydrolyzed in a standard benchtop microwave. Upon hydrolysis, orthosilicic acid was obtained as confirmed by Raman spectroscopy. The Raman spectra also confirmed the complete hydrolysis of silica precursor within one minute. Dynamic light scattering (DLS) was used to measure the hydrodynamic size of the resulting solution, which was less than 2 nm, conforming the formation of silica monomer. During this process, there was a slight amount of methanol that was formed as a result of hydrolysis reaction, which should be removed prior to encapsulation of any biospecimen as it can cause denaturation. Upon addition of an aqueous solution containing the biospecimen of interest, immediate condensation was observed as the result of the transformation of $\text{Si}(\text{OH})_4$ to $-\text{Si}-\text{O}-\text{Si}$ linkages, with a hydrodynamic size of around 70 nm and zeta potential (mV) of -22.07 ± 1.01 . The concentration of silica precursor can be precisely controlled and can be optimized based on the biospecimen of interest.

The key advantages of BioCaRGOS over conventional sol gel techniques are as follows: i) This process is commercially feasible and can be

scaled up as per needs; ii) The entire process does takes less than five minutes to synthesize BioCaRGOS; iii) No additives such as acids, bases, and alcohols are required to carry out the synthesis; iv) Long term storage can be achieved at room temperatures; v) Use of low concentration of silica precursors prevent the formation of glass like matrix which is otherwise deleterious for biospecimen stability; vi) This process is compatible with downstream process and due to the transparent matrix, which is compatible with spectrophotometric techniques; vii) The process is extremely cheap as compared to conventional approaches.

With these wide range of benefits of BioCaRGOS, the remainder of the dissertation will focus on the demonstration of its application to stabilize various proteins and nucleic acids at ambient and room temperatures, the challenges faced, and how they have been overcome to make this technology compatible with multiple downstream processes.

CHAPTER 3

BIOCARGOS: CAPTURE AND RELEASE GELS FOR OPTIMIZED STORAGE OF PROTEINS AND NUCLEIC ACIDS AT AMBIENT TEMPERATURES

3.1 Introduction

The stabilization of protein-based biologics and nucleic acids that serve as biomarkers or therapeutics is important for the diagnosis and treatment of a variety of diseases as introduced in Chapter 1. This typically requires low temperatures (≤ 4 °C) resulting in a dependence on cold storage techniques and expensive transportation network. Additionally, protection from other environmental stresses such as pH and sunlight, in addition to temperature, are often required. To overcome these constraints, a range of alternative techniques have been used such as addition of stabilizing agents, immobilization of proteins onto surfaces, and encapsulation of biospecimens into hydrated matrices.³⁷

Encapsulation in silica sol-gel has particularly been explored due to its relative simplicity, biocompatibility and the ability to control its relative water content and salinity.³⁸⁻⁴⁰ As described in detail in Chapter 2, sol gel silica is a porous and amorphous material, which when added to buffers containing biospecimens allows for immobilization. Although the sol gel process has developed significantly over the years and is widely used, there are certain

limitations to the conventional techniques making them hardly applicable to clinical setting. These include long processing times, high temperatures for sol gel synthesis, difficulties in controlling particle size and distribution, compatibility issues, and costs. Additionally, most sol-gel techniques are marred with a critical issue regarding the release of biospecimen from the gels after long-term encapsulation. The primary reason for the low recovery of biospecimen is the high concentrations of silica precursor (typically 30-50 %) used to obtain intact immobilization in a glass like matrix that restricts molecular motion.

In this chapter, we have engineered capture and release gels for optimized biospecimen storage (BioCaRGOS). This system utilizes minimal concentrations of silica precursors to stabilize the biospecimen and microwave synthesis to provide a rapid and reversible system to store and release biological samples. The key advantages of BioCaRGOS over conventional sol gel techniques are i) a clinically compatible process with hydrolysis taking place in less one minute; ii) the minimal presence of methanol; iii) the effective long-term storage of biospecimens; and iv) an easy post encapsulation recovery method.

To encapsulate a biospecimen in a sol gel matrix, several factors must be taken into consideration such as pH, ionic strength, concentration of silica precursor, and temperature. Hence, in this chapter we have demonstrated the effects of each of these factors by evaluating the stability of a simple protein hemoglobin (Hb) as a proof of concept. Hemoglobin is a protein that is found in red blood cells and is responsible for transporting analytes such as oxygen throughout the body and plays a significant role in the regulation of the blood

pressure. Hemoglobin is an ideal model protein to investigate the preservation of structural integrity under environmental stimuli (heat, mechanical excursions, nuclease/protease/microbial contamination). It has structural diversity with a complex four protein-chain frameworks: each having a heme group and metal center (i.e., iron) in the central cavity. It is also versatile, flexible protein that can be used to study conformational changes and protein-protein interactions.

To carry out preliminary studies as a proof of concept for BioCaRGOS technology, we investigated the room-temperature stability in nearly aqueous BioCaRGOS formulations under 10 v/v % concentration that preserve the metalloprotein's native structure, homogeneity, activity, and reproducibility over long-term storage. Using 5 v/v % BioCaRGOS, greater than 95% of native hemoglobin structure was preserved at room temperature for a period of 33 days. Such strong stability of hemoglobin exhibited in BioCaRGOS is attributed to the scientific premise of isoelectric point (pI) of proteins.

The isoelectric point of a protein is the pH at which the net charge on any biospecimen is zero. At this pH, the number of positively charged amino acids is equal to the number of negatively charged amino acids making the protein less likely to interact with charged molecules in the solution.⁴¹ This results in increased stability of the protein in a narrow pH range near the pI. However, outside this range, the protein can be vulnerable to electrostatic interactions with other charged molecules causing degradation or denaturation. For example, hemoglobin has a pI of 6.8 and therefore, the protein will have a net positive charge at pH higher than its isoelectric point (in this study pH 8.2). Therefore, it stays soluble within negatively charged silica particles whose pI is ~3.0. The hemoglobin stability in BioCaRGOS is therefore attributed to two

main factors. First, the electrostatic repulsions between negatively charged hemoglobin and silica particles drive the protein stability within these colloidal dispersions. Second, immobilization of biospecimens imparted by BioCaRGOS stabilizes hemoglobin due to restricted mobility.

Another important factor to be considered during the storage of biospecimens is the role of electrolytes. Electrolytes are ions such as sodium, potassium, and chloride that are present in solution and affect protein stability by influencing their charge and hydration state. At high concentrations, electrolytes can interfere with the interactions with proteins or nucleic acids and destabilize the structure. On the other hand, at low concentrations, electrolytes stabilize the protein or nucleic acid structure by counteracting the effects of denaturants and maintain proper hydration state.

In this chapter, to evaluate these factors, we have investigated microRNA-21 (miRNA 21), which is a potential biomarker for cancer diagnosis and prognosis. miRNAs are an important class of biomarker for autoimmune diseases and human carcinogenesis.⁴² However, these miRNA molecules are very labile and sensitive to degradation by ribonucleases, which are enzymes that digest the RNA. In addition, various factors such as pH, temperature, and the salt concentration of storage buffer (ionic strength) can affect the overall stability. Hence, in an effort to minimize the degradation caused by the factors described above, in this chapter, we have investigated the effect of variation in pH and ionic strengths on stability of miRNA 21 by encapsulating in BioCaRGOS matrix. In the BioCaRGOS samples, a remarkable resistance against nuclease digestion was observed by demonstrating ~99% integrity of miRNA 21 in

presence of RNase A. We have also demonstrated efficient preservation of miRNA 21 up to 82 days at temperatures of 4, 25, and 40 °C.

3.2 Experimental

3.2.1 Materials

For the hemoglobin experiments, tetramethyl orthosilicate (TMOS, > 98% purity), freeze-dried hemoglobin, polyethylene glycol (2 kDa), sodium phosphate monobasic, sodium phosphate dibasic, 15.0 mL centrifuge tubes and UV-Vis cuvettes were purchased from Sigma Aldrich (St. Louis, MO). UV-Vis absorption spectra were collected using a UV-vis spectrometer (Varian Cary 50 BIO UV, Agilent Technologies, Santa Clara, CA). Raman spectra were acquired on Reva Educational Raman platform (Hellma, Plainview, NY).

For the miRNA 21 experiments, TaqMan microRNA assay (hsa-miR-21; catalog: 4427975), TaqMan® MicroRNA Reverse Transcription Kit (catalog # 4366596), Tris EDTA buffer, Bovine pancreatic RNase A, ethidium bromide, sterile 15.0 ml centrifuge tubes, tetramethyl orthosilicate (TMOS) and sodium chloride were purchased from Sigma Aldrich (Saint Louis, MO, USA). Nuclease free water was purchased from New England BioLabs (MA, USA). miRNA21 (5'-CAA CAC CAG UCG AUG GGC UGU-3') was purchased from IDT technologies. qPCR tubes were purchased from USA scientific (California, USA) and 96 well plates were purchased from Thermo Fisher Scientific (MA, USA).

The reverse transcription thermal cycle was performed at Eppendorf thermocycler (NY, USA). The Dynamic light scattering measurements (DLS) were acquired on a Zetasizer (Zetasizer Nano ZS90, Malvern Instruments Ltd, Westborough, MA, USA). The zeta potential measurements were acquired on

latter samples using a NanoBrook Zeta PALS Zeta Potential Analyzer (Brookhaven Instruments, Holtsville, NY, USA). Fluorescence measurements were acquired on Molecular Devices SpectraMax M2 plate reader (San Jose, California, USA) and modulus fluorimeter's green module with emission range: 580– 640 nm (Sunnyvale, California, USA). FT-IR spectra were measured with the FT-IR spectrometer (PerkinElmer Spectrum 100) with universal ATR (attenuated total reflectance) sample accessory. Raman spectra were acquired on Reva Educational Raman platform (Hellma, Plainview, NY).

3.2.2 BioCaRGOS synthesis

For the hemoglobin studies the following procedure was followed. A 10.0 v/v % TMOS stock-solution was prepared in de-ionized water and transferred to a 40.0 mL glass test tube, screw capped and hydrolyzed via microwave for thirty seconds. Post microwave, the screwcap was removed to evaporate the volatile byproduct (i.e., methanol) of the BioCaRGOS synthesis. This BioCaRGOS stock solution was allowed to cool to room temperature. After room temperature was reached, appropriate amounts of BioCaRGOS were added to 4.0 mL cuvettes to create final concentrations (v/v %) of 0, 1, 2.5, 5 and 7.5 respectively. Phosphate buffer (0.5 M pH 8.2) was added to constitute the remainder of the 3 mL solution, as well as 0.03 mL of 1.0 w/v % hemoglobin. For the miRNA21 studies the process remains same except tris EDTA buffer and 0.1 M NaCl is added to hydrolyzed TMOS solutions to constitute BioCaRGOS, which was further added to ~500 nM miRNA 21 solution to encapsulate.

3.2.3 Storage of hemoglobin in BioCaRGOS

Samples of BioCaRGOS–hemoglobin [(0.0–7.5) v/v % TMOS; 0.01 w/v % hemoglobin; 0.5 M phosphate buffer, pH 8.2; 3.0 mL] solutions were formulated in 4.0 mL UV-Vis cuvettes, capped and stored for a desired amount of time. The UV-Vis spectra of stored BioCaRGOS–hemoglobin [(0.0–7.5) v/v % TMOS; 0.01 w/v % hemoglobin; 0.5 M PB, pH 8.2; 3.0 mL] solutions were measured on 0, 2, 6, 9, 13, 18, 20, 24, 27, 31, 33 days at room temperature, to validate integrity of hemoglobin. For long term studies, the optimized BioCaRGOS concentration of 5.0 v/v % was used, while keeping the rest of the formulation parameters fixed [0.01 w/v % hemoglobin; 0.5 M PB, pH 8.2; 3.0 mL]. Samples were measured over a period of 210 days to validate integrity of hemoglobin over the prolonged room-temperature and refrigerated storage conditions.

3.2.4 Release of hemoglobin

Polyethylene glycol (65.0 mM, 1.0 mL) was added to 3 mL BioCaRGOS containing hemoglobin for facile re-dissolution of the silica-dispersions. After vortexing the sample for 30 seconds, 1.0 mL of the resulting solution was pipetted to a 15.0 mL centrifuge tube. This process was completed until a total of 5.0 mL PEG had been added to each sample, after which the remainder of the dissolved BioCaRGOS was pipetted into the 15.0 mL centrifuge tube. Next, 3.0 mL of the dissolved BioCaRGOS was transferred to two 1.5 mL centrifuge tubes for each sample, after which they were centrifuged for 13 minutes at 10000 rpm. The supernatant hemoglobin solution at the top of each tube was pipetted into the corresponding UV-vis cuvette, where UV-Vis spectroscopy was used to determine the concentration and structure of native hemoglobin.

3.2.5 Evaluation of BioCaRGOS by Raman spectroscopy

The Raman spectra was performed on hydrolyzed TMOS (0.0–10.0) v/v % BioCaRGOS with buffer [(0.0–10.0) v/v % TMOS; 0.5 M PB, pH 8.2; 3.0 mL] and BioCaRGOS with hemoglobin [(0.0–7.5) v/v % TMOS; 0.01 w/v % hemoglobin; 0.5 M PB, pH 8.2; 3.0 mL] using a Reva Educational Raman platform (Hellma, Plainview, NY, USA). The laser power of 450.0 mW and current 959.0 mA was optimized to analyze the samples. The laser temperatures (diode = 30 °C; case = 24.4 °C) and spectrometer temperature (23.1 °C) were optimized for collecting the Raman spectra.

3.2.6 Evaluation of gel formation using IR spectroscopy

FT-IR spectra were measured with an FT-IR spectrometer (PerkinElmer Spectrum 100) with universal attenuated total reflectance (ATR) sample accessory. The BioCaRGOS samples with different concentration were placed on diamond/ZnSe crystal and the spectra were recorded over the range of 500 – 4000 cm^{-1} .

3.2.7 Degradation of miRNA 21 with enhancement of RNase A concentration

The degradation of miRNA21 with respect to change in the concentration of bovine pancreatic RNase A was monitored at pH 7.5 (0.05 M Tris buffer) containing 0.1 M NaCl. The miRNA21 and EtBr solutions were mixed and incubated for 30 min. A 2.7 ml of pH 7.46 'BioCaRGOS Buffer' [1 : 1 : 1 volume ratio of (A) BioCaRGOS (1.5 wt/v %); (B) 0.05 M Tris buffer with 0.1 M NaCl/pH 7.5 and (C) nuclease free water; pH 7.46] or 'Control Buffer' [0.05 M Tris buffer with 0.1 M NaCl; pH 7.5] were mixed with 0.2 ml (1 mg ml^{-1} RNA with 0.077 mM EtBr) and incubated for 100 s. These samples (with or w/o BioCaRGOS) were

added into a respective well in a 96-well reaction plate and mixed gently to bring solution to the bottom of the wells. To the 96-well plates, 1–120 μL of 2.0 μM RNase A were added with the final volume to 200.0 μL and the change in fluorescence intensity monitored.

3.2.8 Reverse transcription

Reverse transcription (RT) master mix was prepared using the TaqMan MicroRNA Reverse Transcription Kit components before preparing the reaction (Table A1†). The RT components were thawed on ice and 5X RT primers were vortexed. The 10 ml of Master mix – 5X RT Primer was pipetted into a respective well in a 96-well reaction plate using 200 μL 96-well plate. The 5.0 ml of miRNA samples (with or w/o BioCaRGOS) were added into a respective well in a 96-well reaction plate, cap-sealed and mixed gently to bring solution to the bottom of the wells. The 96-well plates were further incubated on ice for 5 minutes and transferred to Eppendorf thermocycler at 85 °C for 65 minutes.

3.2.9 Real-time qPCR amplification

A 8.67 μL portion of master mix made for each miRNA 21 (with or w/o BioCaRGOS) was pipetted into a 100 μL PCR 96-well reaction plate respective well, (Table S5†). The 1.33 μL of RT product was transferred into respective 96-well reaction plate well, cap- sealed and gently mixed to bring solution to the bottom of the tube before real time qPCR amplification.

3.3 Results

3.3.1 UV-vis characterization of hemoglobin content within the BioCaRGOS formulations.

Purified proteins in their native state possess a well-defined structure depending on the conditions of their storage. To maintain this native structure,

it is necessary to store the protein under optimum conditions that can minimize the exposure to heat, pH variation, and salt concentrations of buffer solutions in which they are preserved. Therefore, we have investigated the thermal stability (~25 °C) and mechanical handling stability (mixing, vortexing, shaking) of hemoglobin with BioCaRGOS by monitoring the absorbance band of the heme groups. UV-Vis spectra were used to detect loss or alterations in the heme as it is an effective indicator of changes in primary and secondary structure.^{43, 44} In addition, loss of the heme group and the resulting changes in the secondary structure are indicative of alteration of tertiary structure conformation, as each of the subunits are integral to the tertiary structure of the molecule.⁴³ Therefore, in this chapter, we have utilized hemoglobin as a model protein for our studies.

The BioCaRGOS process is based on sol gel technology and utilizes a standard benchtop microwave for rapid hydrolysis of silica precursor (Figure 3-1a). Typically, TMOS is hydrolyzed in an aqueous solution by imparting energy from a benchtop microwave for 30 s. The key hydrolysis reaction is highlighted in Figure 3-1b. TMOS has four hydrolyzable groups and the reaction with water results in the formation of orthosilicic acid [Si(OH)₄] and methanol as the byproduct. The resulting solution is allowed to rest for 5 minutes to reach equilibrium at room temperature and to evaporate some of the methanol. A known concentration of BioCaRGOS is then added to hemoglobin (in buffer), resulting in condensation of the hydrolyzed silica precursor (Figure 3-1).

The Raman spectra of 5 v/v % silica precursor (TMOS) under pre-hydrolysis and post-hydrolysis (microwave for 30 s) conditions and after condensation (evaluated after 7 days) are shown in Figure 3-1c. The theoretical

peak positions of TMOS precursor, intermediates, silicic acid/dimers, and methanol are expected at 640 – 650, 673 – 725, 750 – 780, and 1020 cm^{-1} , respectively.⁴⁵ Experimentally, we observe a peak at 646 cm^{-1} for 10 v/v % TMOS/water solution prior to hydrolysis indicating the presence of intact $\text{Si}(\text{OCH}_3)_4$. Upon ~30 s microwave exposure, the $\text{Si}(\text{OCH}_3)_4$ peak at 646 cm^{-1} disappears and an increase in $\text{Si}(\text{OH})_4$ and methanol peaks was observed at 750 cm^{-1} and 1020 cm^{-1} . Absence of intermediate peaks for partially hydrolyzed TMOS species at 673, 697, and 725 cm^{-1} indicate completed hydrolysis of $\text{Si}(\text{OCH}_3)_4$.⁴⁵ The Raman spectra of serial-diluted TMOS (0.1 – 5.0) v/v % solutions before and after TMOS hydrolysis under microwave irradiation are shown in Figures A1 – A3. Upon addition of the buffer containing hemoglobin, the intensity of methanol peak decreases due to dilution and we also observe emergence of a peak at 980 cm^{-1} , which arises due to the presence of phosphate buffer (Figure A4). The resulting solution undergoes gelation depending upon the concentration of the precursor, which were stored for further analysis. We further performed IR analysis to monitor the formation of Si–O–Si and Si–OH bonds in the gels. IR spectra of the silica gels 0.5, 1, 2.5, 5 and 7.5 v/v % Bio CaRGOS are shown in (Figure A5). The wide band at 1100 – ~1250 cm^{-1} is generated by contribution of the vibrational modes of –Si–O–Si– and –Si–OCH₃. At 1015 cm^{-1} the formation of CH₃OH and Si–OH are also observed. Peak intensity increases as the concentration of silica precursor is increased thus determining the extent of gelation.

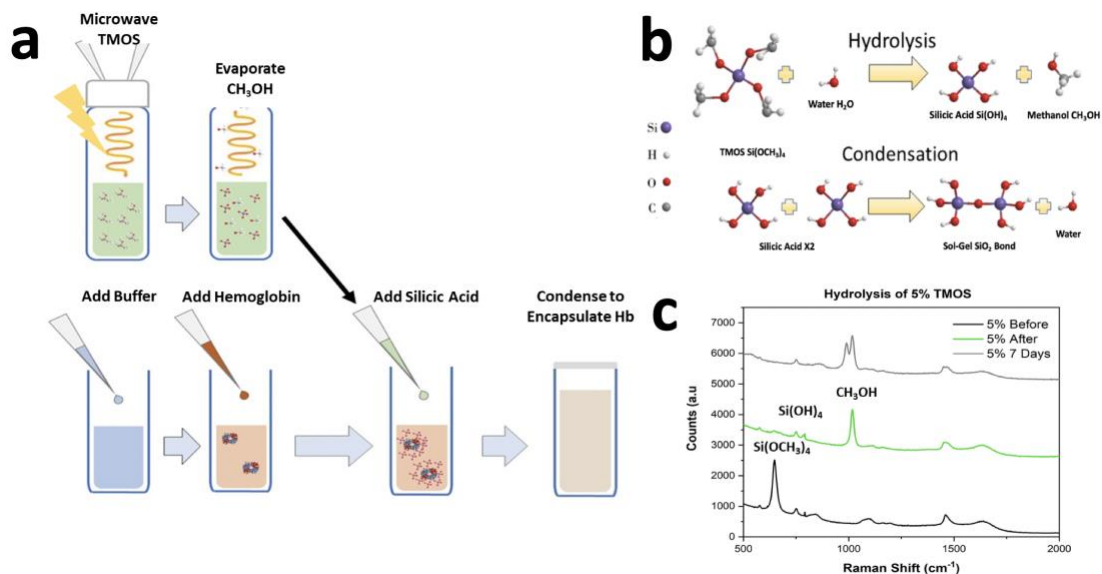


Figure 3-1. Synthesis and Raman characterization of BioCaRGOS formulations. (a and b) Schematic of BioCaRGOS formulations and encapsulation of hemoglobin for long-term room-temperature storage and (c) complete hydrolysis of 5.0 v/v % tetramethyl orthosilicate (TMOS)

The complete self-sterile immobilization of any biospecimen can be achieved in less than 10 minutes utilizing only one chemical and a benchtop microwave. The process is extremely compatible with clinical settings and even for field operations. The integrity of hemoglobin in BioCaRGOS was evaluated using UV-vis spectroscopy. UV-vis spectroscopy is a rapid and routinely used method to validate structural stability of hemoglobin ($\lambda = 406 \text{ nm}$: heme group). A sharp UV-vis band ($\lambda = 406 \text{ nm}$) of the prosthetic heme group ($\text{C}_{34}\text{H}_{32}\text{O}_4\text{N}_4\text{Fe}$) is observed in both aqueous hemoglobin solutions (0.01 v/v %; 0.5 M PB; pH 8.2) and in Bio CaRGOS (1.0–7.5) v/v % formulations immediately after immobilization (Figure 3-2). This absorbance band indicates excellent initial stability of hemoglobin in both the BioCaRGOS and control samples. The intact

absorbance band shown in Figure 3-2 also supports that silica condensation and the presence of the methanol by product do not affect hemoglobin nativity.

Multiple BioCaRGOS + hemoglobin (0.01 wt/v %) samples were evaluated over a period of one month. Relative to control hemoglobin solutions (i.e., w/o BioCaRGOS), a two-fold and three-fold improvement in hemoglobin stability was observed in 1.0 v/v % and 2.5 v/v % BioCaRGOS samples, respectively. This demonstrates a BioCaRGOS concentration dependent trend in determining the physical and chemical stability of hemoglobin. Nearly ~99% stability of the heme group is observed up to three weeks and ~95% stability up to 33 days at room temperature for 5 v/v % and 7.5 v/v %, respectively (Figure 3-2). With this data in hand, BioCaRGOS concentrations of 5.0 – 7.5 v/v %, were determined to be ideal for storing hemoglobin under room temperature and mechanical handling (i.e., mixing, vortexing) conditions. On the other hand, control samples (i.e., w/o BioCaRGOS) demonstrated significant decrease in the heme group absorbance by ~10% in one week, ~20% in three weeks, and nearly ~63% in four weeks (Figure 3-2).

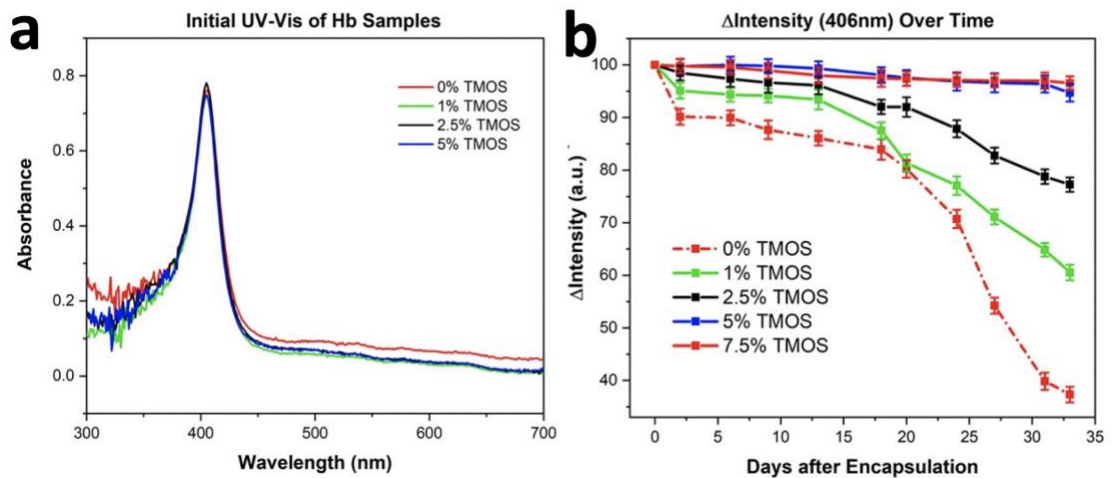


Figure 3-2. UV-vis analysis of hemoglobin content within BioCaRGOS formulations. (a) Incremental increase in the hemoglobin stability with incremental increase in BioCaRGOS concentrations (0–5.0) v/v %. An unaltered UV-vis absorbance band (406 nm) of heme group of hemoglobin framework is observed in BioCaRGOS formulations (5.0 v/v %). (b) Hemoglobin stability with incremental increase in BioCaRGOS concentrations (0–7.5) v/v %. An unaltered UV-vis absorbance band (406 nm) of heme group in hemoglobin framework is observed in BioCaRGOS formulations (5.0 and 7.5 v/v %).

Prolonged storage at low temperatures preserves the quality of biospecimens, inhibits the growth of bacteria, and extends shelf-life. Hence, to investigate the effects of BioCaRGOS at low temperatures, we evaluated the long-term stability of hemoglobin at 5 °C and 23 °C in a similar format to the 33-day hemoglobin storage study described above. As shown in Figure 3-2, BioCaRGOS formulations (5.0 & 7.5 v/v %) demonstrated exceptional hemoglobin storage capabilities over 1 month storage interval. However, the 5.0 v/v % formulation was preferentially chosen over 7.5 v/v % formulation towards investigating hemoglobin integrity over 210 days (7 month) to facilitate

easier biospecimen passage/recovery through BioCaRGOS matrices and reduce cost per sample.

3.3.2 Long term storage of hemoglobin in BioCaRGOS

The optimized BioCaRGOS [(5.0 v/v %) TMOS; 0.01 w/v % hemoglobin; 0.15 M PB, pH 8.2; 3.0 mL] solutions demonstrated an unprecedented hemoglobin stability (~96%) up to 7-month period at 5 °C, under the non-sterile conditions. During prolonged refrigeration, the control samples (0.01 w/v % hemoglobin ; 0.15 M PB; pH 8.2) also displayed robust stability (~96%) up to the 40-day period, demonstrating the short-term stabilizing effect of refrigeration as well as the phosphate buffer environment on control group hemoglobin solutions. However, hemoglobin degraded significantly over the long-term refrigeration period for control samples, with a significant loss of heme group (406 nm) absorbance (~70%) (Figure 3-3). Under room temperature conditions, 5 v/v % BioCaRGOS samples retained 47% absorbance over the 210-day time period, while control samples retained 3% absorbance under the same conditions (Figure 3-3). This supports the long-term storage capabilities of BioCaRGOS under both ambient room temperature (23 °C) and refrigerated conditions (5°C).

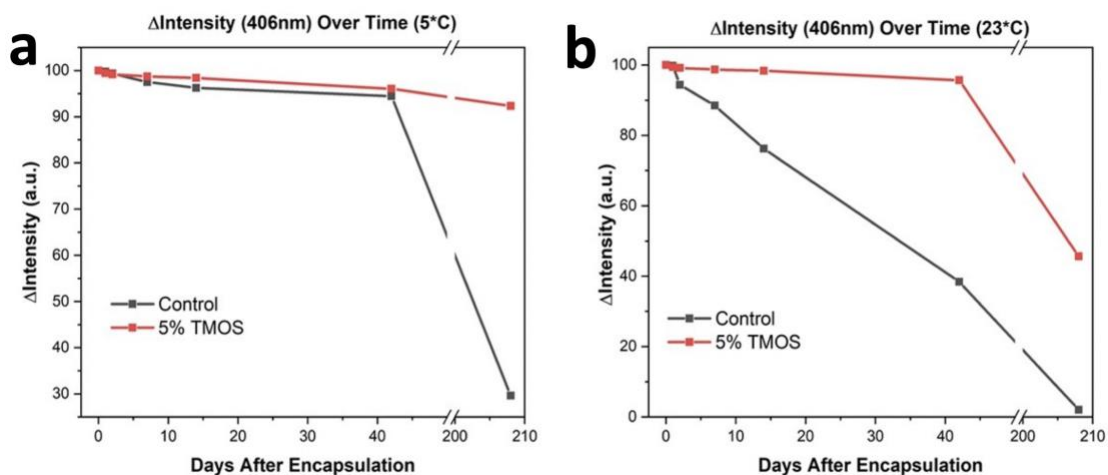


Figure 3-3. Excellent long-term stability of hemoglobin in BioCaRGOS formulations (5.0 v/v % TMOS; 0.01 w/v % hemoglobin; 0.15 M PB, pH 8.2) against control hemoglobin solutions (0.01 w/v % hemoglobin; 0.15 M PB, pH 8.2). (a) Refrigeration (5 °C) and (b) room- temperature (23 °C) conditions.

3.3.3 Raman analysis of BioCaRGOS formulations

Raman spectra of the BioCaRGOS formulations (5.0 v/v % TMOS; PB buffer, pH 8.0) with and w/o hemoglobin was evaluated to investigate the stability of BioCaRGOS at days 7, 14 and 21 respectively. The Raman peaks of TMOS solution was assigned to 646 cm^{-1} , dimerized silica or silicic acid to 830 cm^{-1} and the intense methanol C–O stretch to 1030 cm^{-1} respectively.⁴⁵ Similar peak intensities over 21 days is attributed to the robust physio-chemical stability of BioCaRGOS dispersions under room-temperature and mechanical handling (i.e., mixing, shaking, vortexing) conditions. Also, the unaltered peak intensities of BioCaRGOS formulations, with and without hemoglobin are tentatively attributed to the unique shape recognition capabilities of silica nanostructures (Figure 3-4). Notably, the BioCaRGOS nanoformulations could potentially deposit around hemoglobin and match its shape/conformation,

resulting in similar rotational and vibrational fingerprints of the BioCaRGOS formulations, with and without hemoglobin.⁴⁶

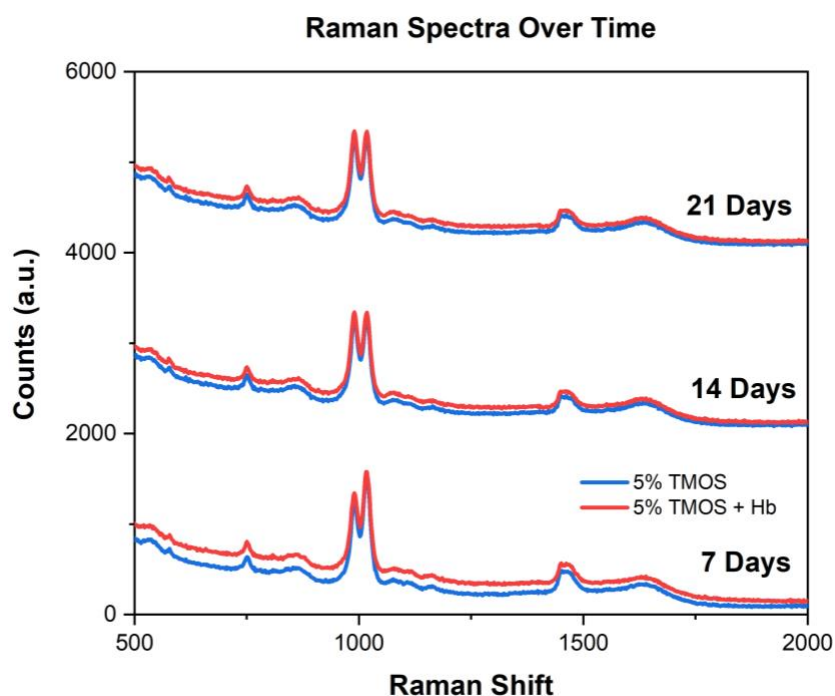


Figure 3-4. Raman spectra of BioCaRGOS. An unaltered Raman spectrum of BioCaRGOS (5.0 v/v %) formulations (with and without hemoglobin) over 21 days.

3.3.4 Polyethylene glycol (PEG) induced hemoglobin release in BioCaRGOS formulations.

The development of a biocompatible release protocol is desirable as it allows lab technicians to run diagnostics on the extracted proteins, . Post-encapsulation of hemoglobin within BioCaRGOS matrices, PEG was systematically added to all the formulations (Figure 3-5). A quick re-dissolution of low-to-high viscous BioCaRGOS–hemoglobin formulations [(1.0–7.5) v/v % TMOS; 0.01 w/v % hemoglobin; 0.5 M PB, pH 8.2; 3.0 mL] was observed upon addition of polyethylene glycol [PEG (65 mM, 2 kDa)]. Upon centrifuging the dissolved BioCaRGOS samples and extracting the supernatant solution, a three

to five-fold increase in hemoglobin's UV-vis absorbance (406 nm) was observed in the resulting solution (Figure 3-5). This large increment in the absorbance intensity of heme group [406 nm] is attributed to a synergistic hydrophilicity imparted by PEG (260 nm) to the BioCaRGOS formulations, indicating a facile passage and release of hemoglobin throughout the BioCaRGOS matrices without any loss of protein nativity as shown in (Figure 3-5). Particularly, an ideal ensilication matrix allows efficient bioanalyte immobilization (i.e., encapsulation entrapment or collaterally depositing) and a facile passage without any physical rupture. Therefore, our highly porous and moderately viscous BioCaRGOS formulations meets these standards, due to the long-term storage capabilities of BioCaRGOS as shown in Figure 3-2, and the biocompatible PEG release protocol as shown in Figure 3-5.

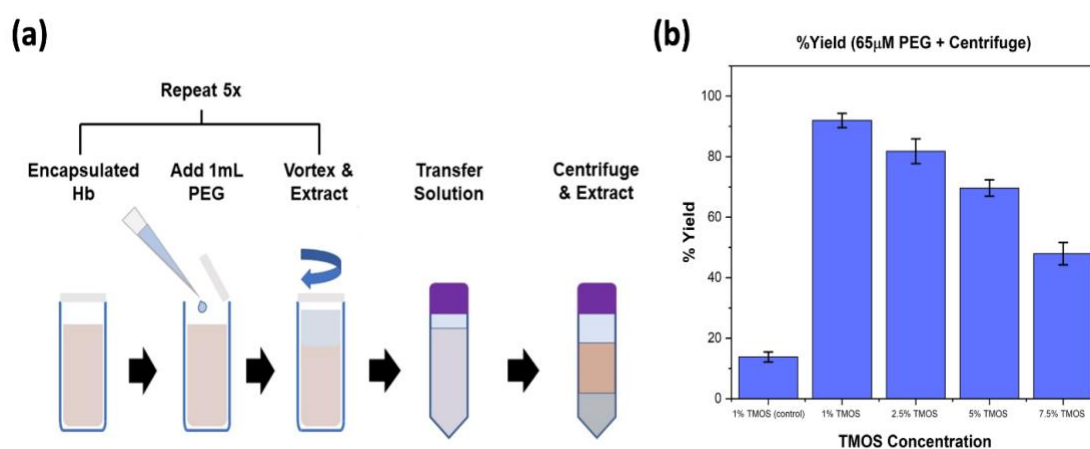


Figure 3-5. Polyethylene glycol (PEG) induced hemoglobin content release. a) Schematic of PEG addition to the BioCaRGOS formulation for facile hemoglobin extraction and b) significant hemoglobin release in BioCaRGOS formulations upon PEGylation.

3.3.5 Investigation of compatibility of BioCaRGOS with miRNA 21

As described in the introduction, preservation of nucleic acids is necessary as it is widely used in diagnosis of various diseases. DNA contains the instructions for building and maintaining a living organism whereas RNA stores the instructions encoded in DNA. Therefore, any degradation to nucleic acids can cause loss of important genetic information. To evaluate the applicability of BioCaRGOS, we selected miRNA 21 as the biospecimen of interest to evaluate parameters such as the effect of pH and ionic strength on the long-term stability. It should be noted that the ionic strength, pH of the BioCaRGOS, and the concentration of silica precursor can drastically impact the stability of biomolecules entrapped within the matrix. For e.g., ionic strength of the solution can directly impact the electrostatic repulsions between negatively charged BioCaRGOS in a buffer environment and consequently affect the size, stability and monodispersity of the silica precursors (Table A2). Also, salinity can dictate the nature of non-covalent interactions between biomolecules and BioCaRGOS matrices. Similarly, pH of the solution can dictate the extent of condensation reaction as well as the stability of the biomolecules. Therefore, a systematic study is performed in this chapter by varying the conditions and simultaneously monitoring miRNA 21 concentrations in each case respectively. miRNA concentration of ~500 nM payload with 0.5 v/v % BioCaRGOS in Tris EDTA buffer with either 0.15 M NaCl or 0.5 M NaCl, while keeping fixed the rest of the BioCaRGOS storage parameters is observed as shown in Figure 3-6. Measurement of miRNA 21 by PCR amplification, utilizes sequence specific primers and is dependent on the structural integrity of the nucleic acid. Thus, this technique allows for the simultaneous analysis of

both the concentration and structural integrity of the miRNA under various BioCaRGOS storage conditions. Reverse transcription (RT) was performed on the miRNA 21 sample aliquots (with and w/o BioCaRGOS) using TaqMan MicroRNA Reverse Transcription Kit and thermal cycler, followed by real-time quantitative polymerase chain reaction (qPCR) amplification with an applied 0.1 C_T threshold value (Tables A1 and A3). The miRNA 21 concentration (nM) of BioCaRGOS aqueous formulations were evaluated by measuring mean C_T values using standard calibration curves (Fig. A6 and A7). A strong correlation between miRNA 21 concentration (nM) of BioCaRGOS aqueous formulations and mean C_T values was observed with $R^2 = 0.99$ respectively (Fig. A6). In response to salt stress, the miRNA concentration levels in low salt buffer were 426.63 ± 46.33 nM ($C_T: 11.5 \pm 6.0$), whereas in high salt buffer the miRNA was not measurable ($C_T: 31.1 \pm 1.2$) [$C_T \geq 30$ are equivalent to nuclease free water].

These conditions are similar to biological pH and ionic strength with an extremely low concentration (0.5 v/v % BioCaRGOS). Under these conditions, the nucleic acids have a negative charge, and the silica colloids also exhibit a negative charge as well. Therefore, electrostatic repulsive forces dominate and the miRNA21 is stabilized. A schematic of miRNA 21 in BioCaRGOS is shown in figure 3-6. We anticipate that at such low concentrations of silica that are slightly viscous in nature, the miRNA 21 will be repelled around silica colloids and will remain stable. These repulsive interactions also allow for ease of measurement in the presence of BioCaRGOS without requirement of a separation step.

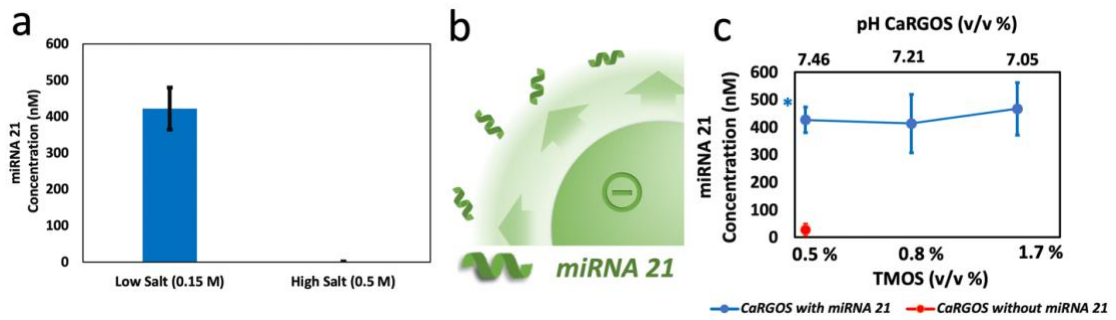


Figure 3-6. Investigation of compatibility of BioCaRGOS with miRNA: (a) miRNA concentration level (nM) in CaRGOS (0.5 v/v %) in low salt buffer and high salt buffer (b) representative schematic of the significant electrostatic-repulsions between negatively charged silica-colloids and miRNA 21 (c) a plot of miRNA concentrations (nM) vs. TMOS concentrations (v/v) % with their pH levels.

Once, the concentration of salt was optimized, we varied the concentration of silica precursor (Figure 3-6). As the concentration of hydrolyzed silica (silicic acid) is increased, a slight decrease in pH is observed for the BioCaRGOS with buffer and biospecimen. Once prepared, the pH of the BioCaRGOS formulations is stable, reproducible [SD < ± 0.2 pH units] and not altered by air exposure. A ~ 500 nM payload of miRNA 21 was added to each BioCaRGOS formulation. Figure 3-6 shows the miRNA concentration of miRNA measured within 1 h from addition to BioCaRGOS formulations with variable TMOS concentrations.

3.3.6 Long term evaluation of miRNA 21 concentration in BioCaRGOS

Based on the observation of better reproducibility and no significant difference in miRNA measurements between 0.5 v/v % vs. 1.7 v/v % BioCaRGOS, the 0.5 v/v % BioCaRGOS formulation was utilized for long-term miRNA 21 storage experiments. At room temperature, the miRNA 21 concentration (nM) in the mixtures without BioCaRGOS sol-gel matrices were

(277.6 ± 18.8) nM within 3 h of addition, (172.0 ± 0.2) nM within 24 hours and was not measurable on day 7, (Figure 3-7). We utilized three temperature conditions (a) refrigeration ($4\text{ }^{\circ}\text{C}$) (b) ambient temperature ($25\text{ }^{\circ}\text{C}$) and (c) physiological temperature ($40\text{ }^{\circ}\text{C}$) respectively. Figure 3-7 shows the quantitative RT-PCR analysis of 0.5 v/v % BioCaRGOS/ miRNA 21 mixtures at (4, 25 and 40) $^{\circ}\text{C}$ over a period of 82 days. In contrast to the absence of BioCaRGOS, we observed $\sim 100\%$ recovery of miRNA 21 (~ 500 nM) in the BioCaRGOS mixtures at each temperature over the 82 day period: (426.63 ± 46.33) nM on day 0, (392.35 ± 8.28) nM on day 1, (524.53 ± 6.54) nM on day 7, (484.32 ± 2.46) nM on day 14, (588.94 ± 0.54) nM on day 21, (505.95 ± 75.00) nM on day 28 and (500.19 ± 59.92) nM on day 82 inferring a thermal stable miRNA 21 within BioCaRGOS formulations.

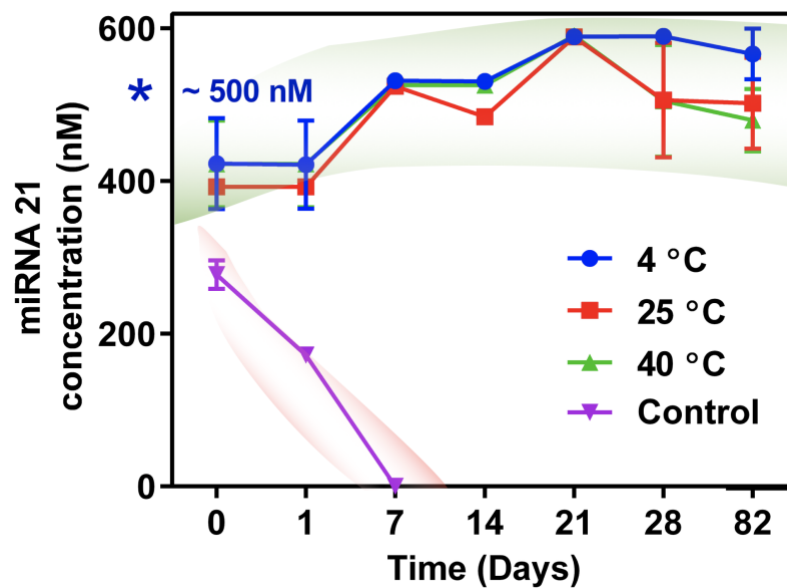


Figure 3-7. Long term evaluation of miRNA concentrations in BioCaRGOS: A plot of miRNA 21 concentrations (nM) with sol-gel for 82 days at varying temperatures (4, 25, 40) $^{\circ}\text{C}$; miRNA 21 concentrations (nM) without BioCaRGOS (Control) at 25 $^{\circ}\text{C}$.

The low concentration of miRNA measured on day 0 and day 1 is attributed to possible interference of PCR amplification by the methanol by product of TMOS generation.⁴⁷ We observed similar results for our DNA preservation studies.⁴⁷ This interference is avoided by preferential evaporation of methanol due to its higher vapor pressure. The mode of miRNA stability in lower concentrations BioCaRGOS sol–gel matrices might be attributed to the combined effect of some miRNA immobilization, caused by sterically-restricted synergistic interactions with BioCaRGOS network and local solvent/pH microenvironment [Tris EDTA buffer/pH > 7] of these aqueous BioCaRGOS formulations.^{48, 49} However, such long-term stability cannot simply arise from repulsive interaction, and we anticipate some other factors play a critical role. A key possibility is that the BioCaRGOS can interact with RNase (which can arise from compromised sterility) and therefore can prevent the denaturation of miRNA by RNase. E.g., previously, Buijs et al.

had reported an electrostatic adsorption induced destabilization of proteins (e.g., RNase A/Lysozyme) on 11 nm sized silica particles.⁵⁰ Also the non-covalent interaction between biological entities and silica nanomaterials are well-known to electrostatically destabilizes nucleases (i.e. RNase) and protease activity, as well as providing stability to biospecimens (e.g. Lipids, proteins, nucleic acids) in their immobilization matrices.^{34, 39, 51-53}

3.3.7 Evaluation of stability in the presence of RNase A

RNase A is a ribonuclease enzyme that specifically cleaves single stranded RNA. It can degrade the RNA samples during storage and can be a source of contamination and hence proper storage of RNA is essential. At pH 7.4, RNase A has asymmetrically stronger positive charge density across the

longest axis of the molecule (PDB 2AAS).^{51, 54, 55} Also, RNase A's active site has been reported to reside in this electropositive region. Therefore, the potential for electrostatic interaction between the positive domain of RNase A and negatively charged BioCaRGOS as shown in Figure 3-8 suggests that BioCaRGOS may inhibit the activity of RNase's.

To validate this hypothesis, we examined BioCaRGOS capability to prevent degradation of RNA in presence of pancreatic RNase A.⁵⁶ As shown in figure 3-8 and A8, the fluorescence emission intensities of yeast RNA intercalated ethidium bromide [EtBr: (em:600 nm; ex 510 nm)] solutions in BioCaRGOS and control buffers were monitored in the presence of incrementally increasing RNase A concentrations (range: 0-320) nM. Normalized with EtBr's fluorescence emission at 0 nM RNase A concentration, a ~40% relative fluorescence quenching was observed in control buffer solutions, (without BioCaRGOS) indicating degradation of yeast RNA with incremental increase in RNase A concentrations.⁵⁶ However, unaltered fluorescence intensity was observed in BioCaRGOS buffer solutions within (0-320) nM range of RNase A concentrations (Figure 3-8). Such unaltered fluorescence emissions were attributed to the electrostatic adsorption induced RNase A inhibition with BioCaRGOS.^{50, 51, 54-58}

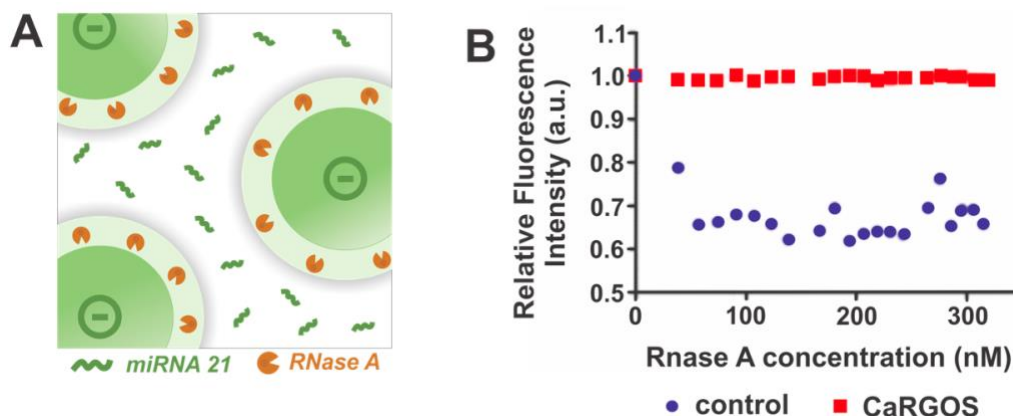


Figure 3-8. Evaluation of stability in the presence of RNase A: (a) A schematic of dual-character of negatively charged silica-colloids demonstrating the electrostatic-attraction induced denaturation of positively charged RNase A and a simultaneous immobilization of miRNA 21 within BioCaRGOS formulations via electrostatic repulsion (b) A plot of relative fluorescence intensity of Ethidium bromide versus RNase A concentrations in (0-320) nM range.

BioCaRGOS demonstrates larger hydrodynamic size of ~69 nm and displayed high stability in their buffer dispersions with zeta potential ~ -21 mV respectively. Therefore, it is an excellent candidate for preventing RNA degradation from environmental RNase contamination (e.g., bacteria, fungi), during transportation/storage and downstream processing.^{59, 60}

3.4 Conclusion

We have developed a highly efficient, convenient, and clinically relevant silica-based sol-gels called BioCaRGOS that allows for long term stabilization of biospecimens such as proteins and nucleic acids. This technique has several advantages as described previously over other conventional sol gel techniques. These gels were used to demonstrate efficient storage for hemoglobin, a metalloprotein as well as miRNA 21, a potential cancer biomarker. Based on our findings, we propose that the final optimal protein storage condition is

utilization of [(5 v/v %) TMOS; 0.01 w/v % hemoglobin; 0.15 M PB, pH 8.2; 3.0 mL], that had demonstrated an unprecedented protein integrity of ~95% at ambient (1 month) and ~96% (7 months) under refrigeration conditions. Using current PEG protocol, the release efficiency is 75%, which can be further optimized. We also demonstrated stability of a highly sensitive cancer biomarker miRNA 21 at ambient and elevated temperatures (4, 25 and 40 °C) for nearly 3 months, with ~100% single-step recovery without the need of any purification protocol. The mode of stabilization is attributed to the RNase (sterile- compromised contaminated environment) inhibition by optimized aqueous formulations of BioCaRGOS [low ionic strength, optimum pH (~7.46), large hydrodynamic sized and high surface potential] as well as miRNA immobilization caused by localized interaction of BioCaRGOS matrix. The results indicate that BioCaRGOS have enormous potential to stabilize biomolecules. The scientific insight gained in the study suggests that if the pI of the protein is below the pH of the BioCaRGOS, it will achieve stabilization and would be amenable to extraction. This robust storage, transport, and extraction are the keystone of this innovation, and present a technology that can encapsulate a plethora of biospecimens including proteins and nucleotides as most of them exhibit a pI of less than 7. Thus, the clinical applications of BioCaRGOS are vast when compared to its predecessors and present a feasible alternative to conventional cryopreservation platforms.

CHAPTER 4

ENHANCING THE COMPATIBILITY OF BIOCaRGOS WITH DOWNSTREAM APPLICATIONS

4.1 Introduction

The process of sol gel encapsulation and its limitations for biospecimen storage were described in Chapter 2 along with our alternative BioCaRGOS approach. The long-term storage of hemoglobin and miRNA21 using BioCaRGOS at ambient temperatures was then demonstrated in Chapter 3. The success of those preliminary studies with isolated protein and RNA are extended in this chapter to the stabilization of pancreatic cancer biomarkers in complex environments, such as plasma. Pancreatic cancer biomarker stability is an important factor in the detection of pancreatic cancer. Biomarkers in general are measurable indicators that can be used to identify the presence of cancer and track its progression. In the case of pancreatic cancer, there are several biomarkers that include CA19-9, CEA, and KRAS, which are the most commonly used. The stability of these biomarkers is crucial as they are used by clinicians to help assess the response to treatment and monitor disease progression. For example, if the biomarker levels are stable or decreasing it suggests the treatment is effective and the cancer is responding, whereas increasing biomarker levels indicate that the cancer is becoming more aggressive, and the treatment needs modification. As such, it is important to ensure that quantification of these biomarkers is reliable and that decreasing biomarker levels are not the result of sample degradation during transportation or storage.

Based on the results presented in Chapter 3, BioCaRGOS is an attractive stabilization agent for these biomarkers at ambient temperatures. However, modifications to BioCaRGOS are necessary to make it compatible with downstream processing and analytical quantification. Notably, the presence of methanol in BioCaRGOS, which arises from hydrolysis of silica precursor (tetramethyl orthosilicate) during the BioCaRGOS synthesis (Equation 1 chapter 2), may interfere with the polymerase chain reaction (PCR). PCR is a technique that uses multiple cycles of temperature changes to amplify a specific region of DNA in a sample, making it possible to produce millions of copies of the target sequence for further analysis. In theory, PCR enables the detection of one single cell or DNA molecule. This makes PCR an important tool in several fields, including clinical diagnostics, food analysis, and forensic analysis. However, the presence of methanol can inhibit the PCR lowering the amplification efficiency, thus lowering the detection limit as well as the precision of sequence-specific nucleic acid quantification in real-time PCR or droplet digital PCR. In order to overcome the problems caused by the presence of methanol, the BioCaRGOS synthesis must be optimized for its removal before encapsulation of any biomarker. Another important aspect is the release of biomarker post encapsulation. Developing a compatible release protocol allows the clinicians to run diagnostics on the extracted biomarkers. Hence, in this study, we report a practical way to release the biomarker post encapsulation and study the effect of silica interference and how it was minimized.

Circulating tumor DNA (ctDNA) in plasma has been demonstrated as a promising predictive and prognostic biomarker for a variety of cancers.^{61, 62} The ctDNA represents a small fraction of the total cell-free DNA (cfDNA) that is

released from cells into the blood stream and can be found in various body fluids including plasma and urine samples.⁶³ KRAS mutation is found in nearly 30% of human cancers, yet the most prevalent and oncogenic is the KRAS(G12D) variant.^{64, 65} Due to the extremely low abundance of ctDNA (<0.1% mutant allele fraction of total cfDNA), current analytical protocols involve extraction and concentration of cfDNA from the biospecimen of interest followed by measurement of the ctDNA mutant allele fraction using ultrasensitive technologies such as droplet digital PCR (ddPCR).^{66, 67} Currently, these biomarkers are stored in ultra-cold storage conditions that are not only expensive but also not practical where access to cold storage is limited. This prompted us to investigate BioCaRGOS for storage of pancreatic cancer biomarkers at room temperature. To achieve this, we first investigated the compatibility of the novel BioCaRGOS silica sol-gel technology with the extraction and downstream analysis of plasma mutant KRAS ctDNA.

Entrapment of biomolecules such as nucleic acids, proteins and other sensitive enzymes into inorganic silica matrices has gained significant attention over the last two decades.⁶⁸⁻⁷¹ Herein, we report the compatibility of BioCaRGOS with a routinely employed plasma ctDNA extraction technology and measurement of mutant KRAS (G12D) ctDNA levels by ddPCR, extracted from a semi-synthetic plasma reference sample. We have demonstrated an efficient way of minimizing the interference of methanol, generated as a by-product during the hydrolysis reaction of BioCaRGOS, with ddPCR and eliminated silica colloidal particles from the BioCaRGOS prior to extraction of cfDNA to eliminate interference with plasma ctDNA extraction.

4.2 Experimental

4.2.1 Materials

Tetramethyl orthosilicate (TMOS) and sodium chloride were purchased from Sigma Aldrich (Saint Louis, MO, US). Nuclease free water was purchased from New England BioLabs (MA, US). The 96 well plates were purchased from Thermo Fischer Scientific (MA, US). Tris EDTA buffer (10 mM Tris-HCl, 1mM EDTA) pH 7.4 and RNase free water were purchased from Bioworld (Dubline, OH, US). Methanol elimination was performed on Buchi R-124 Rotary Vap System (Delaware, US). Raman spectra were acquired on Reva Educational Raman platform (Hellma, Plainview, NY, US). The KRAS (G12D) circulating tumor DNA (ctDNA) based reference materials were purchased from Seracare (Milford, MA, US). QIAamp circulating nucleic acid kit was purchased from Qiagen (Hilden, Germany). Human KRAS (G12D) ctDNA was measured using the BioRad KRAS (G12D) droplet digital PCR (ddPCR) assay reagent with ddPCR supermix from probes per manufacturers recommendations followed by quantification of KRAS (G12D) utilizing the QX200 ddPCR system (BioRad Laboratories, Hercules, CA, US).

4.2.2 BioCaRGOS synthesis

A 10 v/v % TMOS stock solution was prepared in doubly deionized water and transferred to a 40.0 mL glass vial, screw capped and hydrolyzed via a standard benchtop microwave for 30 s. Post microwave hydrolysis, the solution was then subjected to rotary evaporation for 30 mins at a controlled pressure (25 mbar) and temperature of (45 °C) to remove the methanol by-product. This methanol free TMOS stock solution was then allowed to equilibrate to room temperature. After the equilibrium was reached, 10 mM Tris-HCl (pH 7.5), 1mM

EDTA and 0.15 M NaCl were added to formulate the final concentrations of 0, 0.5, 1.0, 1.5 and 2 (v/v %) and this solution was termed as “BioCaRGOS”.

4.2.3 Evaluation of BioCaRGOS using Raman spectroscopy

Raman spectroscopy was performed on BioCaRGOS [5 v/v % TMOS, 10 mM Tris-HCl (pH 7.5), 1mM EDTA, 0.15 M NaCl, 3.0 mL] using a Reva Raman Educational platform instrument. The laser power of 450.0 mW and current 959.0 mA were optimized to analyze the samples. The laser temperatures [diode = 30 °C; case = 24.4 °C] and spectrometer temperature [23.1 °C] were optimized for the collection of Raman spectra.4.2.4 Circulating cell free (cfDNA) nucleic acid extraction

4.2.4 Circulating cell free (cfDNA) nucleic acid extraction

The cfDNA reference material consisting of a synthetic plasma matrix containing ~0.1 ng/ μ L G12D sequence in the presence or absence of BioCaRGOS [0.5 v/v %, 10mM Tris-HCl (pH 7.5), 0.15 M NaCl] samples were formulated in 15.0 mL centrifuge tubes and stored for 2 hours. The extraction was carried out using a nucleic acid extraction kit (QIAamp Circulating Nucleic Acid Kit) as per the instruction manual. The extracted cfDNA was then stored in AVE buffer, provided in the kit, and used for further downstream analysis by ddPCR.

4.2.5 Circulating tumor (ctDNA) analysis using Seracare samples

The measurement was performed using a Seraseq ctDNA reference material v2 (Seracare), which is a full process plasma like reference standard supporting the assessment of the entire workflow from extraction to analysis. It consists of 40 clinically relevant mutations across 28 genes all at the same allele frequency. It includes single well characterized GM24835 human

genomic DNA as background wild-type material. This specific ctDNA mutation mix v2 product has an allele frequency of 2%.

4.2.6 Invert Syringe Filtration

Reference material with and without BioCaRGOS [0.5 v/v %, 10mM Tris-HCl (pH 7.5), 0.15 M NaCl] samples were subjected to invert syringe filtration using a PES filter membrane of 0.45 µm pore size to eliminate silica and release the cfDNA mixture from the silica matrix. The process was completed in 5 mins and subjected to nucleic acid extraction protocol for cfDNA.

4.2.7 Droplet digital PCR (ddPCR)

Droplet digital PCR was performed using the QX200™ Droplet Digital™ PCR System from BioRad (Hercules, CA) according to the manufacturer's instructions. These samples contained cfDNA sample, 2X ddPCR supermix, and 20X primer probe mix in a final reaction volume of 20 µL (Table 4-1). Droplets were generated using the Droplet Generator (DG) with 70 µL DG Oil per well with a DG8 cartridge and cartridge holder, 20 µL PCR reaction mix, and DG8 gasket.

Table 4-1. ddPCR sample preparation

| Component | Volume (μL) per 10 μL reaction | Volume (μL) per 20 μL reaction (Corrected) |
|--|---|---|
| 2X ddPCR Supermix for probe (no dUTP) | 10 | |
| 20X Target (FAM) and wild-type HEX primer probe | 1 | 1.1 |
| AVE Buffer | 4.5 | 4.95 |
| KRAS mutation circulating tumor DNA (Extraction) | 4 | 4.4 |
| Total volume | 19.5 | 21.45 |

*Each 20 μL reaction consists of 10 μL supermix, 1 μL of Target FAM and HEX primer probe, 0.45 μL AVE buffer and 4 μL of KRAS circulating tumor DNA (extracted).

Droplets were dispensed into the 96-well PCR plate by pipetting 40 μL from the DG8 cartridge into each well. The PCR plate was then heat-sealed with a foil seal and the sealed plate was placed in the PCR thermocycler. The S1000 thermal cycler was used for optimal annealing with a 10-minute activation (95 $^{\circ}\text{C}$), 40 cycles, denaturation (15 s, 95 $^{\circ}\text{C}$; 60 s, 60 $^{\circ}\text{C}$), followed by one cycle (98 $^{\circ}\text{C}$, 10 min) (Table 4-2). The data analysis on the results (n=3) is performed using QuantaSoft Software, version 1.7, Regulatory Edition, after carrying out PCR experiments on the QX200 system. After the reaction, the droplets were read using the Droplet Reader, and QuantaSoft software

converted the data into concentrations using Poisson distribution statistical analysis.

Table 4-2. Thermal cycler program

| Step Type | Time (min) | Temperature (°C) |
|------------------|-------------------|-------------------------|
| Hold | 10 | 95 |
| Hold | 30 | 94 |
| Hold | 1 | 55 |
| Hold | 60 | 55 |
| Hold | 10 | 98 |
| Hold | 9 | 12 |

4.2.8 Elimination of Methanol from BioCaRGOS samples

Various rotary evaporation parameters were employed to optimize the methanol removal; temperatures (45 °C, 55 °C, and 70 °C), pressure (10, 20, 25, 30, and 35) mbar, and time (10, 15, 20, 25, and 30) minutes. As a result, the most suitable set of parameters were selected based on the amount of methanol removed. The optimized parameters were temperature (45 °C), pressure (25 mbar), and time (30 mins), which was repeated 3 times (n = 3 trials) to demonstrate ~99% removal of methanol from the hydrolyzed TMOS solution post microwave synthesis. Figure 4-1 demonstrates process optimization for methanol removal at three different temperatures 45 °C, 55 °C, and 70 °C at 25 mbar for specific time intervals.

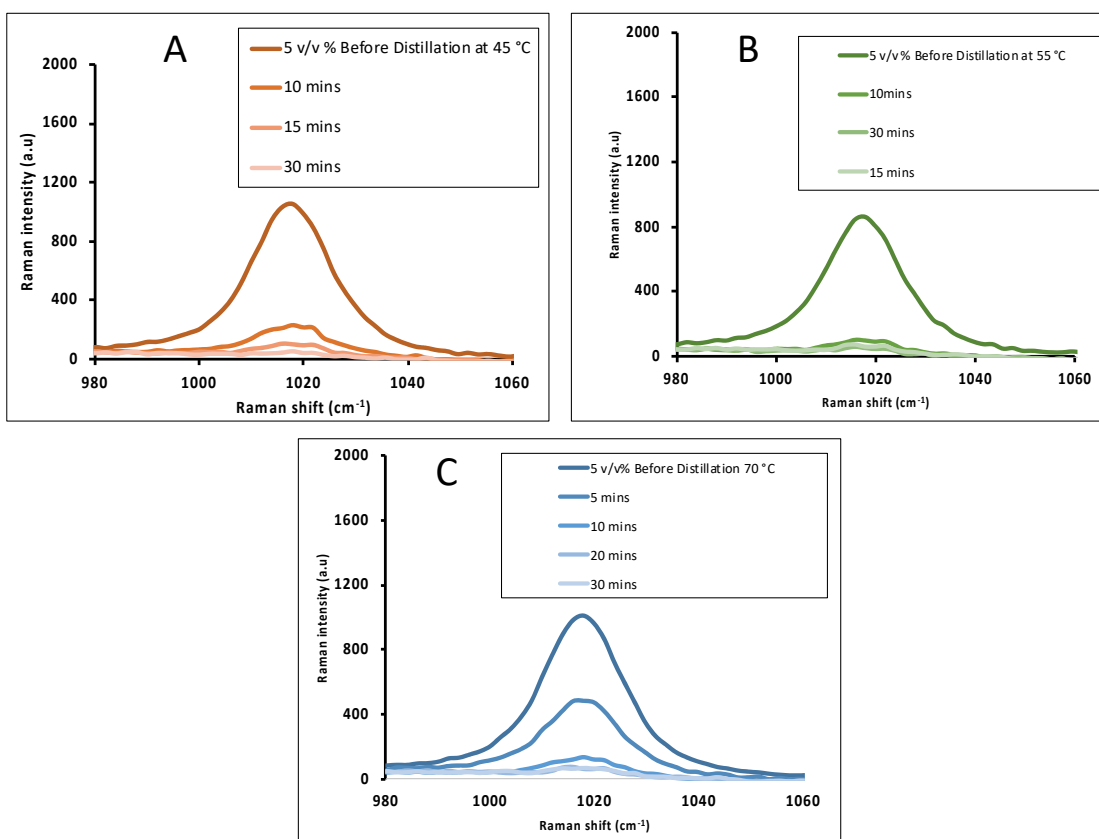


Figure 4-1. Raman spectra of 5 v/v % TMOS pre-distillation demonstrating methanol intensity at A) 45 °C, B) 55 °C, and C) 70 °C at 25 mbar after timed intervals.

4.3 Results

4.3.1 BioCaRGOS compatibility with ddPCR

To extend the application of BioCaRGOS for the storage of pancreatic cancer biomarkers in plasma at ambient temperatures, we first evaluated the compatibility of BioCaRGOS with DNA extraction protocols and ddPCR. This was necessary to establish if BioCaRGOS altered the detection limit or the precision of the sequence-specific nucleic acid. To investigate the compatibility of BioCaRGOS with ctDNA in downstream analysis, ctDNA (~0.01 ng/ μ L KRAS (G12D) concentration) was extracted from BioCaRGOS + ctDNA formulation using the QIAamp cfDNA extraction kit as per the manufacturer's procedure. The extracted KRAS (G12D) ctDNA was spiked into BioCaRGOS [0.5 v/v %,

10mM Tris-HCl (pH 7.5), 0.15 M NaCl] samples and then analyzed by ddPCR. Upon analysis, low quantities of ctDNA copies were observed in BioCaRGOS samples as compared to control samples (without BioCaRGOS) with only 10-15 % KRAS ctDNA recovery [i.e., 15.65 ± 2.19 ng/mL; 4475.15 ± 591.89 copies/mL] from BioCaRGOS, against their control group [52.15 ± 1.05 ng/mL; 14864.20 ± 299.37 copies/mL] as demonstrated in Figure 4-2.

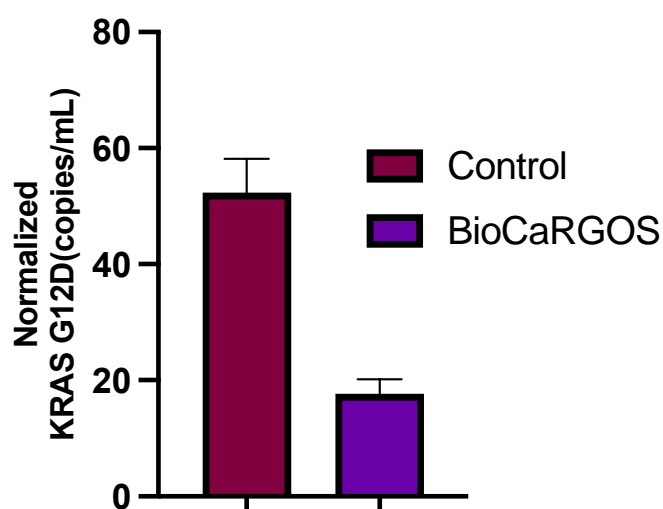


Figure 4-2. ddPCR analysis of KRAS (G12D) ctDNA levels showing low copies due to interference of methanol present in BioCaRGOS.

The rationale for this low count of ctDNA copies is that the hydrolysis reaction for BioCaRGOS synthesis yields methanol as the by-product, which is a known PCR inhibitor. This methanol could interfere with the PCR amplification thereby giving false positives or low count for ctDNA copies. This hypothesis was validated by externally adding 98% MeOH as a negative control, which showed significant reduction in count of ctDNA copies/mL (Figure 4-3). The data confirmed that methanol could be responsible for the reduction in the count of ctDNA copies in the BioCaRGOS samples.

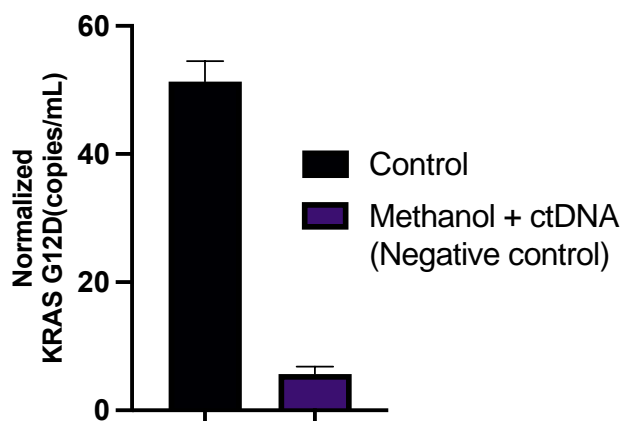


Figure 4-3. Addition of 98% MeOH to control samples [10 mM Tris-HCl (pH 7.5), 1 mM EDTA, 0.15 M NaCl] to see the negative effect on KRAS ctDNA samples.

Raman spectroscopy was used to confirm methanol as the interfering agent as it allows for facile monitoring of reaction progress during BioCaRGOS preparation. The peak positions of the silica precursors ($\text{Si}(\text{OCH}_3)_4$), intermediates [$\text{Si}(\text{OCH}_3)_3\text{OH}$, $\text{Si}(\text{OCH}_3)_2(\text{OH})_2$, $\text{Si}(\text{OCH}_3)(\text{OH})_3$], silicic acid ($\text{Si}(\text{OH})_4$) and methanol (CH_3OH) are expected at $640\text{-}650\text{ cm}^{-1}$, $673\text{-}725\text{ cm}^{-1}$, $750\text{-}780\text{ cm}^{-1}$ and 1020 cm^{-1} , respectively.⁷² Experimentally, we observe a peak at 646 cm^{-1} for 5 v/v% TMOS/water solution prior to hydrolysis indicating the presence of intact $\text{Si}(\text{OCH}_3)_4$. After $\sim 30\text{ s}$ microwave exposure, the $\text{Si}(\text{OCH}_3)_4$ peak at 646 cm^{-1} is absent and new peaks attributed to $\text{Si}(\text{OH})_4$ and methanol are observed at 750 cm^{-1} and 1020 cm^{-1} , respectively. Notably, peaks for partially hydrolyzed TMOS species at 673 cm^{-1} , 697 cm^{-1} , and 725 cm^{-1} are not observed indicating complete hydrolysis of $\text{Si}(\text{OCH}_3)_4$.⁷²

To eliminate this methanol interference, methanol was removed from the hydrolyzed TMOS samples by rotary evaporation. The methanol content was monitored at different time points [0, 15, 20, 25 and 30 minutes] of the rotary evaporation by Raman spectroscopy (Figure 4-1). It was observed that rotary

evaporation at 45 °C, 55 °C and 70 °C did not show any significant difference in terms of elimination efficiency and therefore 45 °C was chosen as the optimum temperature for distillation of MeOH.

After the complete removal of methanol, the hydrolyzed TMOS solution was buffered with 10 mM Tris-HCl (pH 7.5), 1mM EDTA, 0.15 M NaCl, followed by addition of extracted KRAS (G12D) ctDNA and analyzed by ddPCR. The BioCaRGOS formulations (-Methanol) showed analogous levels of KRAS (G12D) ctDNA levels [50.15 ± 1.01 ng/ml; 14859.20 ± 294.12 copies/ml] against controls [52.15 ± 1.05 ng/ml; 14864.20 ± 299.37 copies/ml] as shown in Figure 4-4. These results confirmed that methanol was responsible for the interference observed during analysis of ctDNA from BioCaRGOS samples.

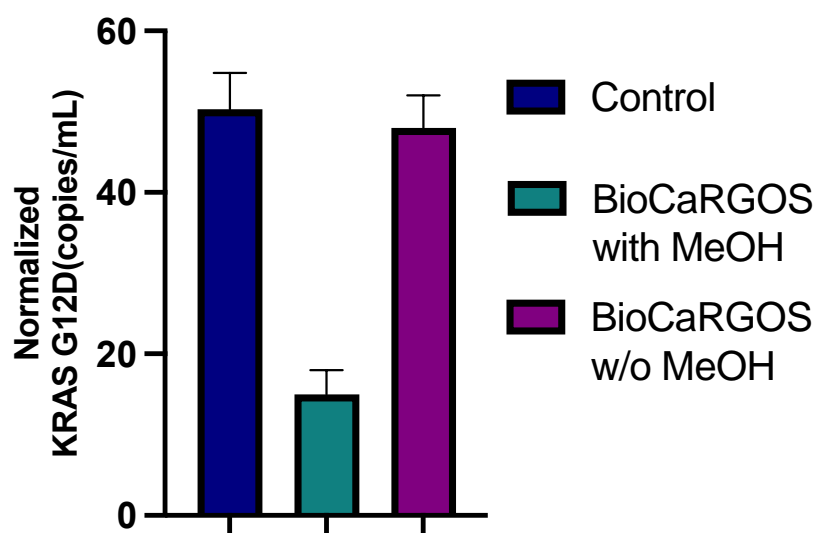


Figure 4-4. ddPCR analysis showing no interference in ctDNA count post removal of methanol by distillation.

4.3.2 BioCaRGOS compatibility with ctDNA extraction process

The next goal was to investigate the compatibility of BioCaRGOS with a complex semi-synthetic plasma matrix requiring ctDNA extraction. To investigate the impact of colloidal silica present in the BioCaRGOS samples on

the DNA extraction protocol, 0.5 v/v % BioCaRGOS was directly added to the plasma reference material. The resulting formulations with BioCaRGOS (pre-extraction) were incubated for 2 hours, along with their control samples, prior to the extraction and ddPCR analysis. Figure 4-5 demonstrates significant interference attributed to colloidal silica with the extraction process and extracted ctDNA with only 5-9 % KRAS ctDNA recovery [i.e., 4.50 ± 2.21 ng/ml; 1268.15 ± 591.89 copies/ml] from BioCaRGOS (-methanol) formulations, against their control group [52.15 ± 1.05 ng/ml; 14864.20 ± 299.37 copies/ml]. Additionally, adsorption of the sample in the presence of BioCaRGOS to the QIAamp Mini membrane took 3-4 hours as compared to control samples which were adsorbed in 5 mins.

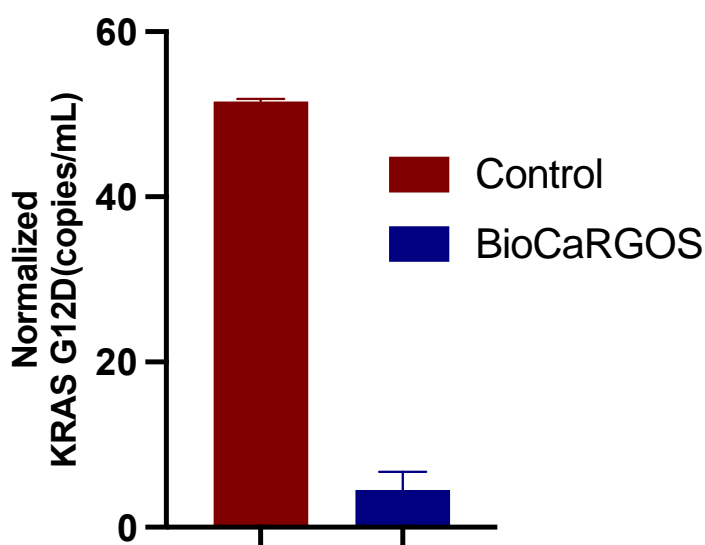


Figure 4-5. ddPCR characterization of KRAS (G12D) ctDNA concentrations (ng/mL) extracted from Seracare reference materials containing BioCaRGOS (+ silica), prior to the ctDNA extraction against controls.

4.3.3 Elimination of silica from BioCaRGOS to minimize the interference

Silica gels have demonstrated a great promise in preserving the structural and functional integrity of proteins and nucleic acids against storing,

shipping, and mechanical variations via encapsulating a wide range of biospecimens. In order to release the biospecimens from the silica matrix it is necessary to develop a compatible protocol that releases the biospecimen (protein/nucleic acid) in its native form. To achieve this, we initially used amicon filters of different Molecular Weight Cut Offs (MWCO) such as 50,000 and 100,000 MWCO. For preliminary studies, hemoglobin was employed as a model protein since it is easy to characterize by UV-Vis spectroscopy. Upon analysis, it was observed that hemoglobin was binding to the cellulose membrane of amicon filters along with silica preventing clear separation post centrifugation. Next, polytetrafluoroethylene membranes were employed with a syringe filtration technique in an attempt to separate the particles. However, no separation of silica and hemoglobin was observed when BioCaRGOS containing hemoglobin was passed through these filters of different pore sizes from 0.20, 0.22 and 0.45 μm .

Finally, polyethersulfone membranes of 0.10, 0.22 and 0.45 μm pore sizes were investigated for the separation of hemoglobin from the silica matrix. Upon analysis, a clear separation of hemoglobin was observed as the filtrate did not contain any silica colloidal particles as confirmed by dynamic light scattering (DLS). Even though it effectively separated silica colloidal particles, this process was very tedious and time consuming. Hence, to develop a more practical approach, and based on the fact that silica nanoparticles were denser than the analyte, we employed the Invert Syringe Filtration (ISF) technique. With ISF, the syringe is inverted and a PES filter membrane of pore size 0.45 μm is attached to the syringe to separate the silica from BioCaRGOS (Figure 4-7). Different pore sizes such as 0.10, 0.22, and 0.45 μm were investigated to

optimize the removal of silica from BioCaRGOS. The data suggested that 0.45 μm worked most efficiently in removing silica. We confirmed the silica elimination by DLS, which showed a significant decrease in the kCPS count rate after invert syringe filtration. The kCPS is a function of size and concentration of scattering particles. In nanoscale particle measurements, kCPS can be used to determine the concentration of sample present.⁷³ (Figure 4-6) shows kCPS count rate of BioCaRGOS [0.5 v/v % TMOS; 10 mM Tris-HCl (pH 7.5), 1 mM EDTA, 0.15 M NaCl] pre and post inverted syringe filtration (ISF). We employed this ISF technique to circumvent silica interference prior to biospecimen analysis in downstream process. Although the hydrodynamic size measurements have demonstrated similar colloidal sizes for pre and post filtered samples, a significant reduction in the colloidal silica count rate (kCPS) was observed in the filtered samples. During the hydrodynamic size measurements for the colloidal particles (2-1000 nm), the silica colloids count rate for pre-filtered samples was observed in 160-175 kCPS range and in 40-50 kCPS range for the post filtered BioCaRGOS formulation [0.5 v/v % TMOS; 10 mM Tris-HCl (pH 7.5), 1 mM EDTA, 0.15 M NaCl] demonstrating 75-80% reduction in colloidal count rate in the filtered samples (Figure 4-7).

Having demonstrated the utility of the ISF method to remove silica from BioCaRGOS, the method was further evaluated to remove silica from the BioCaRGOS solution containing SeraCare reference materials [TMOS 0.5 v/v %; 10 mM Tris-HCl (pH 7.5), 1 mM EDTA, 0.15 M NaCl, 5 ml seracare reference material]. After inverted syringe filtration, the BioCaRGOS (-methanol) formulations [(0.5 v/v % TMOS ; cfDNA (post-extraction))] indicated no significant difference in ctDNA measurements between control and inverted

syringe filtered BioCaRGOS treated reference material KRAS ctDNA levels [51.04 ± 0.6 ng/ml ; 15466 ± 181.8 copies/ml] against controls [51.59 ± 0.4 ng/ml ; 15633 ± 121.21 copies/ml] (Figure 4-6).

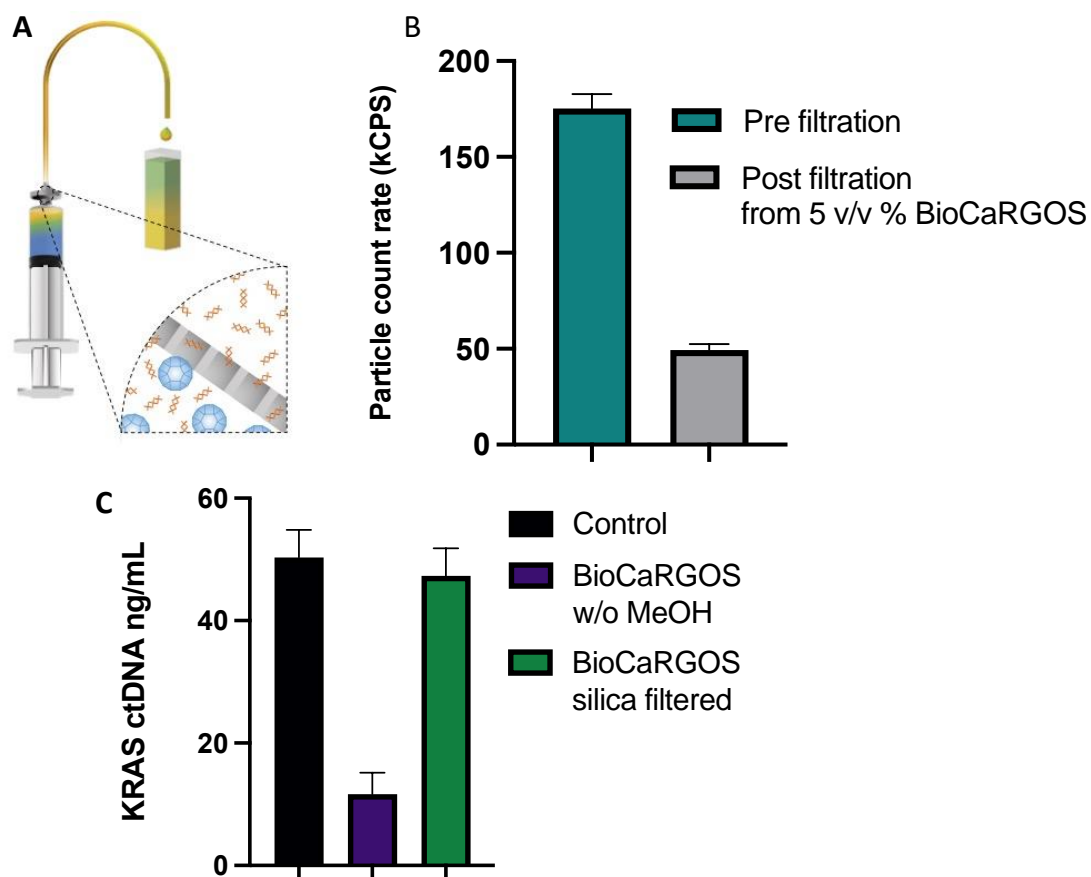


Figure 4-6. A) Representation of Invert Syringe Filtration technique (ISF) using a 0.45 μm pore size filter to remove silica from BioCaRGOS samples prior to analysis. B) Plot of DLS counts showing > 70-80% removal of colloidal silica from BioCaRGOS by ISF. C) KRAS (G12D) ctDNA concentrations (ng/mL) extracted from Seracare reference material containing BioCaRGOS (w/o MeOH and limited silica) employing rotary evaporation and ISF, prior to cfDNA extractions, against controls.

We obtained nearly 96% recovery after removal of silica and methanol from BioCaRGOS solutions demonstrating a very facile and efficient method for release of ctDNA from the silica matrix with comparable integrity to that of ctDNA present in control (buffer) solutions as illustrated in (Figure 4-7).

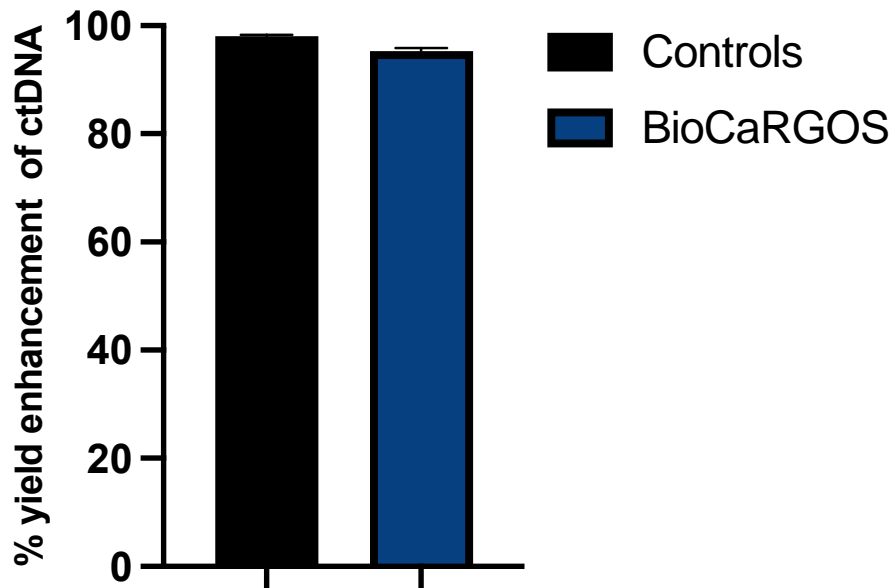


Figure 4-7. Percentage yield enhancement of ctDNA in BioCaRGOS samples demonstrating ~96% recovery.

4.4 Conclusions

In summary, we have demonstrated that BioCaRGOS is highly compatible with sensitive analytical techniques. The mutant KRAS (G12D) ctDNA was selected as the biomarker of interest as it is found in extremely low concentrations in clinical samples. The main goal of this project was to test the compatibility of BioCaRGOS with the extraction of ctDNA from semi-synthetic plasma reference material. Preliminary data suggested that the methanol by-product from BioCaRGOS synthesis interfered with ddPCR measurements. This interference was eliminated by incorporating distillation via rotary evaporation to remove methanol prior to addition of biospecimen. We further demonstrated that BioCaRGOS interfered with the extraction process of ctDNA by causing slow filtration through extraction columns and low recovery of ctDNA was observed by ddPCR analysis. We minimized this interference by incorporating an inverted filtration technique that improved the flow through rate

as well as the yield of ctDNA recovery. These modifications to the workflow of BioCaRGOS containing samples allow for use of BioCaRGOS for stabilization of trace quantities of nucleic acid biomarkers such as plasma ctDNA while retaining the capability of recovery of the biomarker and PCR-based quantification. Figure 4-8 illustrates the complete workflow from the synthesis of BioCaRGOS through the ctDNA extraction process. Moreover, we have developed a highly downstream compatible sol-gel based encapsulation matrix called BioCaRGOS. Thus, we have tailored BioCaRGOS for not only long-term stabilization of biospecimens but improved the compatibility of BioCaRGOS with the downstream applications.

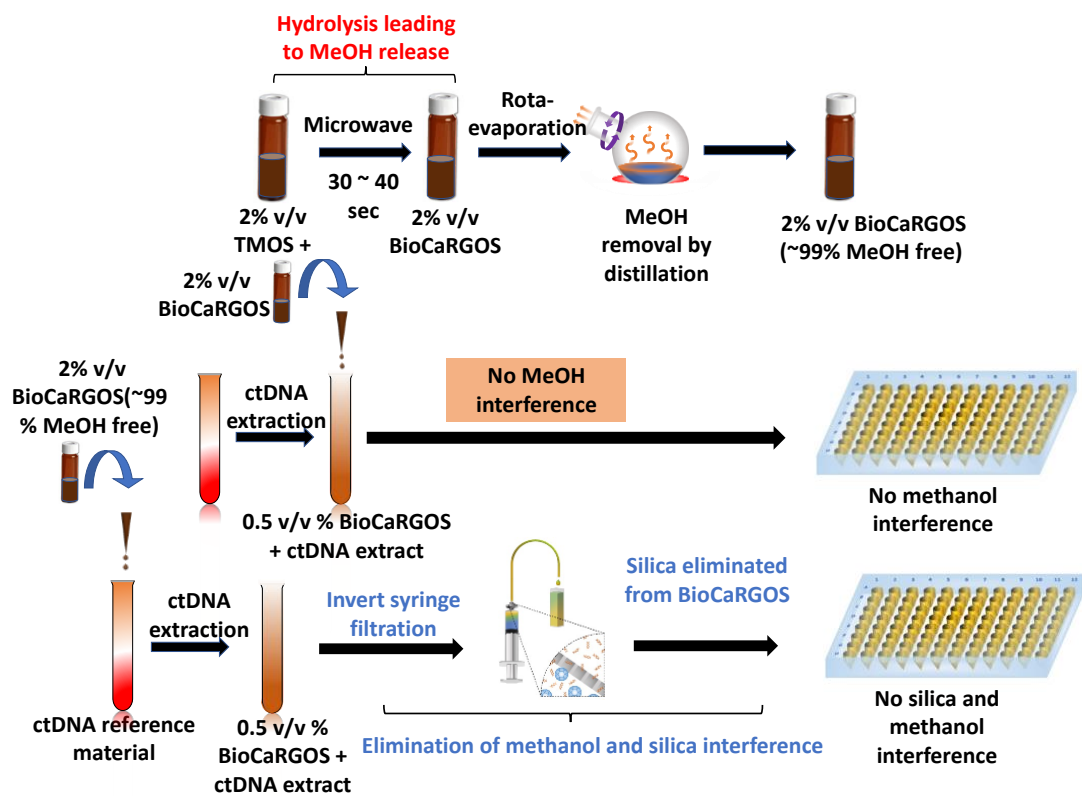


Figure 4-8. BioCaRGOS synthesis and complete workflow of ctDNA extraction

CHAPTER 5
INVESTIGATING BIOCARGOS FOR STABILITY OF HEME
PROTEINS UNDER ENZYMATIC DEGRADATION AND LOW PH

5.1 Introduction

Therapeutic proteins are a class of biologics that are designed to treat a variety of diseases and medical conditions and are an important class of biomolecules that are typically large, complex molecules. Advantages of protein-based drugs include better specificity and lesser side effects relative to other methods. They are also considered safer than gene therapy as they do not alter genetic structure.⁷⁴ Significant challenges to the use of therapeutic proteins include their large molecular size and degradation due to low chemical and physical stability.⁷⁵⁻⁷⁷ Of these, harsh process conditions such as elevated temperature, pH variation, organic solvents, and deactivation enzymes are the major barriers. Due to this, most proteins are typically stored at low temperatures (≤ 4 °C) resulting in a dependence on refrigeration for storage and cold-chain for transportation.⁷⁸ As previously discussed in Chapters 3 and 4, alternative techniques to cold storage methods such as addition of stabilizing agents (sugars, salts, and polyols),^{79, 80} immobilization of the protein onto surfaces, and encapsulation of proteins into hydrated organic and inorganic matrices have been employed. Two of the most common techniques for protein immobilization are sol-gel encapsulation and adsorption onto inorganic porous

materials (e.g., silica, activated carbon, aluminum oxide, iron oxide and metal organic frameworks).

Silica sol-gel is a porous and amorphous material that can be synthesized at low temperatures and mild pHs. As described in Chapter 2, over the past three decades there has been considerable advancement on the sol-gel stabilization of proteins and nucleic acids. However, these techniques have certain limitations, such as the use of highly concentrated silica precursor (30-50 v/v % TMOS/TEOS), the presence of methanol byproduct, and lengthy synthetic procedures. Additionally, the glass like matrix of silica sol-gels requires the use of harsh chemicals to release the biospecimen. To overcome these challenges, we have used BioCaRGOS to encapsulate these proteins and investigate their stability. Our BioCaRGOS (Capture and Release Gels for Optimized Storage of biospecimens) system utilizes a short microwave treatment for the hydrolysis of tetramethyl orthosilicate (TMOS). The resulting solution is then subjected to rotary evaporation to remove the methanol byproduct from the desired orthosilicic acid [Si(OH)₄].

In the current study, we have utilized BioCaRGOS to investigate the stability of the heme proteins myoglobin (Mb) and cytochrome c (Cyt c) and advance BioCaRGOS to be applicable in downstream processes. The two proteins were selected as they have different isoelectric points and are susceptible to denaturation in the presence of proteinase K and low pH conditions. Further, their folding mechanisms in solution are well characterized and easy to assess via spectroscopic techniques.

Myoglobin is a protein found in muscle tissues that plays an important role in the storage and transport of oxygen in muscle cells. It is a globular

protein that contains a heme group, which is responsible for binding and transporting oxygen. It is also important in the diagnosis and treatment of certain medical conditions. For example, elevated levels of myoglobin in the bloodstream can be a sign of muscle damage or injury, such as in the case of a heart attack. It has been the subject of examination with regard to protein structure and its stability against protease digestion has been quantified by monitoring change in heme absorption at 409 nm as a function of proteinase K induced unfolding.⁸¹⁻⁸³ Myoglobin is a relatively stable protein, but its stability against proteinase K depends on several factors such as concentration and activity of the proteinase K enzyme, the pH and temperature of storage condition, and presence of any external denaturants.

Cyt c is primarily known for its function in the mitochondria as a key participant in the life-supporting function of ATP synthesis and electron-transfer processes in the respiratory system. Due to the presence of the heme prosthetic group, it has gained importance for catalysis in presence of organic solvents. It can be also used for various other applications such as electron transfer elements between electrodes and surface bound enzymes.⁸⁴ This makes it very crucial to improve the stability of Cyt c under harsh conditions for various applications.

In this Chapter, we report BioCaRGOS as an efficient and greener silica sol-gel approach for the preservation of Mb and Cyt c. The BioCaRGOS strategy includes an efficient release of the protein in its native form, from the sol-gel matrix without the use of toxic reagents or harsh conditions. The structural stability of the proteins in BioCaRGOS was established using various techniques such as UV-vis and circular dichroism (CD) spectroscopies. To

further confirm the long-term stability in presence of harsh conditions, we demonstrated excellent stability of Mb in presence of proteinase K at ambient temperature (25 °C).

5.2 Experimental

5.2.1 Materials

Tetramethyl orthosilicate, sodium chloride, freeze-dried Mb, Cyt c from equine heart with purity >95%, proteinase K, sodium phosphate monobasic, sodium phosphate dibasic, 15.0 mL centrifuge tubes, and UV-vis cuvettes were purchased from Sigma Aldrich (Saint Louis, MO, USA). Nuclease free water was purchased from New England BioLabs (MA, USA). The 96 well plates were purchased from Thermo Fisher Scientific (MA, USA). Methanol elimination was performed on Buchi R-124 Rotary Evaporator System (Delaware, US). Microwave oven (Panasonic NN-SN651B) for 30 s (400-600W) was used for BioCaRGOS synthesis.

5.2.2 BioCaRGOS Synthesis

A 10.0 v/v % TMOS stock-solution was prepared in doubly deionized water and transferred to a 40.0 mL glass vial. The vial was closed with a screw cap and heated via microwave for thirty seconds to initiate hydrolysis. Post-microwave, the solution was then subjected to rotary evaporation for 30 minutes at a controlled pressure (25 mbar) and temperature (45 °C) to remove the methanol byproduct. This methanol free TMOS stock solution was allowed to cool to room temperature. After the equilibrium was reached, doubly deionized water was added to formulate the final desired concentration of 0, 1, 2.5, 5 and 7.5 v/v %.

5.2.3 Encapsulation of protein in BioCaRGOS

Encapsulation of proteins (Mb and Cyt c) was carried out in BioCaRGOS by addition of 0.06 mL of 10 mg/mL stock to achieve a final concentration of 0.2 mg/mL to which (0-7.5) v/v % BioCaRGOS was added, and 0.5 M phosphate buffer was added to constitute the remainder of the 3.0 mL solution.

5.2.4 Release of Mb post encapsulation

Encapsulated Mb was separated from BioCaRGOS matrix using Millipore Ultrafree MC 0.22 μ m centrifugal filters (Billerica, MA, USA) spun for 15 mins at 14,000 x g. The aqueous filtrate was collected to quantify the amount of Mb released by UV-vis spectroscopy and DLS studies.

5.2.5 Spectroscopic Characterization

Absorbance measurements in the range of 260 to 700 nm were carried out using a Varian Cary 50 Bio UV-visible spectrometer, Agilent Technologies, Santa Clara, CA. Quartz cuvettes were used for the measurements. Circular dichroism (CD) spectra were recorded on a JASCO J-815 spectropolarimeter (JASCO Corporation, Tokyo, Japan) using a cylindrical quartz cell with a path length of 1 mm. Changes in the secondary structure of the protein were monitored in the far UV region between 190 and 260 nm. Four consecutive scans were averaged and corrected by subtracting corresponding blanks.

5.2.6 Proteolysis experiment

For UV-vis absorption measurements, 50 μ L of 0.1 wt/v % proteinase K was added to 3mL of [0-7.5 v/v % BioCaRGOS, 0.2 mg/mL Mb in 0.5 M phosphate buffer pH 7.4]. The samples were incubated for 30 minutes prior to UV-Vis measurements. For CD measurements, the samples were mixed thoroughly and transferred to 1 mm path length quartz cuvettes pre-equilibrated

to the reaction temperature inside the CD sample holder. The CD signal at 222 nm was recorded with an averaging time of 15 seconds.

5.3 Results

5.3.1 BioCaRGOS synthesis and encapsulation of Mb

An overall schematic overview of the BioCaRGOS process developed for encapsulation of biospecimens is shown in Figure 5-1A. First, the silica precursor TMOS is hydrolyzed in an aqueous solution by heating within a standard benchtop microwave for 30 seconds. The key hydrolysis reaction is highlighted in Figure 5-1B. TMOS has four methoxy groups that are hydrolyzed yielding orthosilicic acid $[\text{Si}(\text{OH})_4]$ with the release of methanol as a byproduct. The methanol byproduct, which can be deleterious to the biospecimen stability, is removed by rotary evaporation.⁸⁵ After the removal of methanol (nearly ~99%), a known concentration of the BioCaRGOS is added to (Mb/Cyt c in 0.5 M phosphate buffer) which results in the condensation of hydrolyzed silica precursor as shown in Figure 5-1A. This complete self-sterile immobilization of any biospecimen can be achieved in less than 10 minutes. The process is highly compatible with clinical and downstream processes.

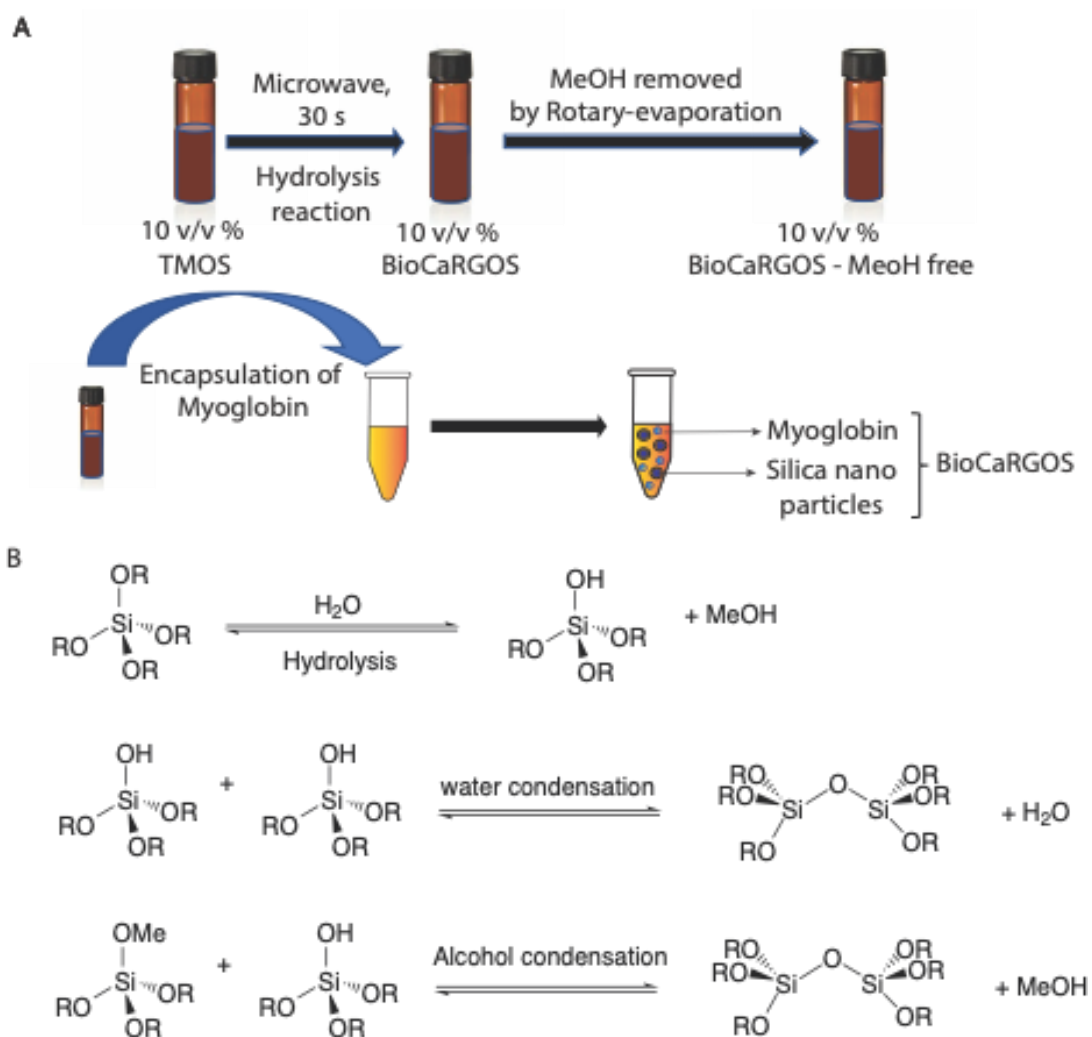


Figure 5-1. (A) Schematic overview of BioCaRGOS synthesis and Mb encapsulation. (B) Mechanism of BioCaRGOS sol gel synthesis.

To compare unfolding of Mb within BioCaRGOS to unfolding in controls (i.e., w/o BioCaRGOS), it is important to establish that the same native structure is the reaction starting point. A previous study encountered difficulties with Mb partially unfolding during encapsulation.⁸⁶ Investigation of this protocol identified insufficient water during the microwave hydrolysis step and ineffective removal of the methanol byproduct as likely sources of the observed Mb degradation. In this study, we have addressed both these issues by increasing the water volume during the hydrolysis step and subjecting hydrolyzed TMOS

to rotary evaporation for 30 mins at 45 °C to remove the methanol from BioCaRGOS. With these simple modifications the UV-vis spectrum of Mb encapsulated in our BioCaRGOS sol gel matrix is identical to the spectrum of a control sample (w/o BioCaRGOS) indicating that our encapsulation process does not perturb the Mb conformation (Figure A9).

5.3.2 Stability of Mb against Proteinase K

Purified proteins in their native state are known to be slightly disordered with certain sections in their unfolded state.⁸⁷ For heme proteins, UV-vis spectroscopy can detect loss or alterations in the heme chromophore and can be an effective indicator of changes in the primary and secondary structure.⁴³⁴⁴ In addition, losses in the heme and the resulting change in the secondary structure are indicative of alteration of tertiary structure conformation as each of the subunits are integral to the tertiary structure of the molecule.⁴³ Changes within the overall globin structure of Mb subunits are complex and are best described by CD and UV-vis spectroscopy. Figure 5-2 shows the UV-vis spectra of metaquo Mb in presence of 0.1 wt/v % proteinase K at pH 7.4 at 25 °C over the period of 24 hr in the absence of BioCaRGOS i.e., control samples. The spectra with the Soret band in the 409 nm region (Figure 5-2A) and a 633 nm band in the Q-band region (Figure 5-2B) are indicative of the metaquo state of the protein.⁸⁸

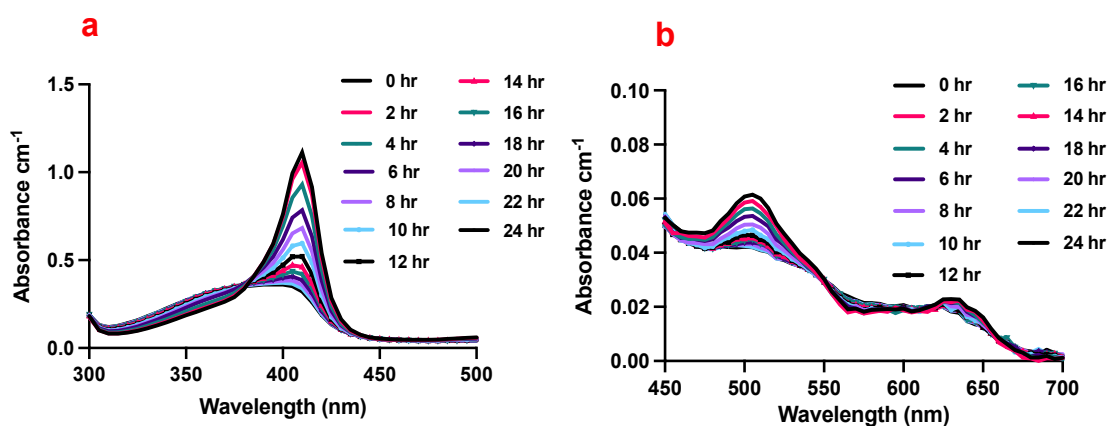


Figure 5-2. UV-vis spectra of metaquo Mb upon addition of 0.1 wt/v % proteinase K at 25 °C at pH 7.4 over 24 h period. The Soret bands of metaquo Mb (409 nm) and the denatured, free heme are shown in (A), while the Q-band region is shown in (B). The 633 nm band in the Q region is from metaquo Mb.

Addition of proteinase K to the control Mb samples in the absence of BioCaRGOS results in the changes to the spectra in both the UV and visible regions. In the presence of relatively high concentrations of proteinase K, the spectra show a substantial shift in the Soret band from the 409 nm to 370 nm region (Figure 5-2A). The broad Soret band in the 370 nm region has been attributed to the absorbance of free heme. Thus, a structural change of the heme pocket upon denaturation results in the release of the heme cofactor.⁸⁹⁻⁹¹ The most likely cause of heme loss within the control samples is unfolding of the helices.

Next, the effect of BioCaRGOS on the stability of Mb in presence of 0.1 wt/v % proteinase K was evaluated. While maintaining a constant Mb concentration (0.2 mg/mL) and buffer environment (0.5 M phosphate buffer, pH 7.4), samples with a variety of BioCaRGOS concentrations (0 – 7.5 v/v %) were prepared and spectroscopically monitored over a period of 24 hours (Figure 3). Relative to the control Mb samples, (i.e., w/o BioCaRGOS), the results show a

two-fold [1.0 v/v % BioCaRGOS] and approximately three-fold [2.5 v/v % BioCaRGOS] increase in Mb stability in BioCaRGOS matrix over 24 h period. This demonstrates a BioCaRGOS concentration dependent trend in determining the physical and chemical stability of Mb. Figure 5-3 shows that 5.0 and 7.5 v/v % BioCaRGOS retained nearly ~95% stability for 24 h. This suggests that higher BioCaRGOS concentrations were, therefore, ideal for storing the Mb against the proteolytic degradation at room temperature.

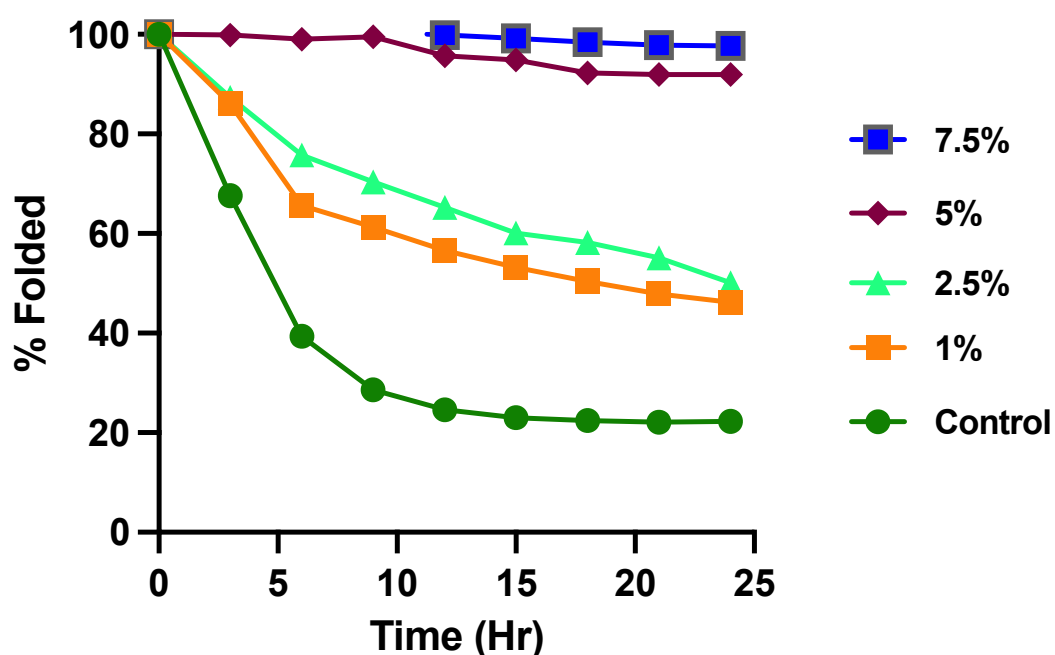


Figure 5-3. Myoglobin stability with incremental increase in BioCaRGOS concentration (0 – 7.5 v/v %). An unaltered UV-vis absorbance band (409 nm) of heme group of Mb was observed in BioCaRGOS formulations (5 and 7.5 v/v %).

Myoglobin contains an abundant amount of helical structure. Helicity of 82% has been estimated by the simulation of the CD spectrum at 25 °C using the reference spectra of protein secondary structures determined by Chen et.al.⁹²
⁹³ The CD spectra of the Mb in controls and BioCaRGOS (1 and 2.5 v/v %) show prominent bands at 208 nm (π - π^* transition) and 222 nm (n - π^* transition).

In the presence of proteinase K, the CD spectrum of native Mb, indicative of α -helix, was preserved to certain extent in 1 v/v % BioCaRGOS but it was nearly ~100 % preserved in 2.5 v/v % BioCaRGOS formulations as shown in Figure 5-4, respectively. The results indicate that the secondary structure of Mb was completely unfolded by proteinase K in control samples, whereas in BioCaRGOS the proteinase K activity was inhibited.

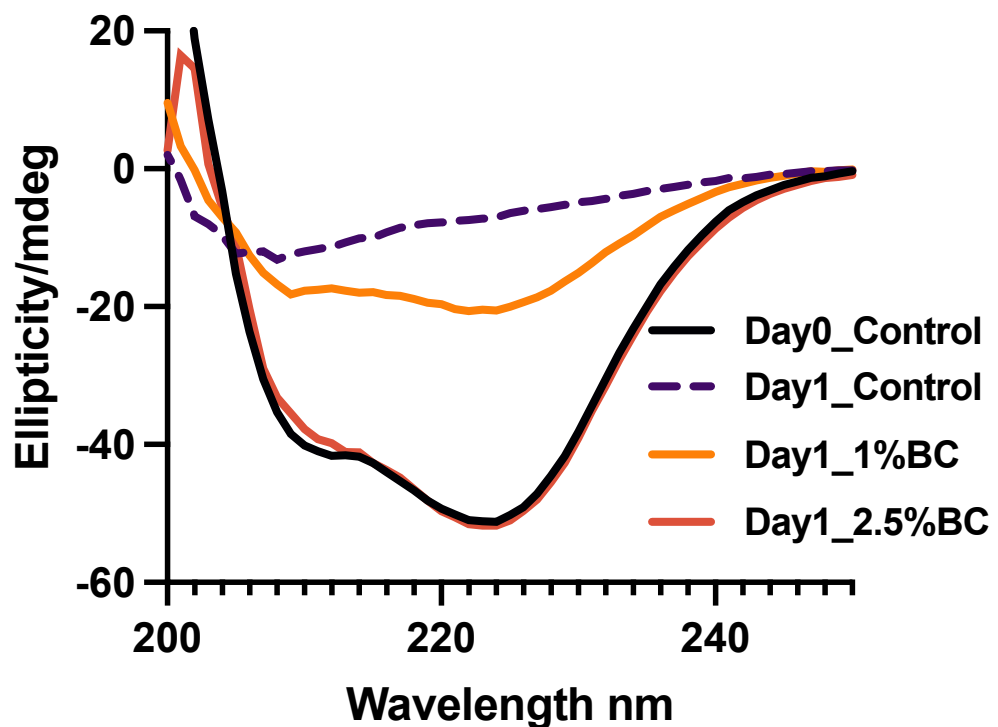


Figure 5-4. CD spectra of Mb encapsulated in 1 and 2.5 v/v % BioCaRGOS vs controls. Note: Day 0 Control was similar to Day 0 1 and 2.5 v/v % BC. Denatured Mb conformation indicated by dotted line (purple). CD spectra of Mb encapsulated in 2.5 v/v % BioCaRGOS vs controls demonstrating intact 2° structure of Mb as compared to Mb in controls which was denatured over 24 h.

The unfolding of Mb is observed in the presence of 1 v/v % BioCaRGOS, albeit more slowly than in control formulations. In controls, complete unfolding occurs within 24 h. Peterson et al. suggested that heme loss from ferric Mb in

their gels and controls occurs only after sufficient unfolding to allow water to enter the pocket, which weakens the Fe-His bond and disrupts hydrophobic interactions.⁹⁴ Sol-gels, such as BioCaRGOS, restrict the motions that open the hydrophobic, folded heme pocket making it difficult for water molecules to encounter the heme group. As a result, we see a slow disruption of the Mb helicity.

The superior protein storage demonstrated by higher (2.5 v/v %) BioCaRGOS formulations highlight another key feature of the system. The conditions mimicked in BioCaRGOS formulations are very similar to biological pH and ionic strength. Under these conditions, the Mb and the silica will exhibit negative charges as the pH of the formulations is greater than their isoelectric points of Mb ~6.5-6.7 and silica nanoparticles ~1.5-3.6, respectively. Therefore, electrostatic repulsive forces dominate, and the Mb is stabilized. On the other hand, proteinase K has an isoelectric point (pI = ~10) greater than its near-physiological pH environment (pH 7-8). As such, it will electrostatically adsorb on the negatively charged silica of BioCaRGOS resulting in deactivation of the proteinase K. Therefore, BioCaRGOS not only provides stabilization to biospecimen encapsulated in it but also denatures enzymes that can degrade them and thus they prove to be an efficient storage solution.

5.3.3 Long term storage of Mb in presence of Proteinase K

It is well known that structural integrity of proteins is disturbed when degrading enzymes, such as proteinase K, are present. To investigate the long-term stability of Mb in presence of proteinase K in BioCaRGOS we evaluated the UV-vis absorbance of the heme group of Mb over 15 days. The data demonstrated that Mb encapsulated in BioCaRGOS (5 and 7.5 v/v %) in

presence of proteinase K was not perturbed by the addition of proteinase K indicating a robust silica network which preserved the Mb structure. On the other hand, Mb in control samples (without BioCaRGOS) showed a steep decrease in terms of stability of Mb upon addition of proteinase K in just 24 hrs (Figure 5-5). As a result, > 90% of the Mb structure is intact over 15 days in BioCaRGOS, whereas Mb in controls is deactivated within the first week of storage.

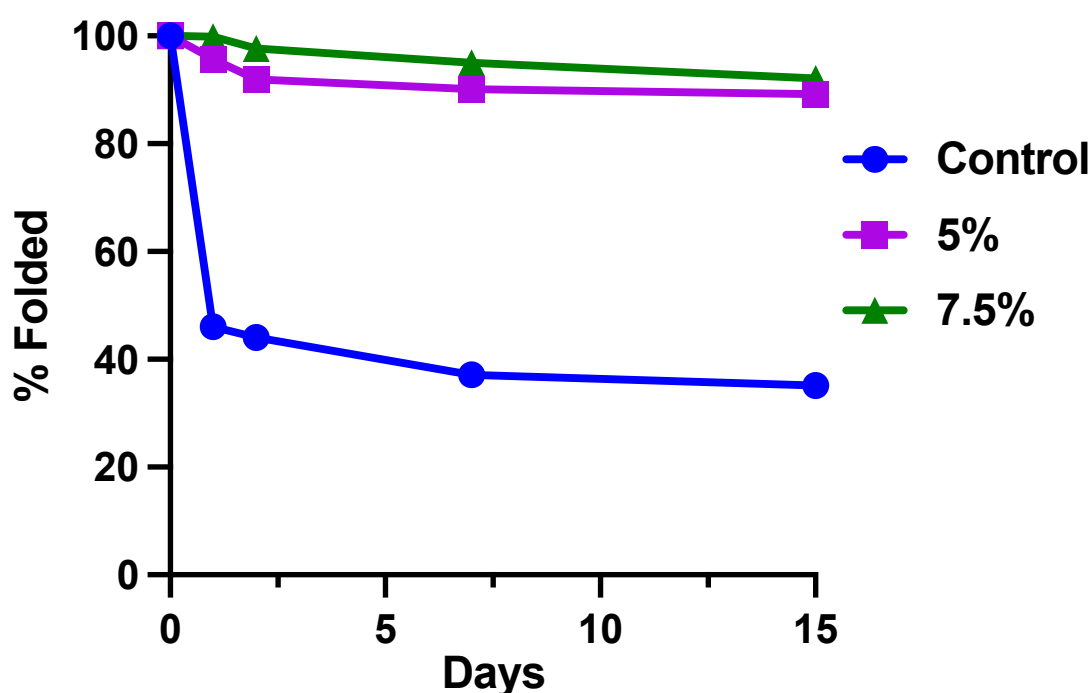


Figure 5-5. Long term storage in presence of proteinase K of Mb encapsulated in 5 and 7.5 v/v % BioCaRGOS demonstrating excellent stability as compared to Mb in control samples.

5.3.4 Release of encapsulated Mb from BioCaRGOS matrix

An important aspect of any stabilizing agent is the ability to release the encapsulated biospecimen. A major advantage of the BioCaRGOS system is the ability to release the biospecimen in an efficient and facile manner. The

encapsulated Mb can be released from the BioCaRGOS formulation [5 v/v % TMOS; 0.01 w/v % 0.2 mg/mL Mb; 0.5 M PB, pH 7.4; 3.0 mL] by centrifugation in a 0.22 μm centrifugal filter for 15 mins at 14,000 x g (Figure 5-6). The recovered Mb in the filtrate displays an intact Mb heme group as compared to its native form. We attribute this excellent release phenomenon to the formulation pH of 7.4, which is higher than the isoelectric points of both silica nano particles and Mb. Thus, electrostatic repulsion between Mb and the BioCaRGOS prevents binding of Mb onto the silica nano particles allowing for ~98% heme recovery, based on absorbance, post encapsulation. (Figure A10)

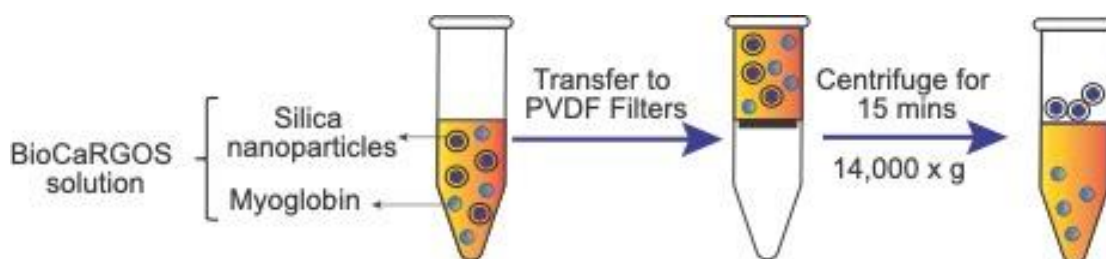


Figure 5-6. Schematic representation of release of Mb from 5 v/v % BioCaRGOS solution.

Dynamic light scattering (DLS) was used to further confirm the removal of silica nanoparticles from the protein solution. No colloidal particles were detected in the filtrate indicating that silica particles from BioCaRGOS formulation had been separated completely. This was further confirmed with a negative control where in the sample [5 v/v % TMOS; 0.01 w/v % Mb; 0.5 M PB, pH 7.4; 3.0 mL] was tested before filtration. Upon measuring the DLS, the nanoparticles exhibited a size of 180 ± 3.29 . This DLS study confirmed the presence of removal of silica from the protein solution.

5.3.5 Effect of BioCaRGOS and their concentration on the stability of Cyt c at low pH

To extend the applicability of BioCaRGOS technology to preserve heme proteins with a higher pI, we investigated Cyt c (pI = ~9.6) as a model protein. Cytochrome c is not susceptible to unfolding by proteinase K under neutral pH conditions due to charge repulsion of the positively charged species. Hence, we investigated the scope of BioCaRGOS as an effective stabilizer of Cyt c against harsh acidic conditions (pH = 2.5). The acid induced denaturation of Cyt c in controls (w/o BioCaRGOS) and encapsulated in BioCaRGOS was investigated following the shift of the Soret absorption band as a function of time. Acidification affects the absorption spectrum of Cyt c in controls as shown in Figure 5-7A, the Soret band (which is sensitive to the spin state of the heme-iron and to the nature of the axial ligands) blue-shifts from 410 nm to ~394 nm, within 10 mins of encapsulation indicating full protein unfolding.⁹⁵ UV-vis absorption allows to infer the conformational changes of proteins in solvent media. Due to the presence of the heme prosthetic group, Cyt c shows some characteristic absorption bands.

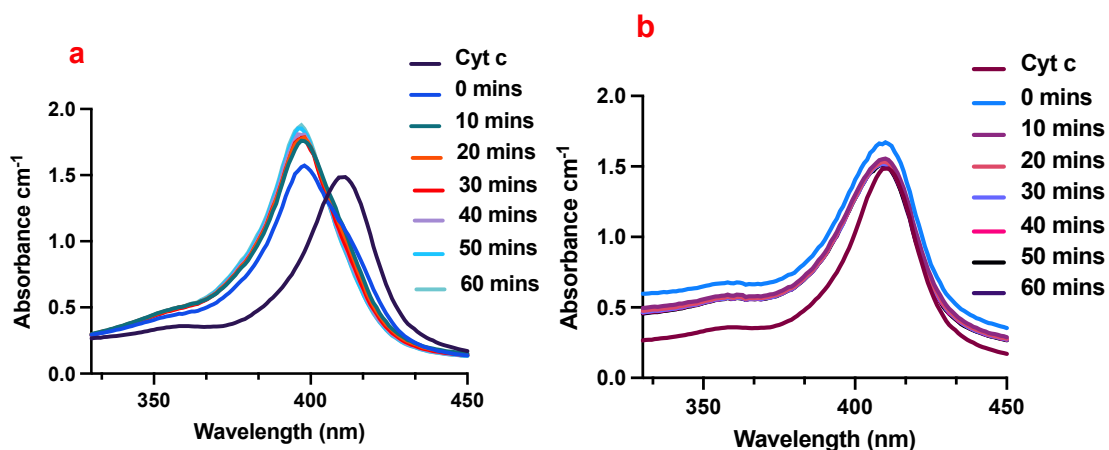


Figure 5-7. UV-vis absorption spectrum of Cyt c encapsulated at pH 2.5 over the period of 1 h (A) in control samples (w/o BioCaRGOS) (B) in 7.5 v/v % BioCaRGOS.

As shown in Figure 5-7B, it is clearly evident that there is no significant shift in wavelength maxima of Cyt c in presence of 7.5 v/v % BioCaRGOS even within 1 hr of encapsulation and did not affect the polypeptide environment around the heme group. However, it was observed that with low concentrations of BioCaRGOS, there was a blue shift observed albeit more slowly. We further evaluated the stability of Cyt c, over 6 hrs in control and BioCaRGOS formulations (Figure 5-8). We attribute this increased stability in 7.5 v/v % BioCaRGOS to greater restrictions in the motion of the biospecimen, which allow the Cyt c structure to remain intact.

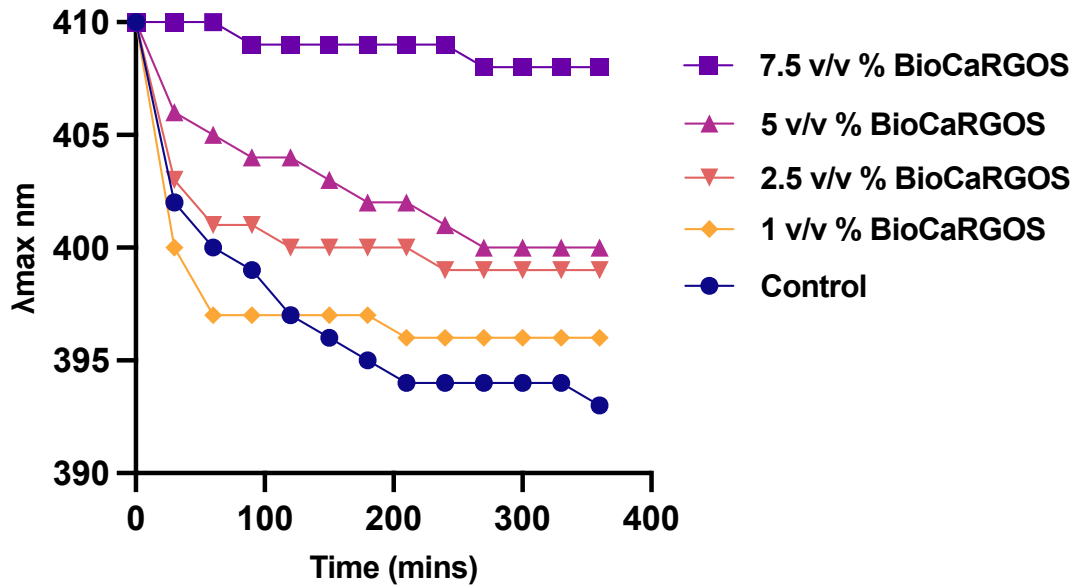


Figure 5-8. Cyt c stability with incremental increase in BioCaRGOS concentration (0-7.5 v/v %). An unaltered UV-vis absorbance band (409 nm) of heme group of Cyt c was observed in BioCaRGOS formulations (7.5 v/v %).

5.4 Conclusions

In summary, we have developed not only a biocompatible approach but a greener and less toxic synthetic approach for the synthesis of sol-gels. This approach was used to demonstrate the effective protein storage against multiple stresses such as protease degradation and low pH conditions. The model protein used in to examine the stability against proteinase K was Mb and, Cyt c was used as a model protein to examine the stability against pH stress. Both the proteins showed exceptional stability in 5 and 7.5 v/v % BioCaRGOS and it was observed that, Mb was preserved efficiently for over 25 days even in the presence of proteinase K. The mode of stabilization is attributed to the proteinase K inhibition by BioCaRGOS formulations caused by electrostatic attractions. Furthermore, a greener, practical, and downstream compatible approach was used to release the biospecimen/ protein post encapsulation

from BioCaRGOS matrix. Thus, BioCaRGOS technology can be used for not only long-term storage but also to preserve biospecimens from getting denatured due to multiple stresses over short term period.

CHAPTER 6

CONCLUSIONS

Sol gel encapsulation has emerged as an important technique for the encapsulation of biomolecules, particularly proteins and nucleic acids. Proteins and nucleic acids are essential biomolecules that play critical roles in various biological processes. They are used extensively in the fields of biotechnology, biomedicine, and food science. However, these biomolecules are highly sensitive to environmental variations such as temperature, pH, and shear forces, which can lead to their degradation, denaturation, and loss of activity. Therefore, the development of effective encapsulation methods that can protect these biomolecules from harsh conditions is essential.

As detailed in Chapter 2, significant progress in recent years has been made in the development of sol-gel encapsulation methods for proteins and nucleic acids. Several studies have demonstrated the effectiveness of sol-gel matrices in protecting these biomolecules from harsh environmental conditions. For example, sol-gel encapsulation has been used to protect enzymes from high temperatures, proteases from proteolysis, and DNA from degradation by nucleases. Sol-gel encapsulation has also been shown to improve the stability and activity of proteins and nucleic acids in various applications, such as biosensors, drug delivery, and food preservation.

One of the advantages of sol-gel encapsulation is that it allows for the controlled release of encapsulated biomolecules. The porous structure of the sol-gel matrix can be designed to release the encapsulated biomolecules at a specific rate or in response to a particular stimulus. This can be particularly useful in drug delivery applications, where the release of drugs can be controlled to ensure optimal therapeutic outcomes.

Another advantage of sol-gel encapsulation is its biocompatibility. The sol-gel matrix is composed of inorganic materials such as silica or alumina, which are non-toxic and do not elicit an immune response. This makes sol-gel encapsulation a safe and effective approach for the encapsulation of biomolecules for biomedical applications. Despite the promising results obtained using sol-gel encapsulation, the inherently complex nature of conventional sol-gel methods make them hardly applicable to clinical setting. Second, most sol-gel techniques are marred with a critical issue. i.e., the release of biospecimen from gels or glasses after long-term encapsulation. The primary reason for the low recovery of biospecimen is due to the use of high concentrations of silica precursor (typically 30–50%), as the techniques always strived to obtain intact immobilization in a glass like matrix, to restrict the motion of biomolecule.

To address these issues, we engineered capture and release gels for optimized biospecimen storage (BioCaRGOS) by hydrolysis of TMOS using standard microwave as discussed in Chapter 2. The key attributes of BioCaRGOS are (i) a clinically compatible ~1 minute hydrolysis process using a standard bench top microwave (ii) minimal presence of methanol (byproduct) that is not deleterious to biospecimen (iii) effective long-term storage of

biospecimen and (iv) ease of biospecimen recovery through BioCaRGOS matrix using the biocompatible molecule PEG. These sol gel silica matrices were utilized to demonstrate effective protein storage over long durations of time. The model protein used in the study was hemoglobin and its stability was monitored using UV-vis measurements. In addition, stability of sol was determined using Raman Spectroscopy. Up to 5.0 v/v %, BioCaRGOS enhance the shelf life as compared to control samples but lose their efficacy over time. High concentration BioCaRGOS (5.0 & 7.5) v/v % formulations, displayed excellent stability of hemoglobin protein over 33 days at room temperature and 7 months at 4 °C. Furthermore, we developed a biocompatible PEG based protocol to release the proteins from the BioCaRGOS with extremely high yields. The results indicated that BioCaRGOS have a strong potential to stabilize molecules. The scientific insight gained in the study suggests that if the pI of the protein is below the pH of the BioCaRGOS solution, it will achieve stabilization and would be easily recovered. These robust storage, transport, and extraction methods are the keystone of this innovation, and present a technology that can encapsulate a plethora of biospecimens including proteins and nucleic acids as most of them exhibit a pI of less than 7.0.

Chapter 3 illustrates the stability of a highly sensitive cancer biomarker, miRNA 21, at ambient and elevated temperatures (4, 25 and 40 °C) for nearly 3 months, with ~100 % single-step recovery without the need of any purification protocol using BioCaRGOS. The mode of stabilization is attributed to RNase (sterile- compromised contaminated environment) inhibition by optimized aqueous formulations of BioCaRGOS [low ionic strength, optimum pH (~7.46), large hydrodynamic sized and high surface potential] as well as miRNA

immobilization caused by localized interaction of BioCaRGOS matrix. BioCaRGOS formulations are completely compatible with current clinical practices and require no technical expertise and we anticipate their utility in storage of several relevant biospecimens as well as in enhancing the shelf life of several drugs including monoclonal antibodies.

Chapter 4 described the workflow modifications to allow for extraction of cell free DNA (cfDNA) from primary samples containing working concentrations of BioCaRGOS, as well as the compatibility of BioCaRGOS with droplet digital PCR (ddPCR) analysis for pancreatic cancer biomarkers i.e., KRAS circulating tumor DNA (ctDNA). Preliminary attempts to extract ctDNA from BioCaRGOS containing samples demonstrated interference in the extraction of primary samples and the interference with ddPCR analysis when BioCaRGOS was directly introduced to stabilize sample extracts. We minimized this interference by incorporating an inverted filtration technique that improved the flow through rate as well as the yield of ctDNA recovery. These modifications to the workflow of BioCaRGOS containing samples allow for use of BioCaRGOS for stabilization of trace quantities of nucleic acid biomarkers such as plasma ctDNA while retaining the capability of recovery of the biomarker and PCR-based quantification. Thus, we have tailored BioCaRGOS for not only long-term stabilization of biospecimens, but also for improved compatibility of BioCaRGOS with the downstream applications.

Chapter 5 demonstrates the applicability of BioCaRGOS for the storage of heme proteins such as myoglobin and cytochrome c under various stresses. The two proteins were selected as they have different isoelectric points and are susceptible to denaturation in the presence of proteinase K and low pH

conditions. Further, their folding mechanisms in solution are well characterized and easy to assess via spectroscopic techniques. The BioCaRGOS sol gel approach was used to demonstrate the effective protein storage against multiple stresses such as protease degradation and low pH conditions. The model protein used in to examine the stability against proteinase K was Mb and, Cyt c was used as a model protein to examine the stability against pH stress. Both the proteins showed exceptional stability in 5 and 7.5 v/v % BioCaRGOS and it was observed that Mb was preserved efficiently for over 25 days even in the presence of proteinase K. The mode of stabilization is attributed to the proteinase K inhibition by BioCaRGOS formulations caused by electrostatic attractions. Furthermore, a greener, practical, and downstream compatible approach was used to release the biospecimen/ protein post encapsulation from BioCaRGOS matrix. Thus, BioCaRGOS technology can be used for not only long-term storage but also to preserve biospecimens from getting denatured due to multiple stresses over short term period.

REFERENCES

1. Rothschild, L. J.; Mancinelli, R. L., Life in extreme environments. *Nature* **2001**, *409* (6823), 1092-1101.
2. Naber, S. P., Continuing role of a frozen-tissue bank in molecular pathology. *Diagn. Mol. Pathol.* **1996**, *5* (4), 253-9.
3. Naber, S. P.; Smith, L. L., Jr.; Wolfe, H. J., Role of the frozen tissue bank in molecular pathology. *Diagn. Mol. Pathol.* **1992**, *1* (1), 73-9.
4. Lou, J. J.; Mirsadraei, L.; Sanchez, D. E.; Wilson, R. W.; Shabihkhani, M.; Lucey, G. M.; Wei, B.; Singer, E. J.; Mareninov, S.; Yong, W. H., A review of room temperature storage of biospecimen tissue and nucleic acids for anatomic pathology laboratories and biorepositories. *Clin. Biochem.* **2014**, *47* (4), 267-273.
5. Hubel, A.; Spindler, R.; Skubitz, A. P., Storage of human biospecimens: selection of the optimal storage temperature. *Biopreserv Biobank* **2014**, *12* (3), 165-75.
6. Ma, S.; Huang, Y.; van Huystee, R. B., Improved plant RNA stability in storage. *Anal Biochem* **2004**, *326* (1), 122-4.
7. Baker, M., Building better biobanks. *Nature* **2012**, *486* (7401), 141-146.
8. Wan, E.; Akana, M.; Pons, J.; Chen, J.; Musone, S.; Kwok, P. Y.; Liao, W., Green technologies for room temperature nucleic acid storage. *Curr. Issues Mol. Biol.* **2010**, *12* (3), 135-42.
9. Crowe, J. H.; Carpenter, J. F.; Crowe, L. M., The role of vitrification in anhydrobiosis. *Annu. Rev. Physiol.* **1998**, *60* (1), 73-103.

10. Montoya, N. A.; Roth, R. E.; Funk, E. K.; Gao, P.; Corbin, D. R.; Shiflett, M. B., Review on porous materials for the thermal stabilization of proteins. *Microporous Mesoporous mat.* **2022**, *333*, 111750.
11. de Vos, P.; Bučko, M.; Gemeiner, P.; Navrátil, M.; Švitel, J.; Faas, M.; Strand, B. L.; Skjak-Braek, G.; Morch, Y. A.; Vikartovská, A., Multiscale requirements for bioencapsulation in medicine and biotechnology. *Biomaterials* **2009**, *30* (13), 2559-2570.
12. Braun, S.; Rappoport, S.; Zusman, R.; Avnir, D.; Ottolenghi, M., Biochemically active sol-gel glasses: the trapping of enzymes. *Mater. Lett.* **1990**, *10* (1-2), 1-5.
13. Wang, X.; Ben Ahmed, N.; S Alvarez, G.; V Tuttolomondo, M.; Hélyary, C.; F Desimone, M.; Coradin, T., Sol-gel encapsulation of biomolecules and cells for medicinal applications. *Curr. Top. Med. Chem.* **2015**, *15* (3), 223-244.
14. Brinker, C. J.; Scherer, G. W., *Sol-gel science: the physics and chemistry of sol-gel processing*. Academic press: 2013.
15. Avnir, D.; Levy, D.; Reisfeld, R., The nature of the silica cage as reflected by spectral changes and enhanced photostability of trapped rhodamine 6G. *J. Phys. Chem.* **1984**, *88* (24), 5956-5959.
16. Sinkó, K., Influence of chemical conditions on the nanoporous structure of silicate aerogels. *Materials* **2010**, *3* (1), 704-740.
17. Gill, I.; Ballesteros, A., Encapsulation of biologicals within silicate, siloxane, and hybrid sol-gel polymers: an efficient and generic approach. *J. Am. Chem. Soc.* **1998**, *120* (34), 8587-8598.

18. Brook, M. A.; Chen, Y.; Guo, K.; Zhang, Z.; Brennan, J. D., Sugar-modified silanes: precursors for silica monoliths. *J. Mater. Chem.* **2004**, *14* (9), 1469-1479.
19. Shchipunov, Y. A.; Bakunina, I. Y.; Burtseva, Y. V.; Tat'yana, N. Z., A new precursor for the immobilization of enzymes inside sol-gel-derived hybrid silica nanocomposites containing polysaccharides. *J. Biochem. Bioph. Meth.* **2004**, *58* (1), 25-38.
20. Schubert, U. S.; Hüsing, N., *Synthesis of inorganic materials*. John Wiley & Sons: 2019.
21. Zhang, Z.; Tanigami, Y.; Terai, R.; Wakabayashi, H., Preparation of transparent methyl-modified silica gel. Google Patents: 1999.
22. Aelion, R.; Loebel, A.; Eirich, F., Hydrolysis of ethyl silicate. *J. Am. Chem. Soc.* **1950**, *72* (12), 5705-5712.
23. Xi, Y.; Liangying, Z.; Sasa, W., Pore size and pore-size distribution control of porous silica. *Sens. Actuators B: Chem.* **1995**, *25* (1-3), 347-352.
24. Brinker, C. J.; Keefer, K.; Schaefer, D.; Assink, R.; Kay, B.; Ashley, C., Sol-gel transition in simple silicates II. *J. Non-Cryst. Solids* **1984**, *63* (1-2), 45-59.
25. Venkateswara Rao, A.; Parvathy, N., Effect of gel parameters on monolithicity and density of silica aerogels. *J. Mater. Sci.* **1993**, *28* (11), 3021-3026.
26. Meador, M. A. B.; Capadona, L. A.; McCorkle, L.; Papadopoulos, D. S.; Leventis, N., Structure-property relationships in porous 3D nanostructures as a function of preparation conditions: isocyanate cross-linked silica aerogels. *Chem. Mater.* **2007**, *19* (9), 2247-2260.

27. Pierre, A. C.; Pajonk, G. M., Chemistry of aerogels and their applications. *Chem. Rev.* **2002**, *102* (11), 4243-4266.
28. Ronda, L.; Bruno, S.; Campanini, B.; Mozzarelli, A.; Abbruzzetti, S.; Viappiani, C.; Cupane, A.; Levantino, M.; Bettati, S., Immobilization of proteins in silica gel: biochemical and biophysical properties. *Curr. Org. Chem.* **2015**, *19* (17), 1653-1668.
29. Rahmani, A.; Jund, P.; Benoit, C.; Jullien, R., Numerical study of the dynamic properties of silica aerogels. *J. Condens. Matter Phys.* **2001**, *13* (23), 5413.
30. Pohl, E.; Osterholtz, F., Kinetics and mechanism of aqueous hydrolysis and condensation of alkyltrialkoxysilanes. In *Molecular characterization of composite interfaces*, Springer: 1985; pp 157-170.
31. Anderson, M. T.; Sawyer, P. S.; Rieker, T., Surfactant-templated silica aerogels. *Microporous Mesoporous mat.* **1998**, *20* (1), 53-65.
32. Ranjit, K. T.; Martyanov, I.; Demydov, D.; Uma, S.; Rodrigues, S.; Klabunde, K. J., A review of the chemical manipulation of nanomaterials using solvents: Gelation dependent structures. *J. Sol-Gel Sci. Technol.* **2006**, *40*, 335-339.
33. Jones, S. M., A method for producing gradient density aerogel. *J. Sol-Gel Sci. Technol.* **2007**, *44*, 255-258.
34. Kandimalla, V. B.; Tripathi, V. S.; Ju, H., Immobilization of Biomolecules in Sol-Gels: Biological and Analytical Applications. *Crit. Rev. Anal. Chem.* **2006**, *36* (2), 73-106.

35. Jin, W.; Brennan, J. D., Properties and applications of proteins encapsulated within sol–gel derived materials. *Anal. Chim. Acta* **2002**, *461* (1), 1-36.
36. Jordan, J. D.; Dunbar, R. A.; Bright, F. V., Dynamics of acrylodan-labeled bovine and human serum albumin entrapped in a sol-gel-derived biogel. *J. Anal. Chem.* **1995**, *67* (14), 2436-2443.
37. Macdougall, L. J.; Wechsler, M. E.; Culver, H. R.; Benke, E. H.; Broerman, A.; Bowman, C. N.; Anseth, K. S., Charged Poly(N-isopropylacrylamide) Nanogels for the Stabilization of High Isoelectric Point Proteins. *ACS Biomater. Sci. Eng.* **2021**, *7* (9), 4282-4292.
38. Meng, H.; Liang, M.; Xia, T.; Li, Z.; Ji, Z.; Zink, J. I.; Nel, A. E., Engineered design of mesoporous silica nanoparticles to deliver doxorubicin and P-glycoprotein siRNA to overcome drug resistance in a cancer cell line. *ACS Nano* **2010**, *4* (8), 4539-50.
39. Zhou, S.; Schlipf, D. M.; Guilfoil, E. C.; Rankin, S. E.; Knutson, B. L., Lipid Pore-Filled Silica Thin-Film Membranes for Biomimetic Recovery of Dilute Carbohydrates. *Langmuir* **2017**, *33* (49), 14156-14166.
40. Shen, J.; He, Q.; Gao, Y.; Shi, J.; Li, Y., Mesoporous silica nanoparticles loading doxorubicin reverse multidrug resistance: performance and mechanism. *Nanoscale* **2011**, *3* (10), 4314-4322.
41. Tokmakov, A. A.; Kurotani, A.; Sato, K.-I., Protein pl and intracellular localization. *Front. Mol. Biosci.* **2021**, 1179.
42. Lan, H.; Lu, H.; Wang, X.; Jin, H., MicroRNAs as potential biomarkers in cancer: opportunities and challenges. *Biomed Res. Int.* **2015**, 2015.

43. Zhu, Y.; Cheng, G.; Dong, S., Structural electrochemical study of hemoglobin by in situ circular dichroism thin layer spectroelectrochemistry. *Biophys. Chem.* **2002**, *97* (2-3), 129-138.
44. Goodarzi, M.; Moosavi-Movahedi, A. A.; Habibi-Rezaei, M.; Shourian, M.; Ghourchian, H.; Ahmad, F.; Farhadi, M.; Saboury, A. A.; Sheibani, N., Hemoglobin fructation promotes heme degradation through the generation of endogenous reactive oxygen species. *Spectrochim. Acta A Mol. Biomol. Spectrosc.* **2014**, *130*, 561-567.
45. Zerda, T. W.; Hoang, G., High-pressure raman study of the hydrolysis reaction in tetramethylorthosilicate (TMOS). *J. Non-Cryst. Solids* **1989**, *109* (1), 9-17.
46. Chen, Y.-C.; Smith, T.; Hicks, R. H.; Doekhie, A.; Koumanov, F.; Wells, S. A.; Edler, K. J.; van den Elsen, J.; Holman, G. D.; Marchbank, K. J.; Sartbaeva, A., Thermal stability, storage and release of proteins with tailored fit in silica. *Sci. Rep.* **2017**, *7* (1), 46568.
47. Narvaez Villarrubia, C. W.; Tumas, K. C.; Chauhan, R.; MacDonald, T.; Dattelbaum, A. M.; Omberg, K.; Gupta, G., Long-term stabilization of DNA at room temperature using a one-step microwave assisted process. *Emergent Mater.* **2021**.
48. Carrasquilla, C.; Lau, P. S.; Li, Y.; Brennan, J. D., Stabilizing Structure-Switching Signaling RNA Aptamers by Entrapment in Sol–Gel Derived Materials for Solid-Phase Assays. *J. Am. Chem. Soc.* **2012**, *134* (26), 10998-11005.

49. Perumal, S.; Ramadass, S.; Madhan, B., Sol-gel processed mupirocin silica microspheres loaded collagen scaffold: a synergistic bio-composite for wound healing. *Eur. J. Pharm. Sci.* **2014**, *52*, 26-33.
50. Larsericsdotter, H.; Oscarsson, S.; Buijs, J., Thermodynamic Analysis of Proteins Adsorbed on Silica Particles: Electrostatic Effects. *J. Colloid Interface Sci.* **2001**, *237* (1), 98-103.
51. Shang, W.; Nuffer, J. H.; Dordick, J. S.; Siegel, R. W., Unfolding of Ribonuclease A on Silica Nanoparticle Surfaces. *Nano Lett.* **2007**, *7* (7), 1991-1995.
52. Vertegel, A. A.; Siegel, R. W.; Dordick, J. S., Silica Nanoparticle Size Influences the Structure and Enzymatic Activity of Adsorbed Lysozyme. *Langmuir* **2004**, *20* (16), 6800-6807.
53. Lee, C. J.; Jung, J. H.; Seo, T. S., 3D Porous Sol–Gel Matrix Incorporated Microdevice for Effective Large Volume Cell Sample Pretreatment. *J. Anal. Chem.* **2012**, *84* (11), 4928-4934.
54. Lee, C. S.; Belfort, G., Changing activity of ribonuclease A during adsorption: a molecular explanation. *Proc. Natl. Acad. Sci. U.S.A.* **1989**, *86* (21), 8392.
55. Santoro, J.; González, C.; Bruix, M.; Neira, J. L.; Nieto, J. L.; Herranz, J.; Rico, M., High-resolution three-dimensional structure of ribonuclease A in solution by nuclear magnetic resonance spectroscopy. *J. Mol. Biol.* **1993**, *229* (3), 722-34.
56. Tripathy, D. R.; Dinda, A. K.; Dasgupta, S., A simple assay for the ribonuclease activity of ribonucleases in the presence of ethidium bromide. *Anal. Biochem.* **2013**, *437* (2), 126-129.

57. Vertegel, A. A.; Siegel, R. W.; Dordick, J. S., Silica nanoparticle size influences the structure and enzymatic activity of adsorbed lysozyme. *Langmuir* **2004**, *20* (16), 6800-7.
58. Roach, P.; Farrar, D.; Perry, C. C., Surface Tailoring for Controlled Protein Adsorption: Effect of Topography at the Nanometer Scale and Chemistry. *J. Am. Chem. Soc.* **2006**, *128* (12), 3939-3945.
59. Fabre, A. L.; Colotte, M.; Luis, A.; Tuffet, S.; Bonnet, J., An efficient method for long-term room temperature storage of RNA. *Eur. J. Hum. Genet.* **2014**, *22* (3), 379-85.
60. Mutter, G. L.; Zahrieh, D.; Liu, C.; Neuberg, D.; Finkelstein, D.; Baker, H. E.; Warrington, J. A., Comparison of frozen and RNALater solid tissue storage methods for use in RNA expression microarrays. *BMC Genom.* **2004**, *5* (1), 88.
61. Ma, Y.; Gamagedara, S., Biomarker analysis for oncology. *Biomark. Med.* **2015**, *9* (9), 845-50.
62. McGuigan, A.; Kelly, P.; Turkington, R. C.; Jones, C.; Coleman, H. G.; McCain, R. S., Pancreatic cancer: A review of clinical diagnosis, epidemiology, treatment and outcomes. *World J. Gastroenterol.* **2018**, *24* (43), 4846-4861.
63. Fernandez-Garcia, D.; Hills, A.; Page, K.; Hastings, R. K.; Toghil, B.; Goddard, K. S.; Ion, C.; Ogle, O.; Boydell, A. R.; Gleason, K.; Rutherford, M.; Lim, A.; Guttery, D. S.; Coombes, R. C.; Shaw, J. A., Plasma cell-free DNA (cfDNA) as a predictive and prognostic marker in patients with metastatic breast cancer. *Breast Cancer Res.* **2019**, *21* (1), 149.
64. Mao, Z.; Xiao, H.; Shen, P.; Yang, Y.; Xue, J.; Yang, Y.; Shang, Y.; Zhang, L.; Li, X.; Zhang, Y.; Du, Y.; Chen, C.-C.; Guo, R.-T.; Zhang, Y.,

KRAS(G12D) can be targeted by potent inhibitors via formation of salt bridge.
Cell Discov. **2022**, 8 (1), 5.

65. Wang, L.; Barth, C. W.; Sibrian-Vazquez, M.; Escobedo, J. O.; Lowry, M.; Muschler, J.; Li, H.; Gibbs, S. L.; Strongin, R. M., Far-Red and Near-Infrared Semianaphthofluorophores for Targeted Pancreatic Cancer Imaging. *ACS Omega* **2017**, 2 (1), 154-163.

66. Johansson, G.; Andersson, D.; Filges, S.; Li, J.; Muth, A.; Godfrey, T. E.; Ståhlberg, A., Considerations and quality controls when analyzing cell-free tumor DNA. *Biomol. Detect. Quantif.* **2019**, 17, 100078-100078.

67. Thierry, A. R.; El Messaoudi, S.; Gahan, P. B.; Anker, P.; Stroun, M., Origins, structures, and functions of circulating DNA in oncology. *Cancer Metastasis Rev.* **2016**, 35 (3), 347-376.

68. Livage, J.; Coradin, T.; Roux, C., Encapsulation of biomolecules in silica gels. *J. Condens. Matter Phys.* **2001**, 13 (33), R673-R691.

69. Pierre, A. C., The sol-gel encapsulation of enzymes. *Biocatal. Biotransformation* **2004**, 22 (3), 145-170.

70. Tu, J.; Boyle, A. L.; Friedrich, H.; Bomans, P. H. H.; Bussmann, J.; Sommerdijk, N. A. J. M.; Jiskoot, W.; Kros, A., Mesoporous Silica Nanoparticles with Large Pores for the Encapsulation and Release of Proteins. *ACS Appl. Mater. Interfaces* **2016**, 8 (47), 32211-32219.

71. Tang, F.; Li, L.; Chen, D., Mesoporous Silica Nanoparticles: Synthesis, Biocompatibility and Drug Delivery. *Adv. Mater.* **2012**, 24 (12), 1504-1534.

72. Woignier, T.; Fernandez-Lorenzo, C.; Sauvajol, J. L.; Schmit, J. F.; Phalippou, J.; Sempere, R., Raman study of structural defects in SiO₂ aerogels. *J. Sol-Gel Sci. Technol.* **1995**, 5 (3), 167-172.

73. Smeraldi, J.; Ganesh, R.; Safarik, J.; Rosso, D., Statistical evaluation of photon count rate data for nanoscale particle measurement in wastewaters. *J. Environ. Monit.* **2012**, *14* (1), 79-84.
74. Gu, Z.; Biswas, A.; Zhao, M.; Tang, Y., Tailoring nanocarriers for intracellular protein delivery. *Chem. Soc. Rev.* **2011**, *40* (7), 3638-3655.
75. Deodhar, G. V.; Adams, M. L.; Trewyn, B. G., Controlled release and intracellular protein delivery from mesoporous silica nanoparticles. *Biotechnol. J.* **2017**, *12* (1).
76. Leader, B.; Baca, Q. J.; Golan, D. E., Protein therapeutics: a summary and pharmacological classification. *Nat. Rev. Drug. Discov.* **2008**, *7* (1), 21-39.
77. Xu, C.; Lei, C.; Yu, C., Mesoporous Silica Nanoparticles for Protein Protection and Delivery. *Front. Chem.* **2019**, *7*.
78. Welch, R. P.; Lee, H.; Luzuriaga, M. A.; Brohlin, O. R.; Gassensmith, J. J., Protein-Polymer Delivery: Chemistry from the Cold Chain to the Clinic. *Bioconjug. Chem.* **2018**, *29* (9), 2867-2883.
79. O'Shea, T. M.; Webber, M. J.; Aimetti, A. A.; Langer, R., Covalent Incorporation of Trehalose within Hydrogels for Enhanced Long-Term Functional Stability and Controlled Release of Biomacromolecules. *Adv. Healthc. Mater.* **2015**, *4* (12), 1802-12.
80. Piskiewicz, S.; Gunn, K. H.; Warmuth, O.; Propst, A.; Mehta, A.; Nguyen, K. H.; Kuhlman, E.; Guseman, A. J.; Stadtmiller, S. S.; Boothby, T. C.; Neher, S. B.; Pielak, G. J., Protecting activity of desiccated enzymes. *Protein Sci.* **2019**, *28* (5), 941-951.

81. Ballew, R. M.; Sabelko, J.; Gruebele, M., Direct observation of fast protein folding: the initial collapse of apomyoglobin. *Proc. Natl. Acad. Sci. U. S. A.* **1996**, *93* (12), 5759-64.
82. Schechter, A. N.; Epstein, C. J., Spectral studies on the denaturation of myoglobin. *J. Mol. Biol.* **1968**, *35* (3), 567-89.
83. Sykes, P. A.; Shiue, H.-C.; Walker, J. R.; Bateman, R. C., Determination of Myoglobin Stability by Visible Spectroscopy. *J. Chem. Educ.* **1999**, *76* (9), 1283.
84. Bisht, M.; Mondal, D.; Pereira, M. M.; Freire, M. G.; Venkatesu, P.; Coutinho, J. A. P., Long-term protein packaging in cholinium-based ionic liquids: improved catalytic activity and enhanced stability of cytochrome c against multiple stresses. *Green Chem.* **2017**, *19* (20), 4900-4911.
85. Potnis, C. S.; Chauhan, R.; Kalbfleisch, T. S.; Alexander, E.; Eichhold, L.; Bansal, M.; Grapperhaus, C. A.; Keynton, R. S.; Linder, M. W.; Gupta, G., Enhancing the compatibility of BioCaRGOS silica sol-gel technology with ctDNA extraction and droplet digital PCR (ddPCR) analysis. *RSC Adv.* **2022**, *12* (45), 29399-29404.
86. Edmiston, P. L.; Wambolt, C. L.; Smith, M. K.; Saavedra, S. S., Spectroscopic Characterization of Albumin and Myoglobin Entrapped in Bulk Sol-Gel Glasses. *J. Colloid Interface Sci.* **1994**, *163* (2), 395-406.
87. Raynal, B.; Lenormand, P.; Baron, B.; Hoos, S.; England, P., Quality assessment and optimization of purified protein samples: why and how? *Microb. Cell Factories* **2014**, *13* (1), 180.

88. Flanders, K. G.; Pessagno, L. R.; Cerda, J. F., Hemoglobin and myoglobin stabilization by heme-fluoride complexes. *Polyhedron* **2021**, *203*, 115238.
89. Palaniappan, V.; Bocian, D. F., Acid-induced transformations of myoglobin. Characterization of a new equilibrium heme-pocket intermediate. *Biochem. J.* **1994**, *33* (47), 14264-14274.
90. Sage, J. T.; Morikis, D.; Champion, P. M., Spectroscopic studies of myoglobin at low pH: heme structure and ligation. *Biochem. J.* **1991**, *30* (5), 1227-1237.
91. Tang, Q.; Kalsbeck, W. A.; Olson, J. S.; Bocian, D. F., Disruption of the Heme Iron– Proximal Histidine Bond Requires Unfolding of Deoxymyoglobin. *Biochem. J.* **1998**, *37* (19), 7047-7056.
92. Chen, Y.-H.; Yang, J. T.; Chau, K. H., Determination of the helix and β form of proteins in aqueous solution by circular dichroism. *Biochem. J.* **1974**, *13* (16), 3350-3359.
93. Takeda, K.; Wada, A.; Yamamoto, K.; Hachiya, K.; Batra, P. P., Secondary structure change of myoglobin induced by sodium dodecyl sulfate and its kinetic aspects. *J. Colloid Interface Sci.* **1988**, *125* (1), 307-313.
94. Peterson, E. S.; Leonard, E. F.; Foulke, J. A.; Oliff, M. C.; Salisbury, R. D.; Kim, D. Y., Folding Myoglobin within a Sol-Gel Glass: Protein Folding Constrained to a Small Volume. *Biophys. J.* **2008**, *95* (1), 322-332.
95. Deriu, D.; Pagnotta, S. E.; Santucci, R.; Rosato, N., Spectroscopic and electrochemical characterization of cytochrome c encapsulated in a bio sol-gel matrix. *Biomaterials* **2008**, *21* (4), 417-23.

APPENDIX

Appendix for Chapter 3

Table A1. Reverse Transcription (RT) reaction mixture for a 15 μL reaction: 15 μL reaction consists of 7 μL master mix, 3 μL of 5X primer and 5 μL miRNA 21 sample (with or w/o BioCaRGOS).

| Component | Volume (μL) per 15- μL reaction |
|--|--|
| 100 mM dNTPs | 0.15 |
| MultiScribe Reverse Transcriptase, 50 U/ μL | 1.00 |
| 10X Reverse Transcription Buffer | 1.50 |
| RNase Inhibitor 20 U/ μL | 0.19 |
| Nuclease-free water | 4.16 |
| 5X miRNA | 3.00 |
| Total volume(μL) | 10.00 |

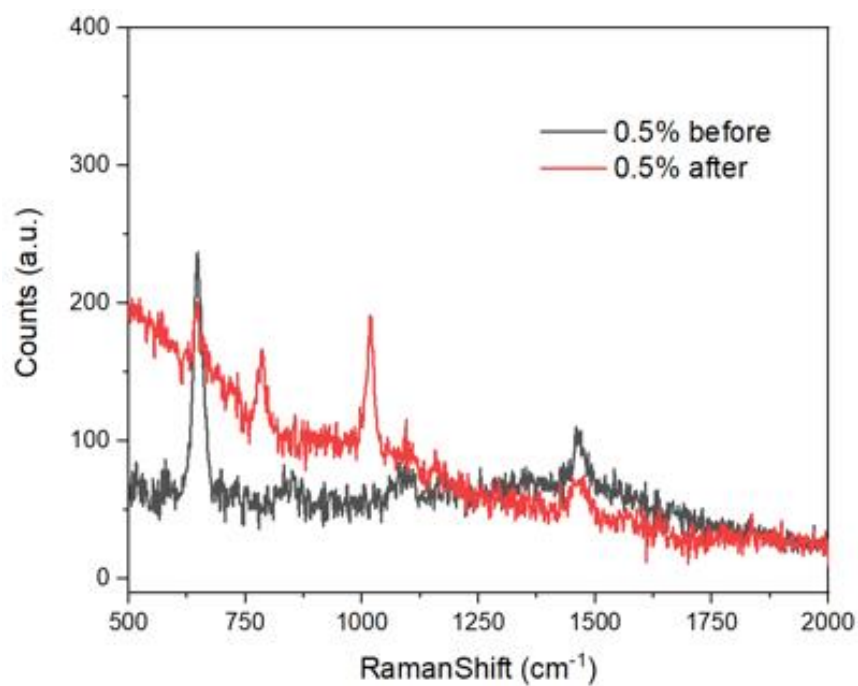


Figure A1. Complete hydrolysis of 0.5 v/v % tetramethyl orthosilicate (TMOS) was demonstrated by Raman spectra with an elimination of TMOS peak (646 cm⁻¹) and formation of methanol peak (1030 cm⁻¹) after a standard microwave synthesis.

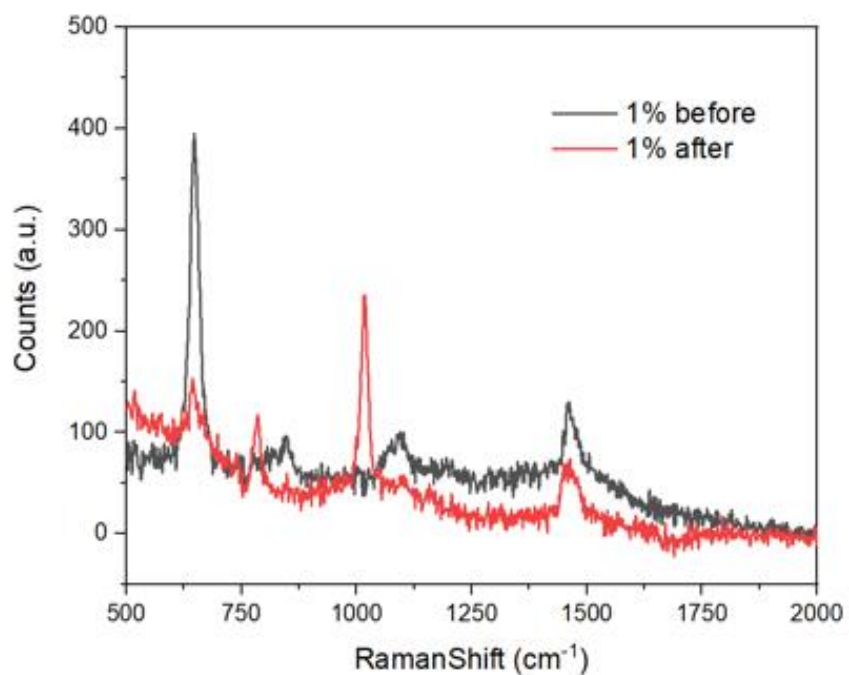


Figure A2. Complete hydrolysis of 1.0 v/v % tetramethyl orthosilicate (TMOS) was demonstrated by Raman spectra with an elimination of TMOS peak (646 cm⁻¹) and formation of methanol peak (1030 cm⁻¹) after a standard microwave synthesis.

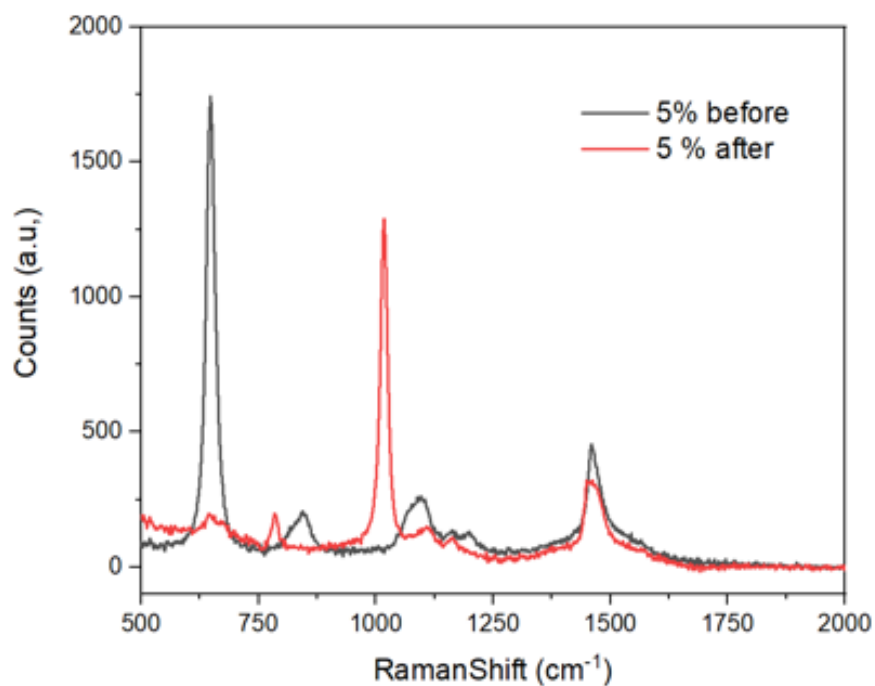


Figure A3. Complete hydrolysis of 5.0 v/v % tetramethyl orthosilicate (TMOS) was demonstrated by Raman spectra with an elimination of TMOS peak (646 cm⁻¹) and formation of methanol peak (1030 cm⁻¹) after a standard microwave synthesis.

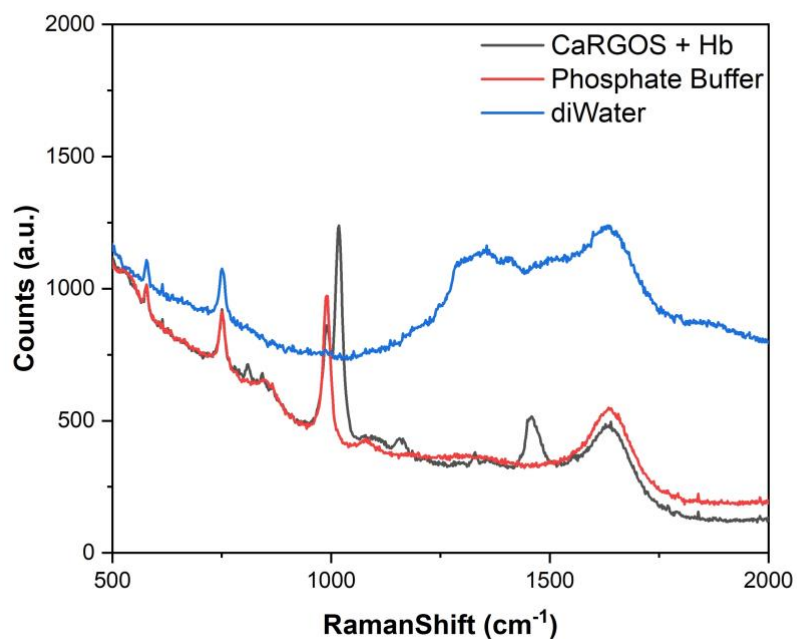


Figure A4. Raman spectra of CaRGOS formulations (5.0 v/v %) with hemoglobin and control solutions (phosphate buffer and Deionized water).

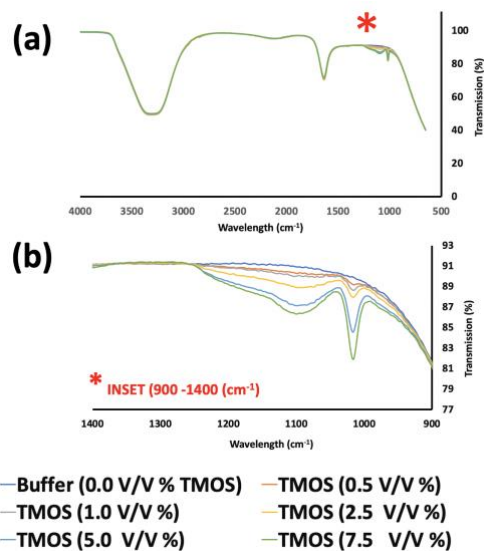


Figure A5. TMOS gel formation as displayed by FT-IR (ATR) spectra at (A) 500 -4000 cm⁻¹ (B) TMOS region (900-1400) cm⁻¹

Table A2. Size and stability characterization of CaRGOS formulations

:Hydrodynamic Size (DLS), Polydispersity Index (PDI) and Stability [zeta potential (ζ)] characterization of CaRGOS.

| Sample | DLS (nm) | PDI | Zeta Potential (mV) |
|--|-----------------|------------------|--------------------------------|
| CaRGOS without buffer (1.25 v/v %) | *0.79 ± 0.11 | 0.983 ± 0.026 | -22.07 ± 1.01 |
| CaRGOS without buffer (0.5 v/v %) | ** | ** | -26.58 ± 7.69 |
| CaRGOS with Buffer (0.5 v/v %) | 67.22 ± 1.65 | 0.248 ± 0.006 | -10.50 ± 1.66 |
| CaRGOS with Buffer (0.5 v/v %) <i>and</i> miRNA 21 | 69.95 ± 0.47 | 0.308 ± 0.004 | -20.04 ± 1.26 |
| CaRGOS with Buffer (0.5 v/v %) <i>without</i> miRNA 21 | 70.02 ± 2.09 | 0.338 ± 0.035 | -22.07 ± 1.01 |

Table A3. PCR reaction mixture for a 10 μL reaction: Each 10 μL reaction consists of 5 μL master mix, 0.5 μL of 20X primer, 3.17 μL of nuclease-free water and 1.33 μL of cDNA (RT product).

| Component | Volume (μL) per 10- μL reaction |
|----------------------|---|
| 20X miRNA Primer | 0.5 |
| Universal Master Mix | 5.00 |
| Nuclease-free water | 3.17 |
| Total Volume | 8.67 |

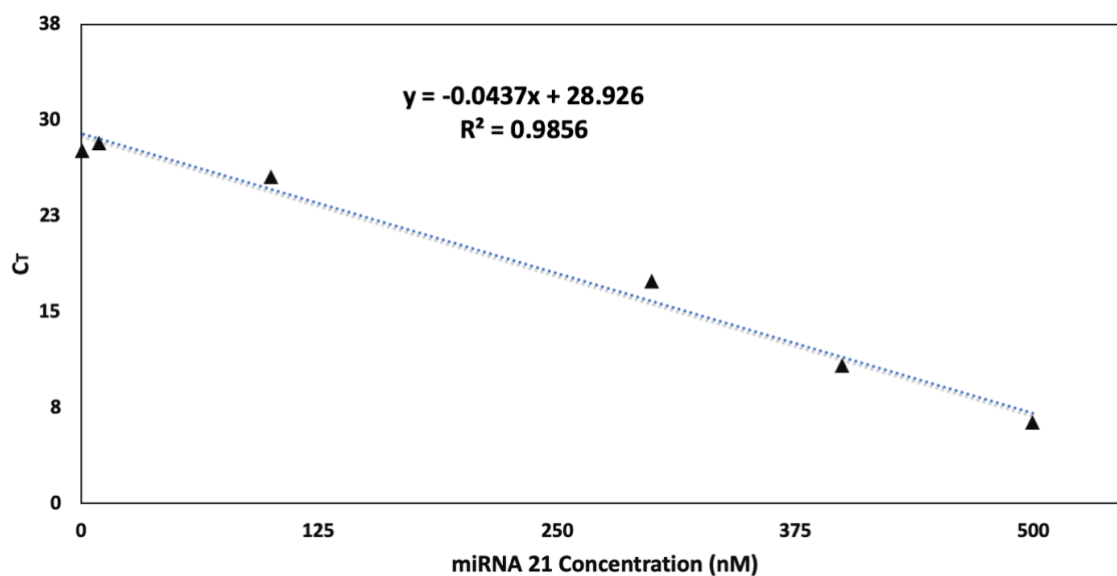


Figure A6. miRNA 21 concentration (nM) calibration curve in CaRGOS using qRT-PCR analysis: Formulation parameters used were 0.5 v/v % CaRGOS, Low-salt Tris EDTA buffer and nuclease free water.

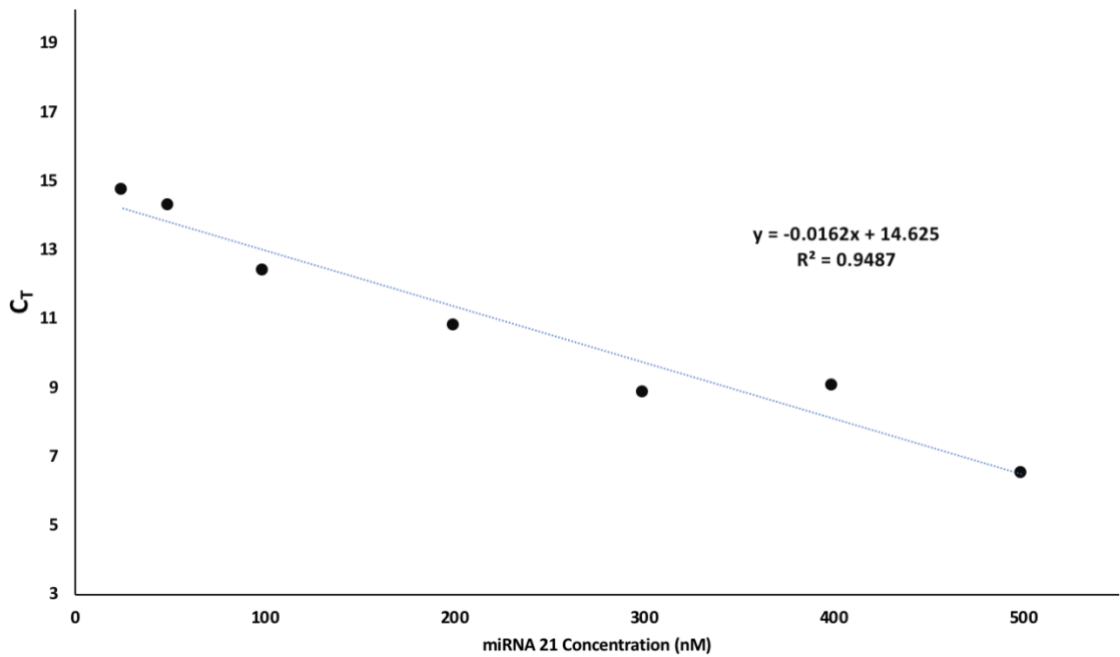


Figure A7. miRNA 21 concentration (nM) calibration curve in nuclease free water using qRT-PCR analysis: Formulation parameters used were low-salt buffer and nuclease free water.

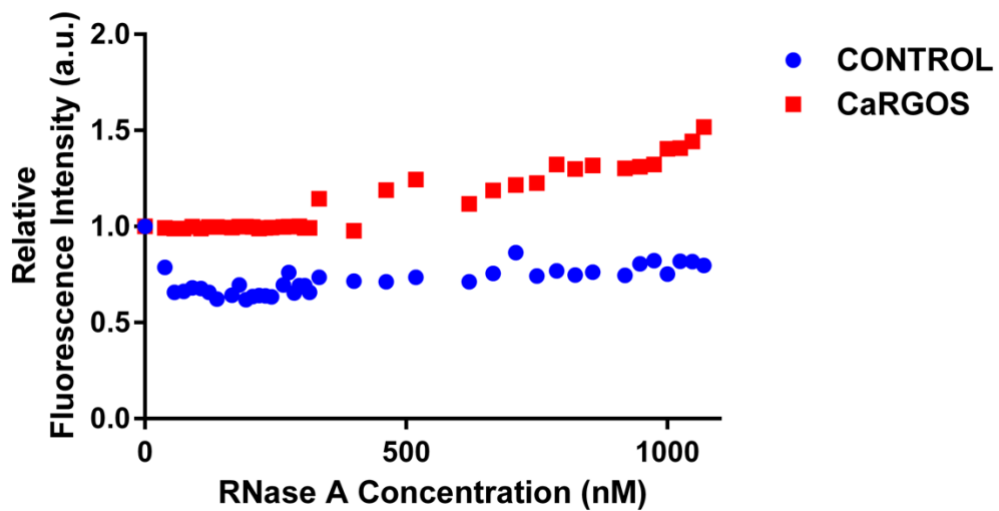


Figure A8. A plot of relative fluorescence intensity of Ethidium bromide against RNase A concentrations in (0-1200) nM range: An increase in relative fluorescence emission intensities of EtBr was observed in (320-1200) nM RNase A concentrations range.

Appendix for Chapter 5

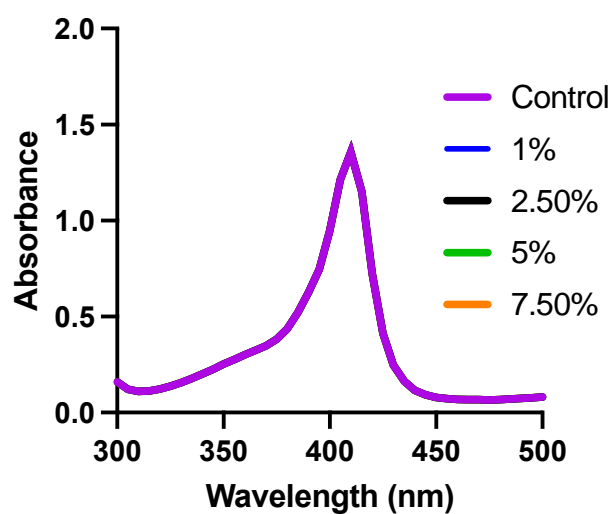


Figure A9. UV-Vis absorbance of myoglobin with different concentrations of BioCaRGOS demonstrating no interference post encapsulation.

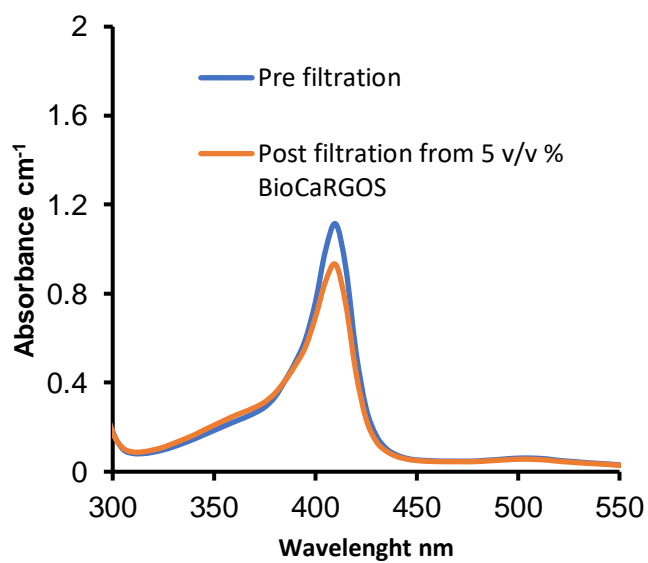


Figure A10. UV-Vis analysis of myoglobin demonstrating 95% recovery post encapsulation from 5 v/v % BioCaRGOS samples.

CURRICULUM VITA

Chinmay Shashank Potnis

Phone – 502-387-0006, email: chinmay.potnis@louisville.edu

LinkedIn: www.linkedin.com/in/ChinmayPotnis

Professional Summary

As a highly skilled and experienced formulation scientist, I bring over 5 years of expertise in Chemical Biology, Synthetic Organic Chemistry, and Catalysis to the table. My research background includes developing novel synthetic methodologies and optimizing sol-gel formulations for encapsulation of bio-specimens, with a keen focus on troubleshooting and improving the stability of temperature-sensitive bio-specimens using patented silica sol-gel technology. Well-versed in handling advanced instrumentation and developing analytical techniques commonly used in chemical and pharmaceutical research. With a strong track record of interdisciplinary collaboration in clinical and translational settings, I possess exceptional analytical thinking and project management skills. I am highly detail-oriented and possess leadership skills that enable me to excel in leading teams and driving projects to success. As a collaborative team player with excellent interpersonal and motivational abilities, I am well-prepared to excel in a dynamic environment.

Key Skills

Molecular Biology: Proficient in RNA/DNA isolation, PCR amplification, protein purification, Gel Electrophoresis, Western Blots, ddPCR and qPCR, assay development, and process optimization. Extensive experience with RNA, DNA, and protein formulations.

Protein Characterization: Skilled in UV-Vis spectroscopy, plate-based fluorescence assays, FTIR, HPLC, GC-MS, enzyme activity assays, Circular Dichroism (CD), ELISA, Zeta analyzer, and DLS, along with method development.

Organic Chemistry: Strong understanding of organic chemistry techniques, Scale-up support, multi-step synthesis, process optimization, purification methods, 1D and 2D NMR methods, Crystallization techniques, and small molecule synthesis.

Software Proficiency: Working knowledge of Origin, Graph-pad Prism, MestreNova, Chem Draw, and knowledgeable in statistical tools such as ddPCR QuantaSoft, SoftmaxPro, JMP, and Microsoft Office applications.

Project Management: Experienced in validation protocols, Good Laboratory Practices (GLPs), authoring technical documents such as protocols, test methods, text reports, certificates of analysis, and standard operating procedures (SOPs). Familiar with tech transfer processes.

Education

Doctor of Philosophy (Ph.D. Chemistry)

2018-present

University of Louisville, Kentucky, USA

Supervisors: Dr. Craig A. Grapperhaus and Dr. Gautam Gupta

Expected graduation date: Summer 2023

Thesis title: BioCaRGOS: Capture and Release Gels for Optimized Storage of Biologics.

Research Area: Chemical Biology; improving biospecimen stability by using patented silica sol-gel technology and developing a downstream compatible approach.

MS Chemistry (Organic Chemistry) 2018-2021

University of Louisville, Kentucky, USA

MS Chemistry (Organic Chemistry) 2016-2018

University of Mumbai, Maharashtra, India

BS Chemistry 2013-2016

University of Mumbai, Maharashtra, India

Work Experience

University of Louisville, Kentucky, USA

Department of Chemistry and Chemical Engineering

Graduate Research Assistant 2018-present

2018-present

Scope of research: Chemical Biology; Formulating and evaluating novel sol-gel technology as a platform for improving the stability of temperature sensitive bio-specimens.

- Optimized silica sol-gel formulations termed as BioCaRGOS (Capture and Release Gels for Optimized Storage), for outlining the stability and release pattern of biologics (proteins and nucleic acids).
- Improved the patented BioCaRGOS technology by developing protocols for toxicity removal prior to encapsulation of biospecimens.
- Established biocompatible protocols for the analysis of encapsulated nucleic acids using downstream analytical techniques such as ddPCR, qPCR, and ELISA.
- Characterized RNA, DNA, and proteins encapsulated in silica sol-gels for their size, zeta potential, morphology, encapsulation efficiency, structural integrity, and stability using methods such as DLS, Bradford, Ribogreen, SDS-PAGE, UV-Vis, HPLC, and CD spectroscopy.
- Optimized and formulated BioCaRGOS for stabilizing pancreatic cancer biomarkers such as KRAS ctDNA, CA-19-9 in plasma samples at room temperature, assessing stability using ddPCR and other relevant techniques.
- Investigated the stability of heme proteins in the presence of highly denaturing conditions and assessed structural integrity using spectroscopic techniques such as CD, UV-Vis, and Raman spectroscopy.
- Developed novel approaches for release of biospecimens post encapsulation for downstream analysis and efficient recovery.
- Designed, executed, and analyzed biophysical and biochemical characterization of biologics.

Scope of research: Synthetic Organic / Green Chemistry and Photocatalysis

- Developed a novel photoredox strategy for deformylative alkynylation of aldehydes, utilizing a green chemistry approach with no radical initiator or co-solvent. High functional group tolerance was observed in the synthesis of C(sp³) - C(sp) coupling of dihydropyridines and alkynylbenziodoxolones.
- Investigated the synthesis of alkylaryldiazenes via formal, photoredox-catalyzed, deformylative C-N bond formation. Characterized compounds using NMR, HPLC, and GCMS.
- Developed an efficient and greener approach for synthesizing nitriles from aldehydes using HCl.DMPU catalyst assisted one pot conversion. Achieved high yield and high purity compounds in the synthesis of nitriles from aldehydes.

Summer Research Intern

2017-2017

Institute of Chemical Technology, Maharashtra, India

Department of Pharmaceutical Sciences and Technology

Scope of research: Synthetic Organic Chemistry

- Developed a novel catalyst (aluminized polyborate) for synthesis of alkyl 1,2,6-trisubstituted-4-[(hetero)arylamino]-1,2,5,6-tetrahydropyridine-3-carboxylates and characterized the organic compounds by NMR.

Teaching and Leadership Experience

I. Graduate Teaching Assistant

2018-2021

University of Louisville

Department of Chemistry

- Assisted in the development and implementation of course curriculum and materials
- Developed strong communication and leadership skills while working with diverse groups of students and faculty.

II. Treasurer, CGSA. 2019-2020

- Successfully organized all event logistics associated with the 41st annual Derby Lecture Series. Invited the 2016 Nobel Laureate, Sir J. Fraser Stoddart to the university for two lectures.
- Responsible for fundraising efforts and secured university and corporate funding for the event

Certifications and Awards

-
- Dissertation Completion Award 2023
 - University of Louisville LaunchIt Innovation Bootcamp Graduate and NSF I-corps award 2022

Conference Presentations

-
- Oral presentation in 3rd Pfizer's Chemistry connect symposium for chemical engineering 2022
 - Oral presentation in American Chemical Society (Fall) 2022
 - Poster presentation in Bioorganic Chemistry Gordon Research Conference 2022
 - Oral presentation in Pfizer's Biotech connect symposium 2022
 - Poster presentation in American Chemical Society (Spring) 2022
 - Oral presentation in 2nd Pfizer's Chemistry connect symposium for chemical engineering 2021

- Poster presentation in international e-conference on Chemicals and Materials for Emergent Technologies

2020

Publications

- I. Potnis, C.S.; Grapperhaus. C.A.; and Gupta. G, Investigating BioCaRGOS for stability of heme proteins under enzymatic degradation and low pH. ACS Omega, 2023, manuscript under review.
- II. Potnis, C.S.; Chauhan, R.; Kalbfleisch, T.; Alexander E.; Eichhold. L.; Bansal. M.; Grapperhaus. C.A.; Keynton. R.S.; Linder. M.W.; and Gupta. G, Enhancing the compatibility of BioCaRGOS silica sol gel technology with ctDNA extraction and droplet digital PCR (ddPCR) analysis. RSC Advances 2022, 12, 29399-29404
- III. Chauhan, R.; Kalbfleisch, T.; Potnis, C. S.; Bansal, M.; Linder, M.; Keynton, R. S.; Gupta, G., Long term storage of miRNA at room and elevated temperatures in silica sol-gel matrix. RSC Advances 2021, 50, 31505-31510.
- IV. Boylan, J.; Chauhan, R.; Koneru, K.; Bansal, M.; Kalbfleisch, T.; Potnis, C. S.; Hartline, K.; Keynton, R. S.; Gupta, G., Bio-CaRGOS: capture and release gels for optimized storage of hemoglobin. RSC Advances 2021, 22, 13034-13039.
- V. G. Hammond, , S. R. Mudshinge, C. S. Potnis and B. Xu, HCl•DMPU-Assisted One-pot and Metal-free Conversion of Aldehydes to Nitriles, Green Chem. 2020, 22, 4161-4164.
- VI. R. A. Angnes, C. Potnis, S. Liang, Carlos R. D. Correia, and G. B. Hammond, Photoredox-Catalyzed Synthesis of Alkylaryldiazenes: Formal

Deformylative C–N Bond Formation with Alkyl Radicals, *J. Org. Chem.* 2020, 85, 4153-4164.

- VII. Liang, S., Angnes, R.A., Potnis, C.S., Hammond, G.B., Photoredox catalyzed C(sp³)-C(sp) coupling of dihydropyridines and alkynylbenziodoxolones, *Tet. Lett.* 2019, 45, 151230.
- VIII. Mali, A.S., Potnis, C.S. & Chaturbuj, G.U. Aluminized polyborate: a novel catalyst for the multicomponent solvent-free synthesis of alkyl 1,2,6-trisubstituted-4-[(hetero)arylamino]-1,2,5,6-tetrahydropyridine-3-carboxylates. *J Iran Chem Soc.* 2018, 15, 1399–1409.